CHARACTERIZATION OF ELECTROMAGNETIC WAVE ABSORBING PROPERTIES OF SiC-BASED AND ALUMINA WOVEN FABRICS

A THESIS SUBMITTED TO
THE GRADUATE SCHOOL OF NATURAL AND APPLIED SCIENCES
OF
MIDDLE EAST TECHNICAL UNIVERSITY

BY

ELVAN TAN

IN PARTIAL FULFILLMENT OF THE REQUIREMENTS
FOR
THE DEGREE OF MASTER OF SCIENCE
IN
METALLURGICAL & MATERIALS ENGINEERING

JUNE 2008

Approval of the thesis:

CHARACTERIZATION OF ELECTROMAGNETIC WAVE ABSORBING PROPERTIES OF SiC-BASED AND ALUMINA WOVEN FABRICS

Submitted by **ELVAN TAN** in partial fulfillment of the requirements for the degree of **Master of Science in Metallurgical and Materials Engineering Department, Middle East Technical University** by,

Prof. Dr. Canan ÖZGEN _____
Dean, Graduate School of **Natural and Applied Sciences**

Prof. Dr. Tayfur ÖZTÜRK _____
Head of Department, **Metallurgical and Materials Engineering**

Assist. Prof. Dr. Arcan Fehmi DERİCİOĞLU _____
Supervisor, **Metallurgical and Materials Engineering Dept., METU**

Examining Committee Members:

Prof. Dr. Muharrem TİMUÇİN _____
Metallurgical and Materials Engineering Dept., METU

Assist. Prof. Dr. Arcan Fehmi DERİCİOĞLU _____
Metallurgical and Materials Engineering Dept., METU

Prof. Dr. Macit ÖZENBAŞ _____
Metallurgical and Materials Engineering Dept., METU

Prof. Dr. Kadri AYDINOL _____
Metallurgical and Materials Engineering Dept., METU

Assoc. Prof. Dr. Özlem AYDIN ÇİVİ _____
Electrical and Electronics Engineering Dept., METU

Date: 24.06.2008

I hereby declare that all information in this document has been obtained and presented in accordance with academic rules and ethical conduct. I also declare that, as required by these rules and conduct, I have fully cited and referenced all material and results that are not original to this work.

Name, Last name : Elvan TAN

Signature :

ABSTRACT

CHARACTERIZATION OF ELECTROMAGNETIC WAVE ABSORBING PROPERTIES OF SiC-BASED AND ALUMINA CERAMIC WOVEN FABRICS

Tan, Elvan

M.Sc., Department of Metallurgical and Materials Engineering

Supervisor: Assist. Prof. Dr. Arcan Fehmi Dericioğlu

June 2008, 128 pages

Electromagnetic wave absorbing properties of SiC-based and alumina ceramic woven fabrics have been investigated. Electrical conductivities of SiC-based ceramic woven fabrics were modified by heat treatment in air resulting in their oxidation. Surface properties of alumina woven fabrics were altered by gold-sputtering resulting in a high conductivity layer on the surface of the wovens. Electromagnetic wave interactions of single layer and double layered combinations of these ceramic woven fabrics were determined in 17-40 GHz frequency range using "free-space" method. Electromagnetic wave absorption potential of ceramic woven fabrics with different chemical compositions and woven types were correlated with their material properties by X-ray diffraction, scanning electron microscopy and electrical conductivity measurements. Effects of modifications and varying woven fabric arrangements in combinations on the electromagnetic wave absorption potential of the ceramic woven fabrics have been discussed. Various double layer combinations of SiC-based and alumina woven fabrics revealed a

promising potential in terms of both reduced reflection and transmission resulting in more than ~95% absorption in millimeter wavelength range, which makes them powerful candidate materials for electromagnetic wave absorption applications.

Keywords: SiC-based woven fabrics, alumina woven fabrics, electromagnetic wave absorbing materials, free-space method.

ÖZ

SiC-BAZLI VE ALUMİNA FİBER DOKUMALARIN ELEKTROMANYETİK DALGA EMİCİ ÖZELLİKLERİNİN KARAKTERİZASYONU

Tan, Elvan
Yüksek Lisans, Metalurji ve Malzeme Mühendisliği Bölümü
Tez Yöneticisi: Yrd. Doç. Dr. Arcan Fehmi Dericioğlu

Haziran 2008, 128 sayfa

Bu çalışmada farklı dokuma türü ve kimyasal kompozisyona sahip SiC-bazlı ve alumina seramik dokumaların elektromanyetik dalga soğurma özellikleri incelenmiştir. Isıl işlem sonucu elektriksel iletkenlikleri değiştirilen SiC-bazlı dokumalar ile altın kaplanarak yüzey özellikleri değiştirilen alumina dokumaların tek ve çok katmanlı kombinasyonlarının elektromanyetik dalga geçirim ve yansıtma kayıpları 17-40 GHz frekans aralığında "free-space" metodu kullanılarak belirlenmiştir. Farklı kimyasal kompozisyonlara ve dokuma tiplerine sahip seramik dokumaların malzeme özellikleri ile elektromanyetik dalga soğurma potansiyelleri arasındaki ilişki X-ışınları kırınımı, taramalı elektron mikroskobu ve elektriksel iletkenlik ölçümleri kullanılarak incelenmiştir. Malzemelere uygulanan modifikasyonların ve kombinasyonlardaki dokuma dizilişlerinin, sistemlerin elektromanyetik dalga ile etkileşiminde doğurduğu sonuçlar araştırılmıştır. SiC-bazlı ve alumina dokumalarla yapılan iki katmanlı birçok kombinasyonun düşük geçirim ve yansıtma değerleri ile malzemeye gelen elektromanyetik

dalganın %95'inden fazlasını soğurduğu görülmüştür. Milimetre dalga boyundaki yüksek soğurma potansiyelleri bu çok katmanlı seramik dokuma kombinasyonlarını elektromanyetik dalga soğurma alanında kullanılabilecek kuvvetli aday malzemeler yapmaktadır.

Anahtar Kelimeler: SiC-bazlı dokumalar, alumina dokumalar, elektromanyetik dalga soğurucu malzemeler, free-space metot

To My Family,

ACKNOWLEDGEMENTS

I would like to express my sincere appreciation to Assist. Prof. Dr. Arcan Dericioğlu for his supervision, guidance, support and encouragement throughout the study.

I must also thank to my brother Evren Tan for his never-ending patience, motivation, physical and moral support in the completion of this thesis.

I am grateful to all the stuff of the Department of Metallurgical and Materials Engineering. I must express my special thanks to my dear labmate Selen Gürbüz for her valuable supports and motivation, and also thanks to Burcu Kayıplar, Gökhan Kıdıl, Göksu Gürer for their supports and friendships.

I must also express my great thanks to my friends Nurdan Gürkan, Özge Acarbaş, Yankı Başaran, Ali Erdem Eken, Sıla Süer, and the ones which I could not record all their names at the Department of Metallurgical and Materials Engineering, METU, for their help and support.

Finally, I owe a depth to my family İbrahim and Sema Tan for their endless love, support and encouragement throughout my life.

TABLE OF CONTENTS

LIST OF TABLES

LIST OF FIGURES

CHAPTER 1

INTRODUCTION

In today's technology many commercial and military applications such as data transmission, telecommunication, wireless network systems and satellite broadcasting as well as radars, diagnostic and detection systems utilize and emit electromagnetic (EM) waves. Rapid development of many advanced electronic systems and telecommunications has resulted in a growing interest in electromagnetic interference (EMI) shielding and absorbing materials.

Interaction of EM waves originating from different sources can cause severe interruption of electronically controlled systems such as device malfunctioning and performance reduction due to system to system coupling. This situation leads to decrease in quality and misinterpretation of the transferred data. Therefore, it becomes vital to avoid resulting EMI and EM wave pollution by the use of appropriate shielding and absorbing materials.

There are many researches on the development of EM wave absorbers which can be capable of absorbing unwanted EM radiation and suppress EMI. Choice of the suitable material for a certain application depends on many factors such as whether narrow or broadband absorption is required or low or high frequency effectiveness is necessary. Moreover, high mechanical performance, low thickness, lightweight and environmental durability with minimized production cost can be the important design criteria especially for aerospace and aeronautical applications. Magnetic and/or electrical properties of materials can altered to allow absorption of EM energy at discrete or broadband frequencies. Any sort of material that exhibits ohmic, dielectric polarization and/or magnetic polarization loss can be utilized as an EM wave absorbing material and various magnetic and dielectric lossy materials are being used for this purpose.

In the present study, EM wave absorbing potential of SiC-based and alumina ceramic woven fabrics was investigated. These materials are known as two of the main reinforcements of structural ceramic matrix composites. SiC-based woven fabrics are used in high temperature structural applications, where lower creep and grain growth rate allow better dimensional stability and strength retention under the combined conditions of elevated temperature and stress. Moreover, SiC-based woven fabrics can also provide great thermal and electrical conductivity with low density. On the other hand, alumina woven fabrics are used in applications where oxidation resistance, chemical stability and high temperature durability are needed with flexibility and lightweight. Owing to these application areas of SiC-based and alumina woven fabrics, intrinsic properties of them such as their specific modulus and strength, density and environmental durability related to their structural use are quite well known. However, there is very limited knowledge about their interaction with EM radiation; especially, there is no study available on alumina woven fabrics in this respect to the best of our knowledge. The desired property set of lightweight, high environmental durability, low thickness and wide electrical resistivity range (for SiC-based woven fabrics only) draw attention to these materials for EM wave absorbing applications.

Present study has focused on the interaction of SiC-based and alumina ceramic woven fabrics and EM waves. Following to the determination of EM wave absorption potential of as-received ceramic woven fabrics, properties of woven fabrics were altered with various treatments. For this manner, electrical conductivities of SiC-based woven fabrics were modified by heat-treatment in air, and surface properties of alumina woven fabrics were modified by gold-sputtering. EM wave absorption potential of single as well as various double layer combinations of SiC-based and alumina woven fabrics were determined in 17-40 GHz frequency range. “Free-space” method which has several advantages being non-destructive, contactless and conductable without any specific sample preparation etc. over the conventional measurement methods, was used for this purpose. Effects of modifications and varying woven fabric arrangements in combinations on the EM wave absorption potential of the ceramic woven fabrics have been discussed.

Throughout this thesis, in the first chapter basic information about EM waves and their interactions with materials are given together with requirements of EM wave absorbers. Following the first chapter, “Experimental Procedure” chapter describes the ceramic woven fabrics, measurement set up and methodology which is used to characterize EM wave absorbing properties of the woven fabrics. Results on the general characteristics of SiC-based and alumina woven fabrics as well as results on single and multilayer combination interaction with EM radiation are given and discussed in “Results and Discussion” chapter. Finally, a guideline is suggested in the “Conclusion” chapter to obtain high EM wave absorption potential in multilayer ceramic woven fabric systems.

CHAPTER 2

THEORY AND LITERATURE REVIEW

This chapter includes basic information about EM wave absorbing materials and their interaction with EM waves. Prior to explaining their characteristics, information about the basic features of EM waves together with their properties and interactions with materials are provided. A literature review is given about the materials which are commercially used as EM wave absorbers and measurements techniques used for the characterization of EM wave absorbing materials are reviewed. Chapter is concluded with general production routes, properties and application fields of the silicon carbide and alumina fibers, which are the broad class of materials used in this study.

2.1. Electromagnetic Waves

EM waves are formed when an electric field couples with a magnetic field. These waves are generated by accelerating electric charges. The radiated waves consist of oscillating electric and magnetic fields, which are of at right angle to each other and also at right angle to the direction of wave propagation [1]. A linearly polarized EM plane wave propagating in the +z-direction is shown in Figure 2.1.

According to Maxwell theory, the electric (E) and magnetic (B) field amplitudes in EM wave are interrelated via Eq. (1) where c shows the speed of light. At large distances from the source of the waves, the amplitudes of oscillating fields diminish with distance, r, being proportional to 1/r [1]. The radiated waves can be detected at extreme distances from the oscillating charges.

$$E = c * B \tag{1}$$

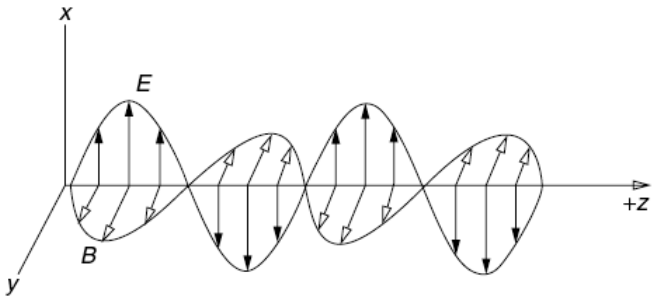

Figure 2.1 Schematic representation of linearly polarized EM wave [2].

A wavelength (λ) represents the repeat distance associated with the wave, in other words, the distance between two adjacent peaks (or troughs) at a fixed instant. A period (*T*), on the other hand, is the time for one complete wavelength of the disturbance to pass a given point in space. Inverse of the period is frequency (*f*) of the wave which is measured in units of cycles/s or Hertz (Hz). Figure 2.2 shows the wavelength (λ) and period (*T*) of a wave which is gravelling at the speed of light.

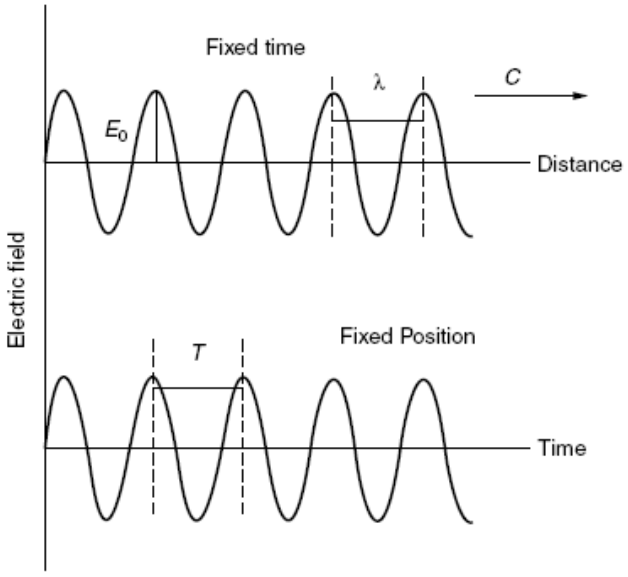

Figure 2.2 Wavelength (λ) and period (*T*) of a wave of amplitude E_0 that travel at c [2].

The wavelength and frequency are related simply through the speed of the wave by Eq. (2).

$$c = f * \lambda \tag{2}$$

EM waves carry energy and momentum, and hence, exert pressure on a surface. Transport of EM radiation energy occurs via photons. A photon is a quantum, or excitation, of the radiation field. It has zero rest-mass and propagates at the speed of light. Each photon carries energy (*E)* that is determined by *f* or λ of the radiation according to Eq. (3), where *h* is Planck's constant, which has the experimentally determined value of 6.6261×10^{-34} J.s [1].

$$E = h * f = \frac{h * c}{\lambda} \tag{3}$$

2.2. Energy Levels and Transitions in Atomic, Molecular and Nuclear System

Electrons, protons and neutrons are the main blocks of matter. They are bound together so that the total energy of an atom, molecule or atomic nucleus can only take well-defined, discrete values. Transition from one energy level to another is satisfied by the absorption or emission of a photon.

2.2.1. Atomic Transitions

To excite an atom from a low-energy level to a higher level, a photon must be absorbed, and its energy must match the energy difference between the initial and final atomic states. When an atom deexcites to a lower energy level, it must emit a sequence of one or more photons of the proper energy. Atomic transitions are characterized by photon energies that range from a few eV to the order of keV depending on the type of the atom and the particular transition involved [2].

The frequency of the absorbed or emitted radiation is determined by photon energy according to the allowed transitions of atomic electrons. As a result, only certain selected frequencies appear in atomic absorption.

2.2.2. Vibrational and Rotational States in Molecules

Electron transitions in molecules exhibit energy spacings that are similar to those in individual atoms; they are on the order of eV to keV. The spacing of vibrational levels is on the order of 100 times lower than that of the electronic levels where rotational energy level is typically about 100 times lower than the spacing between the vibrational levels of a molecule [2].

2.2.3. Nuclear Transitions

Protons and neutrons are bound within atomic nuclei at discrete, quantized values of energy. Nuclear levels and photon energies are orders of magnitude higher than those of atomic transitions. The spacings between nuclear levels are also typically in the MeV range or greater [2].

2.3. Electromagnetic Spectrum

EM waves cover a wide range of frequencies related to large range of photon energies. The EM spectrum is the distribution of EM radiation according to energy (or frequency or wavelength) which is indicated in Figure 2.3. It covers different EM waves having wavelengths from thousands of meters down to fractions of the size of an atom.

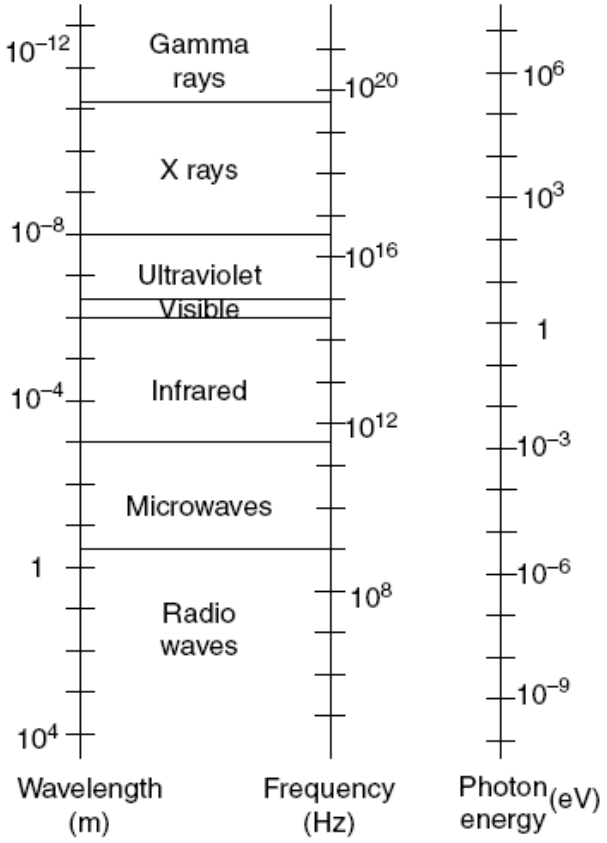

Figure 2.3 Electromagnetic spectrum [2].

Basic properties of EM waves observed in the spectrum are summarized below [1, 2]:

Radio waves are used for radio and television broadcasting and mobile phone communication. They reveal a much longer wavelength than light waves. The corresponding photon energies of the waves are about 10^{-5} eV or less. These energies are too small to be associated with electronic, molecular or nuclear transitions. Radio waves are the basis of magnetic resonance imaging, since corresponding photon energies are in the proper range for transitions between nuclear spin states (nuclear magnetic resonance).

Microwaves have wavelengths ranging between 1 to 300 mm, and their frequencies are in the GHz range. They are generated by electronic devices. Related

to their short wavelength, they are well suited for radar system used in aeronautical as well as naval navigation and for studying atomic and molecular properties of matter. Photon energies of microwaves are typically between about 10^{-6} and 10^{-3} eV. These energies correspond to transitions between rotational states of molecules.

Infrared waves reveal a wavelength range between 1 mm down to the longest wavelength of visible light. These waves are produced by hot bodies or molecules, and they are absorbed by majority of materials. Infrared energy which is absorbed by a substance appears as heat. The energy disturbs the atoms of the body by increasing their vibrational or translational motion, which results in temperature rise. Some of the application areas of these waves are thermal imaging and vibrational spectroscopy. Human eye cannot detect infrared radiation but heat can be felt by human skin. Corresponding photon energy values are on the order of 10^{-3} eV up to a few eV.

Visible light is the most familiar form of EM waves, since it can be detected by human eye. Light is produced by the arrangement of electrons in atoms and molecules. Various wavelengths of visible light are classified in terms of colors ranging from violent to red. Photon energies in the visible region are between 1.6 eV (red) and 3.2 eV (violet). These photon energies are generally associated with the excitation and deexcitation of outer shell electrons in atoms and molecules.

Ultraviolet waves have very high energy and very short wave lengths (shorter than visible light). Their photon energies range between about 3 and 100 eV which are comparable to the order of magnitude of ionization energies and molecular dissociation energies of many chemical reactions. Sun is an important source of ultraviolet light, which is the main cause of suntans and skin cancer. Most of the ultraviolet light from the sun is absorbed by atoms in the upper atmosphere. Ultraviolet light cannot be detected by human eye; however human skin can be irritated by the light emerging from the sun.

X-rays have significantly high energy levels and short wavelengths which can transmit through human body. Deceleration of high energy electrons which are bombarding a metallic target is the most common source of X-rays. These rays are used as a diagnostic tool in medicine, as a treatment for certain diseases and in the study of crystal structure, since their wavelengths are comparable to the atomic

separation distances (~0.1 nm) in solids. Photon energies of these rays are approximately between 100 eV to the order of a few hundred keV, which is associated with transitions at inner, most tightly bound atomic electrons.

Gamma rays have very high energies and they can transmit through metals, consequently they can be used to find tiny cracks in metals for example hairline cracks in aircraft components. Some radioactive materials produce gamma rays during certain reactions. Since their photon energies are extremely high on the order of keV to GeV, gamma rays are highly penetrating radiation and produce various damages when absorbed by living tissues. Photons in this regime readily produce ionization and, in some cases, can initiate photonuclear reactions.

2.4. Interaction of Electromagnetic Waves with Materials

In the previous sections, basic information about the features of EM wave, energy levels, transitions at atomic and molecular levels and properties of EM waves in the spectrum was given. In this section, material properties which affect the interaction of EM wave with materials is described.

EM properties of materials are controlled by the interactions between material constituents at atomic and molecular level and the electric and magnetic force fields. Material behavior or response to EM forces depends on three basic material parameters, namely permittivity (ε), permeability (μ) and conductivity (σ) [1-5]. These parameters are complex in general, since response of material is frequency dependent. Such complex EM parameters determine the depth to which the EM energy can couple to the material at a given frequency.

The depth of penetration (skin depth) of the EM energy in material could be so small that the interaction may just be limited to the surface only. This situation is generally observed at higher frequencies. In such cases, response of the material refers not only to the bulk characteristics but also to the surface properties of the materials [4].

2.4.1. Dielectric Characterization of Materials

The basis of dielectric properties arises from the interaction of matter with an external electric field at the microscopic level. Electric field between electric charges (q_1 and q_2) in a medium is quantified by Coulomb's law (Eq. (4)) where F is the columbic force of interaction between two charges separated by a distance r, and ε is the constant that specifies the dielectric properties of a material.

$$F = \frac{1}{4\pi\varepsilon} * \frac{q_1 q_2}{r^2} \tag{4}$$

ε is generally expressed as $\varepsilon_0 * \varepsilon_r$ where ε_0 is the absolute dielectric permittivity of free space ($(1/36\pi)*10^{-9}$ farad/m), and ε_r is the dimensionless permittivity of the medium relative to the free space and is known as dielectric constant.

Dielectric materials are the materials which are polarized in the presence of an electric field and have an electrostatic field within them under the state of polarization [4]. Polarization is the molecular alignment along the direction of an applied electric field.

Dielectric materials can be classified as polar (dipole) dielectrics and nonpolar (neutral) dielectrics. If charges in a molecule of a material form a lumped entity positive-negative pair in the common center of gravity, this molecule is termed as nonpolar molecule. Unpolarized set of nonpolar molecules and polarized set of these molecules under the influence of an electric field are shown in Figure 2.4.

On the other hand, if charges can be separated by a distance with respect to their positional centers, the molecule is said to be polar which exhibits a permanent or rigid dipole moment even in the absence of an external electric field. Unpolarized and polarized polar molecule under the influence of an electric field is shown in Figure 2.5.

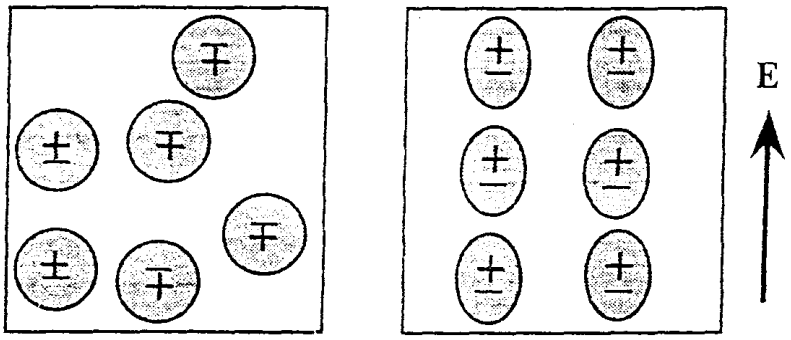

Figure 2.4 (a) Unpolarized set of nonpolar molecules and (b) polarized set of nonpolar molecules under the influence of an electric field E [4].

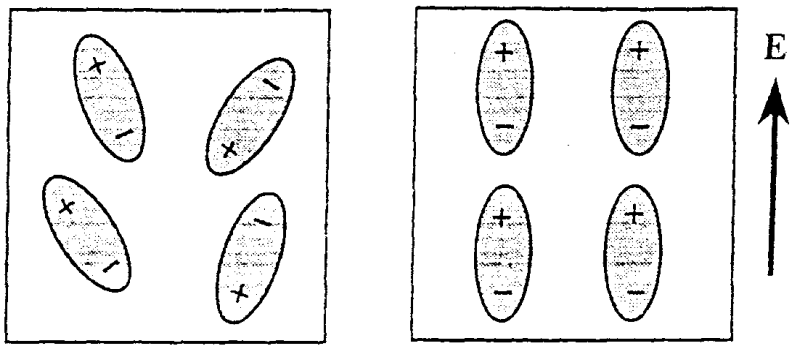

Figure 2.5 (a) Randomly oriented unpolarized set of polar molecules and (b) polarized set of polar molecules under the influence of an electric field E [4].

Polarization types can be summarized in three main groups:

An external electric field causes an elastic displacement of electronic shells relative to the nucleus of the atoms of a dielectric. This polarization known as *electronic polarization* and occurs in all dielectrics. Nonpolar dielectrics exhibiting pure electronic polarization possess low relative permittivity on the order of 1 to 3 where the relative permittivity of polar dielectrics is higher.

Dielectrics of an ionic crystal structure exhibit *ionic polarization*. An applied field acts to displace cations in one direction and anions in the opposite direction, which gives rise to a net dipole moment.

Orientation polarization can be only observed in substances that possess permanent dipole moment. It involves displacement of dipoles. When dipoles are subjected to alternating electric field force, there is a time-dependent polarization response which is known as relaxation process. The rate of response of the molecular polarization influences polarizability of the medium and hence the bulk dielectric property. As a consequence, permittivity become complex numbers which can be expressed as shown in Eq. (5).

$$\varepsilon = (\varepsilon' - j\varepsilon'') \tag{5}$$

The real part of the complex permittivity, ε', shows the capacitive term (energy storage part), and the imaginary part, ε'', represents the energy dissipative (loss part) term. At microwave frequencies the absorbed energy can be transferred to the molecules, and when the wave energy is transferred to the material, the molecular dipoles start to oscillate. The loss amount is measured by loss tangent which is given in Eq. (6).

$$\tan\delta = \frac{\varepsilon''}{\varepsilon'} \tag{6}$$

Various types of charges or groups in any material lead to corresponding interactions with the applied EM field resulting in either relaxation or resonance phenomenon which are briefly explained in the following [4]:

- ❖ Inner bound electrons are tightly bound to the nuclei and are little influenced by the external field. They only resonate with a high energy (~10^4 eV).
- ❖ Outer bound electrons are the valance electrons of outer electronic shells, and they contribute to atomic and/or molecular polarizabilities.

❖ Free electrons are in the conduction band and contribute to electric current through free movement under an electric field.

❖ Bound ions represent ionic dipoles which are permanent and experience orientational polarization under an applied field.

❖ Free ions are dissociated ions as in electrolytes which move in the direction of applied field with a low mobility.

Depending on the type of charges, the EM field versus material interaction may result in either relaxation or resonance which is shown in Figure 2.6.

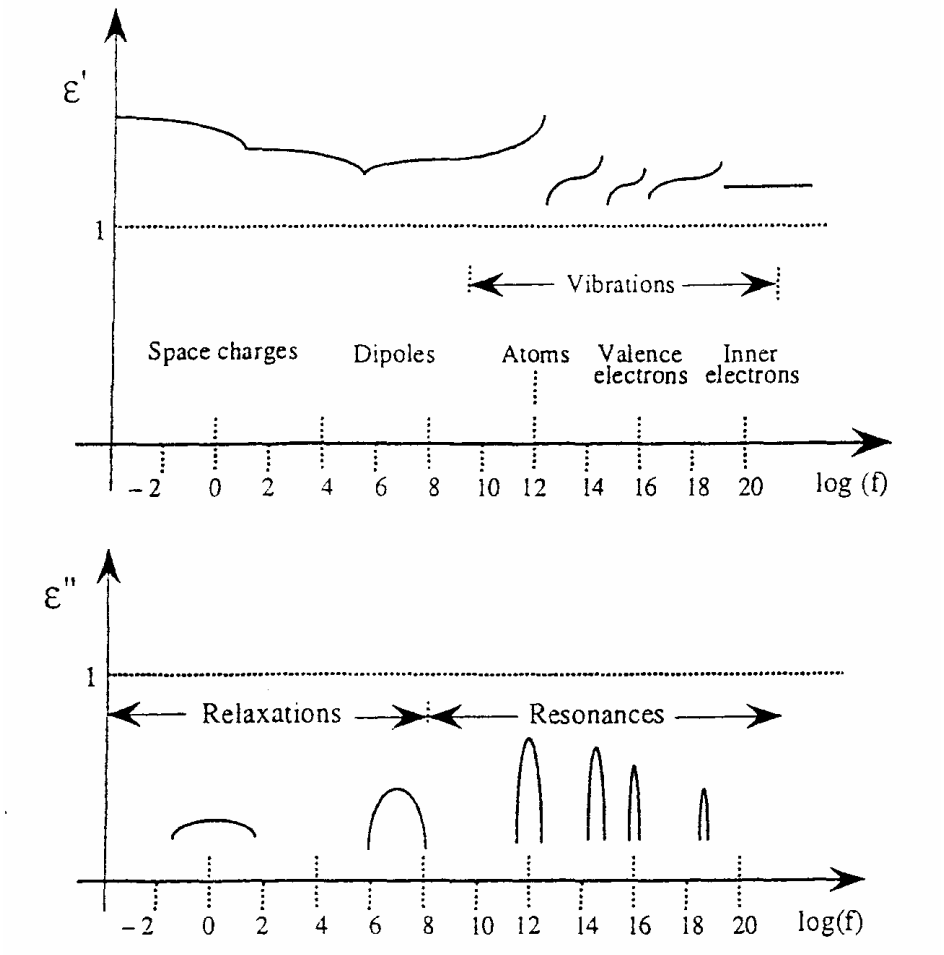

Figure 2.6 Response of a dielectric material interacting with an EM wave: Relaxation and resonance effects [4].

2.4.2. Magnetic Characterization of Materials

Response of a material to magnetism is determined by the extent of its interaction with a magnetic field force. The parameter that quantifies such an interaction is the magnetic permeability, μ. Presence of charges generates an electric field force, and the movement of such charges induces a magnetic field force $(\vec{H})$. Permeability is defined according to Eq. (7) where $\vec{B}$ is magnetic flux density, for linear, homogeneous, isotropic medium.

$$\vec{B} = \mu \vec{H} \tag{7}$$

μ is generally expressed as $\mu_0 * \mu_r$ where μ_0 is the absolute dielectric permeability of free space ($(4\pi)*10^{-7}$ henry/m), and μ_r is the relative permeability of the medium.

Magnetic materials can be classified broadly on the basis of the atomic structure of the material and values of relative permeability:

Diamagnetic materials have relative permeability slightly less than unity. They exhibit a negative magnetism where their magnetic susceptibility is independent of external magnetic field and temperature. Diamagnetic materials are nonmagnetic and have no use as magnetic materials.

Paramagnetic materials have relative permeabilities slightly larger than unity. When the permanent magnetic moments (resulting from an electric current due to electronic spin, orbital motion and nuclear spin angular momentum) in the atoms or ions do not mutually interact and are dispersed with isotropic randomness corresponding materials are known as paramagnetic.

Ferromagnetic materials are characterized by the presence of parallel orientation of magnetic dipole moments. It occurs in materials with partly filled inner electron shells. In these materials magnetization is spontaneous. Relative permeability is much higher than unity.

Ferrimagnetic materials have non-zero net magnetization of magnetic sublattices. Consequently, they possess a net magnetic moment which disappears at $T>T_c$ due to thermal energy. These materials are known as ferrites.

2.4.3. Characterization of Electrical Conductivities of Materials

Individual atoms are characterized by discrete energy levels surrounding it, in which the electrons form orbital paths around the parent nuclei (Bohr's model). The interaction between atoms results in the formation of bands of energy level. When atoms are brought together to constitute a solid, the discrete atomic energy levels change under the influence of neighboring nuclei. Although total number of energy levels remains constant, discrete levels which correspond to a given isolated atomic level become closely packed in energy and form a band.

Individual atoms are in the ground state at absolute zero temperature which implies that electrons reside and fill all the energy levels below a reference energy level called Fermi level. On the other hand, electrons acquiring thermal energy may shift to the band of energy levels higher than Fermi level at higher temperatures. Fermi level specifies the probabilistic dividing line below which the fully occupied energy levels exist and above which fully empty energy levels exist at 0 K [4].

Valance band is the band of energy levels which are closest to the nuclei and energy levels are totally filled at 0 K. Forbidden band (band gap) is the disallowed states between the uppermost occupied shell of valance band and an empty band. At temperatures higher than 0 K thermal energy imparted to the electrons in the valance band could allow the electrons jump across the forbidden gap and reach the unoccupied energy levels. The electrons which reach these levels are less influenced by the columbic force of attraction by the nuclei, and hence are free to move. These electrons are called free electrons and conduction band is the band in which the free electrons are present.

The extent of forbidden gap permits the classification of a material as a dielectric, semiconductor or conductor. The simple band theory suggests that the availability of a number of free electrons in the conduction band depends on the forbidden gap energy [4]. In case of a large forbidden gap, it may be impossible for the free electrons to be present in conduction. This refers to the electrical insulation property of a material which is known as dielectric. The availability of electrons in the conduction band is limited when forbidden gap energy is rather small. This situation permits an electrical conduction, and such materials are known as

semiconductors. When conduction and valance bands overlap permitting a copious amount of free electrons available at ambient temperatures, such materials are termed as conductors.

Electrical conductivity, σ, is used to specify the electrical character of the material. Range of electrical conductivities of conducting, semiconducting and insulating materials are given in Figure 2.7.

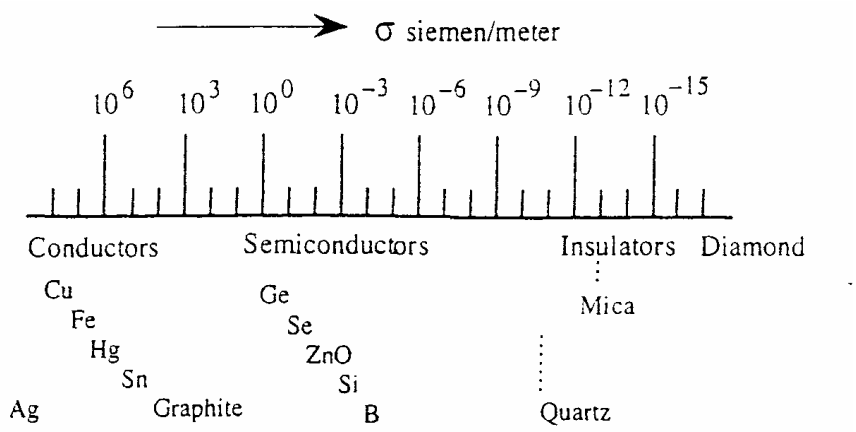

Figure 2.7 Range of conductivities of conducting, semiconducting and insulating materials [4].

Electrical conductors are characterized by the property of finite electrical conductivity depicting its ability to transport electric charges under the influence of an applied electric field force. Semiconductors are materials which have conductivities between the metallic conductors (with $\sigma>10^5$ S/m) and insulators (with $\sigma<10^{-10}$ S/m).

Materials which are intrinsically semiconductors (with no impurities added) are known as intrinsic semiconductors. These are group IV elements namely carbon (C), silicon (Si), germanium (Ge) and tin (Sn). An atom of this group shares its four valence electrons with its neighboring atoms and forms covalent bonding. As a covalently bonded pure semiconductor they prefer to be chemically inactive.

In the absence of thermal energy, at 0 K the valance band of semiconductor is fully occupied, and the conduction band has no electrons. As the temperature rises, small fraction of electrons in the valance band would acquire enough thermal energy to jump across the forbidden energy gap. The removal of electrons from the valance band corresponds to holes which would be occupied by an electron. Thus, the migration of electrons from atom to atom would necessitate filling and creation of holes. Flow of electrons means a concurrent movement of holes as well.

Extrinsic semiconductors are materials with deliberately added impurities (dopants) so that electrical conductivity is dominantly dictated by the dopants. Substitutional impurities occupy the atomic sites in the host lattice, whereas the interstitial impurities fit between regular lattice sites. When a group IV semiconductor is doped, it is known as an extrinsic semiconductor, since its electrical behavior is more predominantly dictated by the added impurities than by the intrinsic characteristics of the group IV element.

Addition of group V impurities renders the extrinsic semiconductor to have a set of easily achievable electrons in the conduction band as the free electrons. Therefore, such an extrinsic material has acquired donor atoms by addition of group V impurities. Addition of group III impurities would render the extrinsic material with excess of holes in the valance band or the material is rich in acceptor atoms due to presence of group III impurity. Donor type of semiconductors is known as n-type semiconductors, where others are p-type semiconductors.

2.5. Electromagnetic Wave Absorbing Materials

In today's technology, there is a growing interest in EMI shielding and absorbing materials with the rapid growth in the field of advanced electronic devices. Many commercial and military applications such as data transmission, telecommunication, wireless network systems and satellite broadcasting as well as radars, diagnostic and detection systems utilize and emit EM waves. Interaction of EM waves originating from different sources leads to decrease in quality and misinterpretation of the transferred data. Therefore, it becomes vital to avoid

resulting interference and EM wave pollution by the use of appropriate shielding and absorbing materials.

EM shields confine EM energy within the bounds of a specific region and/or prevent the proliferation of such energy into designated locale [4]. EMI shielding is based on three basic mechanisms: absorption, reflection and multiple reflection [6, 7]. Shielding by reflection loss is based on reflecting EM energy back to its source with minimum transmission through the shielded region. Multiple reflection mechanism refers to the reflections at various interfaces in the shield due to inhomogeneity within the material. Typical metals like copper and aluminum which possess high conductivity and high dielectric constant reveal high EMI shielding efficiency; nevertheless, high weight, and low corrosion and wear resistance limit their usage in shielding applications [8-10]. Electrically conductive polymers such as polyaniline, polypyrrole eliminate the drawbacks of metals [10-12]; however, they are not common and have poor mechanical properties. Shielding by absorption is complied by the usage EM wave absorber materials.

In both EMI shielding and EM wave absorption applications, various EM wave absorbing materials are being used. These materials absorb and dissipate EM energy to which they are exposed so that the reflected and/or scattered EM component is significantly small [4]. Any sort of material that exhibits ohmic, dielectric polarization and/or magnetic polarization loss can be utilized as EM wave absorbing materials. These materials can be in the form of monolithic, composite, fluid, gel, colloid sol or slurry [4].

2.5.1. Requirements of Electromagnetic Wave Absorbing Materials

The fundamental requirements and properties of EM wave absorbers are defined according to following considerations [3, 4, 13, 14]:

- Extent of absorption: Maximum absorption of EM wave.
- Frequency of operation: Whether the absorber is intended for resonance absorption (at a single, multiple or discrete frequency) or for broadband applications.

- High mechanical properties: Mechanical stability against aging and physical or chemical degradation due to the continual exposure to EM radiation.
- Capability to operate over wide limits of temperatures: Environmentally durable.
- Easily applied: Feasibility aspects of molding or forming into required shapes and sizes.
- Inexpensive: Cost-effective.
- Minimum thickness and weight.

2.5.2. Application Areas of Electromagnetic Wave Absorbers

Basic application areas of EM wave absorbers are summarized below:

- Radar Cross Section (RCS) Reduction: Radar cross section is a measure of power scattered in a given direction when a target is illuminated by an incident wave [3]. Minimizing RCS of an aircraft or warship is essential to reduce the detectability of the vehicles. Two basic methods are used to reduce RCS [15, 16]. First one is shape optimization of the body so that incident EM wave can be scattered yielding minimum reflective wave. Researches on shaping of the target show that RCS reduction is achieved only in a limited angular region and is effective only at high frequencies, which frequently conflicts with structural and aerodynamic requirements in designing the aerospace vehicles. [16, 17]. As a result of this, the second method, usage of radar absorbing material, is preferred to make the vehicle transparent or absorptive to the incident EM energy.
- EMI reducers: EM wave absorbers prevent EMI and improve the performance of the electronic systems.
- Antenna applications: EM wave absorbers remove unwanted reflections, reduce side lobes [4] and enhance system performance of the antennas.
- Protective screen: Microwave absorbers used as shielding screens in test environments where powerful radars may cause nonionizing radiation hazards to nearby personnel.
- Bioelectromagnetic phantoms: EM wave absorber is synthesized to exhibit characteristic complex permittivity and permeability values which imitate

biological substances like tissue or bone [18]. These materials are called as bioelectromagnetic phantoms which are used in evaluating the interaction between EM energy and biological media.

2.5.3. Classification of Electromagnetic Wave Absorbers

The absorption of microwaves by a material depends on the properties of the material and its structure. One technique used to produce low reflectivity is to match the impedance of the EM radiation at the air-absorber interface allowing the EM radiation to propagate into the absorber. Another technique used is to create destructive interference between the EM waves reflecting from different layers of the absorber. The second class of absorbers is called resonant absorbers.

2.5.3.1. Resonant Absorbers

The Dallenbach layer (Figure 2.8) is a resonant absorber which uses the bulk of material for absorption. This layer consists of a homogeneously lossy layer backed with a metal plate. The reflection from outer surface cancels the reflection from the back surface. Therefore, if a material can be found whose impedance relative to free-space equals 1 meaning $\mu_r=\varepsilon_r$ there will be no reflection at the surface. In this case the overall attenuation will depend on the loss properties of the materials (ε_r", μ_r") and the electrical thickness. Dallenbach layers specifically contain magnetic materials or a combination of conductive and magnetic materials.

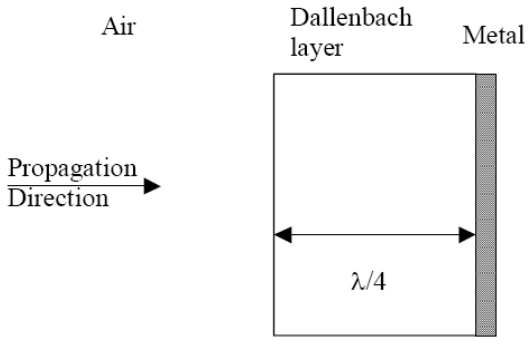

Figure 2.8 Dallenbach layer [19].

The Salisbury Screen is the simplest layered resonant absorber which consists of a resistive sheet placed an odd multiple of 1/4 wavelengths in front of a metal (conductive) backing separated by an air gap (Figure 2.9). A low dielectric material such as foam is often used to replace the air gap reducing the gap thickness at the expense of bandwidth. The quarter wavelength transmission line transforms the short circuit at the metal into an open circuit at the resistive sheet [19]. The effective impedance of the structure is the sheet resistance. If the sheet resistance is 377 ohms/m^2 (the impedance of air), then good impedance matching occurs and a reflective null appears at the frequency corresponding to the spacer thickness.

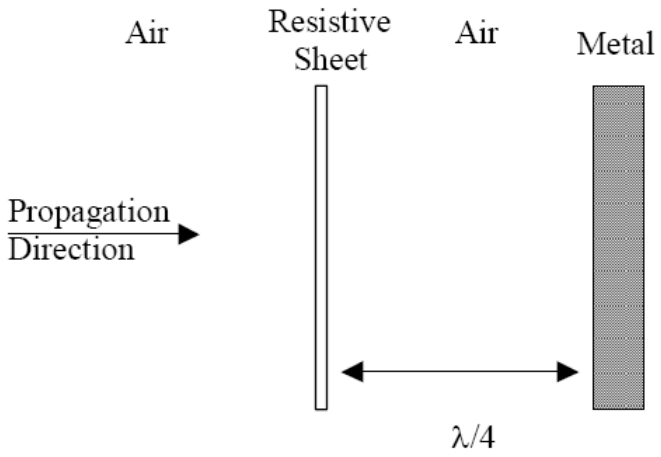

Figure 2.9 Salisbury screen [19].

Jaumann layers are used to increase the bandwidth of the Salisbury screen. The number of layers is proportional to the bandwidth of the absorber. For instance, a device consisting of two equally spaced resistive sheets in front of a conducting plane (Figure 2.10) produce two minima in the reflectivity, and hence increase the absorber's bandwidth over the Salisbury screen [20].

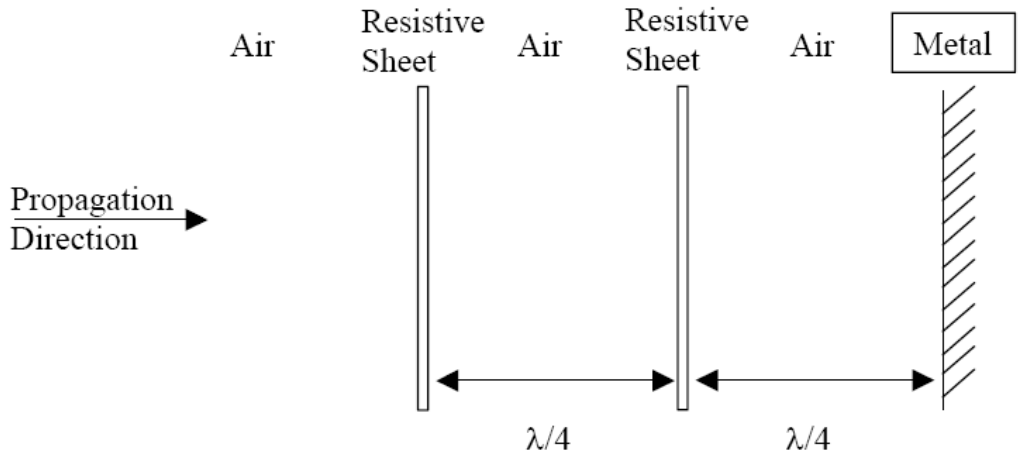

Figure 2.10 Jaumann layers [19].

An EM wave absorber which is based on the complete dissipation of the EM energy rather than suppressing reflection can be classified into two groups according to the absorbing principle: the absorbers using magnetic loss (large imaginary part of permeability) known as magnetic absorbers and the ones which use dielectric loss (large imaginary part of permittivity) known as dielectric absorbers.

2.5.3.2. Magnetic and Dielectric Materials for Electromagnetic Wave Absorbers

Losses of magnetic absorbers are dependent upon the applied magnetic field. Magnetic metal alloys such as Permalloy have very high permebilities; however due to low skin depth the conductor attributes dominate above a few Hertz [4]. As a result of this, non-conducting magnetic materials are generally used for EM wave absorption applications like ferrites [21-24]. Various magnetic lossy materials like carbonyl iron, cobalt etc. dispersed in polymers are also used as magnetic absorbers [22, 25-27]. Existence of resonance frequencies in the MHz range and heavy weight are the main drawbacks of these materials [17, 28]. In high frequency ranges, the weakness of magnetic materials can be compensated by improving their molecular

composition and compounding with other materials, yet a critical weakness of being heavy still remains [22, 24].

On the other hand, lossy dielectric materials attract attention with their low density and effectiveness in GHz frequency range. Since maximum electric fields occur away from conductors, conductor backing is not important for dielectric absorbers. Generally, thick layers are utilized. The absorption requirement is that internal wave impedance should be nearly that of free space [4]. Since relative permeability of dielectric absorber is one, relative permittivity should be as close to one as possible. Composites with conductive powders such as carbon black and graphite [10, 17, 29-31] as well as continuous or discontinuous conducting fillers [32-34] such as stainless steel and nickel-coated carbon fibers are used as dielectric absorbers which generate dielectric loss by improving electrical conductivity of the mixture.

2.6. Measurements Techniques Used for the Characterization of Electromagnetic Wave Absorbing Materials

This section presents a review of various measurement techniques which are used to characterize the interaction of materials with EM waves. The choice of the measurement system depends on various factors such as material under consideration, cost and flexibility of the system, frequency of interest, accuracy required, shape of the sample, physical modification of the sample etc. [3, 35].

Characterization techniques can be investigated in three main groups as reflection techniques, transmission/reflection techniques and resonance techniques. For reflection techniques sample should be backed with a metal plate, and only reflection coefficient is recorded [36, 37] whereas the transmission/reflection techniques measure both transmission and reflection coefficients [38].

Resonance techniques normally consist of a slab of a dielectric material introduced into a resonator. Dielectric properties of the material are obtained from the resonance frequency and the width of the resonance peak [39, 40]. Relative loss

and the resonant frequency of the cavity with and without a test sample are used to determine the intrinsic properties of test material.

Reflection and transmission/reflection techniques are the broadband techniques, whereas resonance techniques only provide the information near the resonance frequency. Therefore, resonance techniques are not suitable for characterization of materials which possess a large variation of the permittivity over frequency [35].

Transmission/reflection techniques are inaccurate in measuring the loss tangent of low-loss materials (loss tangent< 0.005) and medium-loss materials (loss tangent between 0.005-0.1) [38]. Reflection techniques are suitable for high-loss and medium-loss materials, but it is not accurate for low-loss materials [37]. Resonance techniques are usually very sensitive, which makes them good for measuring low-loss materials and medium-loss materials with loss tangents up to about 0.05 [39].

Transmission/reflection techniques allow the measurement of any type of material including magnetic and anisotropic materials [35]. Two basic and widely applied transmission/reflection techniques are introduced in the following sections.

2.6.1. Transmission Line

Bulk materials are characterized by their relative permeabilities and permittivities, whereas thin sheets are generally characterized by their complex impedances. Properties of bulk materials are most accurately measured in small fixtures which are short sections of transmission lines. These fixtures minimize the escape of energy from the system and reduce the risk of energy losses which might be attributed to nonexistent losses within the test sample.

A well-machined test sample is placed in a sample holder which is a short section of transmission line. The reflected energy from the sample or the transmitted energy through it or both are measured. According to application theory of transmission line, sample holder should be uniform which means that the transverse dimensions of the line and the test sample as well as its properties do not vary along the length of the line. The uniformity requirement in material properties restricts the types of materials which can accurately be measured.

During the measurement a signal is launched in the line and the signal at the far end is measured. The signal is assumed to be monochromatic and characterized by propagation factor, γ, which is complex in general. When there are no ohmic losses in the line, γ describes the shift in the phase of the signal as it travels along the line (in the absence of loss there is no change in the amplitude). If there are energy losses in the line due to either the finite conductivity of the conductors of the line or losses in the material filling it, decay in amplitude as well as shift in phase is observed [3].

2.6.1.1. Transverse Electromagnetic (TEM) Lines and Waveguides

TEM lines and rectangular waveguides are two kinds of transmission line which are used for evaluation of bulk EM properties. Inside the TEM line the electric and magnetic fields are both transverse to the axis of the line. On the other hand, the fields in waveguides (hollow conducting pipes) have components along the direction of propagation as well as transverse to it. The existence of these longitudinal waves together with transversal fields can be thought of or two plane waves alternatively bouncing off the top and bottom plates. This is due to the fact that the waveguide has only one conducting boundary. As a result of this, at least two waves must exist to enforce the boundary condition that the tangential electric field vanishes at the conducting walls of the guide. According to this when the frequency drops below well-defined cut-off values, the wave pair can no longer satisfy the boundary conditions and propagation ends.

A consequence of cut-off phenomenon is that if the frequency is high enough, waveguide may support more than one mode of propagation. The method ordinarily used to prevent higher order mode propagation is to choose the transverse waveguide dimensions so that only the dominant (lowest order) mode can exist over the investigated range of operating frequencies.

Waveguide propagation modes are grouped according to the direction of propagation known as transverse electric (TE) where there is no component of electric field and transverse magnetic (TM) modes where there is no component of magnetic field along the axis of the waveguide.

2.6.1.1.1 Sample Holders

Frequencies and physical sizes of any inhomogeneities that may be present in the test sample is effective in choosing TEM or waveguide systems for the evaluation of material properties. The coaxial line (a TEM transmission line) is more convenient to use than the rectangular waveguide if the frequencies of interest cover more than an octave. This is because waves propagating in the coaxial line do not suffer the cut-off phenomenon. Higher order modes in coaxial lines may be prevented by making the sample holder small enough. Smaller holder necessitates smaller test samples, as a result of this, cost of the system increases. Small, undetected inhomogeneitites in the sample can have a greater effect on the accuracy of the test data in smaller lines and samples compared to the larger ones. The samples should be well fabricated to fit within the sample holder and to make a good contact with all conducting surfaces. This situation complicates the design of the sample holder.

2.6.1.1.2 Open- and Short-Circuit Measurements

Major elements of the systems are a signal source, a slotted section of waveguide or transmission line, the sample holder, a sliding short circuit and a signal detector. The standing wave in the line is the sum of two waves traveling in opposite directions. Measurement of voltage standing wave ratio (VSWR) is sufficient to determine the strength of the backward traveling wave compared to that of the incident wave. This characterizes the amplitude of reflection from the test sample. A precision short circuit (a carefully machined metal plug) is used to determine the phase of reflection. It is inserted in the sample holder so that the position of the front face of the plug matches that of the sample. The nulls are sharp and deep for the short-circuited condition, and their positions establish the reference plane for measurements of the test specimen. Amplitude is determined by the comparison of the two VSWR readings, and phase is determined by the distance which the nulls shift toward or away from the generator. If the sample is thin, an open circuit is used to maximize the electric field on the sample. Open circuit

condition can be created at the rear face of the sample by positioning the shorting plunger $\lambda_0/4$ behind the sample [3].

2.6.2. Free-Space Measurement Systems

EM properties of thin sheets are not readily measured in transmission lines, since it is difficult to install them in the sample holders. Due to the variations in the EM properties of the final product from one point to another, and because the final product is much thicker than any of its component parts, transmission line measurements cannot be used. In free-space methods test samples are not enclosed by the conductors like those in transmission-line sample holder.

Free space systems are composed of a pair of horn antennas (transmitting and receiving), a specimen holder and network analyzer. Network analyzer is the basic tool of all measurement techniques which provides test data for dozens of frequencies with a great convenience in relatively short time. As the measurement frequency increases, losses inside many transmission media of the measurement system increase, and phase measurements become inaccurate. Horn lens antennas which have far-field focusing ability make it possible to measure the EM properties accurately with free-space method at microwave frequencies (300 MHz–300 GHz) [37, 38].

At the point of measurement, antennas are connected to the two ports of an S-parameter test set by using circular-to-rectangular waveguide adapters, rectangular waveguide to coaxial line adapters and precision coaxial cables. S-parameter measurements in free space are performed with a network analyzer and a computer is used for automation, data acquisition, printing and plotting. Two antennas are separated by a distance equal to twice of the focal distance of the lenses. The horn lens antenna consists of two equal Plano-convex dielectric lenses mounted back to back in a conical horn antenna. Specimen holder is placed at the common focal plane and is mounted on a micrometer driven carriage.

The errors in free-space measurement are presumed to be due to the diffraction effects at the edge of the sample and multiple reflections between the horn lens antennas and the mode transitions. Diffraction effects at the edge of the sample are

minimized by using spot focusing horn antennas and errors due to multiple reflection are eliminated by free-space TRL (through, reflect, line) calibration technique. For the measurement, transmitting antenna sends the EM wave onto the specimen surface; the waves which transmit through the specimen and reflect its surface are collected by receiving and transmitting antennas, respectively. By this manner S-parameters of the material are determined.

When most widely used two techniques, waveguide and "free-space" system are compared, following conclusion can be drawn: Waveguides are known to be efficient at high frequencies. However, using waveguide technology requires high-precision machining of the sample under investigation. Positioning of the sample is also critical, especially at high frequency since the dimensions of the waveguide are small, making the alignment more difficult. All these issues lead to increased process cost. On the other hand "free-space" measurement is a contactless and non-destructive method. Sample preparation is relatively simpler compared to other methods. Large sized sample characterization can easily be done using this method, and high frequency broadband measurements are also possible. Possible diffraction at the edge of the samples and misalignment can cause errors in the measurement results and the method is inadequate in measuring loss tangents of low and medium loss materials. Detailed information about "free-space" measurement system and its calibration can be found in the "Experimental Procedure" chapter.

2.7. General Information about the Fibers Used in This Study

2.7.1. Silicon Carbide Fibers

Silicon carbide fibers have been produced since the mid-1960s by chemical vapor deposition onto a tungsten or carbon filament core. Their large filament diameters (100-140 μm) and the lack of flexibility limited their use as the reinforcement of metals such as aluminum, titanium and intermetallics. In the 1990s the application of ceramic composites at higher temperatures started to receive great demand. It became necessary to produce continuous SiC-based ceramic fibers with

excellent properties for the thermal stability of these ceramic composites. The development of fine silicon carbide fibers with diameters of 10 μm opened up the possibility of reinforcing ceramic materials to produce high-temperature structural composites [41].

Fine silicon carbide fibers are prepared by melt spinning, crosslinking and pyrolysis of an organosilicon polymer. General polymer pyrolysis fiber processing diagram is shown in Figure 2.11.

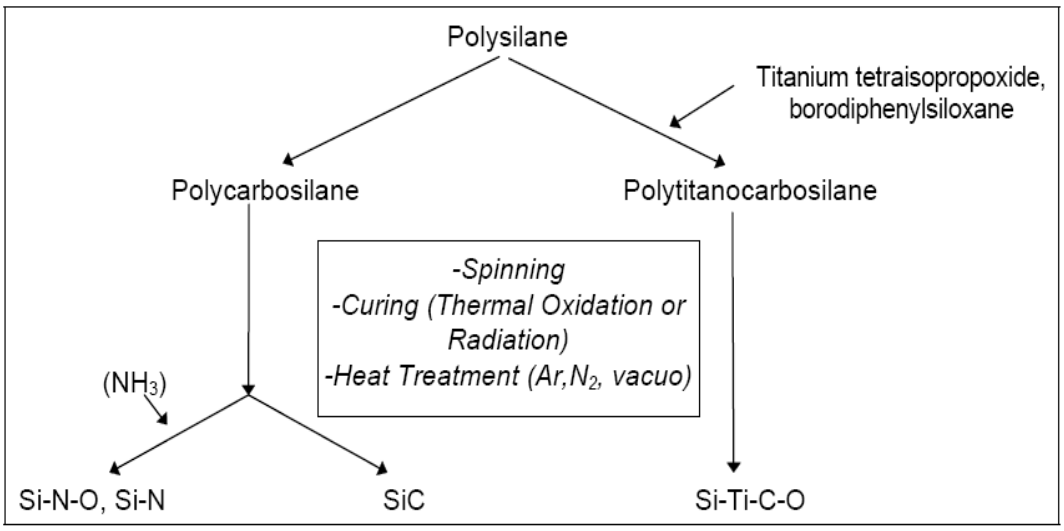

Figure 2.11 General polymer pyrolysis fiber processing diagram [42].

SiC-based ceramic fibers, through the conversion of polycarbosilane of an organosilicon polymer, were firstly developed by Yajima, and the fibers have been industrially produced as continuous fibers. The method of preparing ceramic materials via organic to inorganic conversion is called the polymer precursor method or Yajima's method [43]. Fibers primarily consist of fine SiC grains and several phases which considerably influence the characteristic behavior of the fibers. Physical properties of representative SiC-based fibers are shown in Table 2.1. Heat-

resistance of fibers improves when the microstructure converts from amorphous to polycrystalline which is schematically shown in Figure 2.12.

Table 2.1 Physical properties of representative SiC-based fibers [41].

: *Nearly stoichiometric SiC fiber*

	SiC Fibers							
	Nicalon			Tyranno				Sylramic
	NL-200	Hi-Nicalon	Hi-Nicalon–s	Lox M	ZMI	ZE	SA*	
Atomic Composition	$SiC_{1.34}O_{0.36}$	$SiC_{1.39}O_{0.01}$	$SiC_{1.05}$	$SiTi_{0.02}C_{1.37}O_{0.32}$	$SiZr_{<0.01}C_{1.44}O_{0.24}$	$SiZr_{<0.01}C_{1.52}O_{0.05}$	SiC $O,Al_{<0.008}$	$SiCTi_{0.02}B_{0.09}O_{0.02}$
Tensile Strength (GPa)	3.0	2.8	2.6	3.3	3.4	3.5	2.8	3.0
Tensile Modulu (GPa)	220	270	410	187	200	233	410	420
Elongation (%)	1.4	1.0	0.6	1.8	1.7	1.5	0.7	0.7
Density ($g \cdot cm^{-3}$)	2.55	2.74	3.10	2.48	2.48	2.55	3.02	>3.1
Diameter (μm)	14	14	12	8 & 11	8 & 11	11	8 & 10	10
Specific Resistivity ($\Omega \cdot cm$)	10^3-10^4	1.4	0.1	30	2.0	0.3	—	—
Thermal Expansion coeff. (10^{-6}/K)	3.2 (25-500℃)	3.5 (25-500℃)	—	3.1	4.0	—	4.5 (20-1320℃)	—
Thermal Conductivity (W/mK)	2.97(25℃) 2.20(500℃)	7.77(25℃) 10.1(500℃)	18.4 (25°C) 16.3 (500°C)	—	2.52	—	64.6	40·45

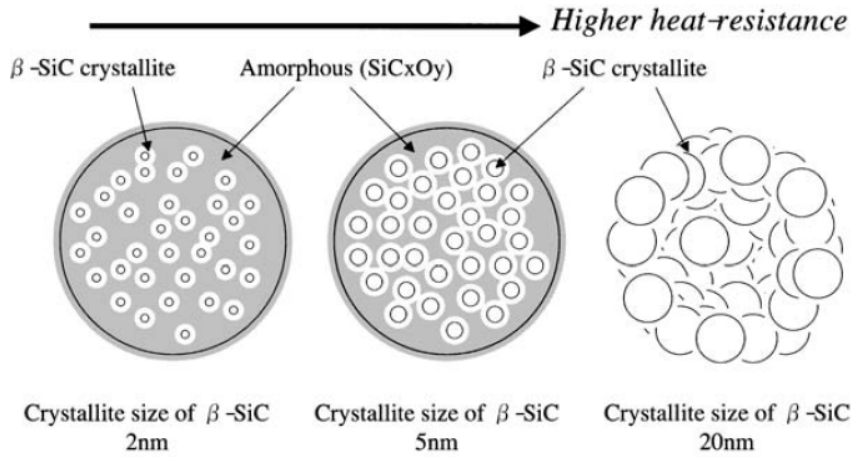

Figure 2.12 Microstructures of some SiC-based fibers [41].

Si-C-O fibers are used as reinforcement fibers for refractory matrix composites, glass-ceramic matrix composites, SiC matrix composites and high-temperature materials such as diesel particulate filters [44, 45].

The Si-C-O fiber produced from polycarbosilane by the thermal oxidation curing method is amorphous and has a high oxygen content along with excess carbon [46]. These fibers are a mixture of β-SiC nanocrystals, free carbon and an amorphous silicon oxycarbide (SiC_xO_y) [47-50].

Up to around 1573 K there exists no modification in the intergranular phase (SiC_xO_y) as a result of this, SiC grain size stays roughly unchanged [51]. When fibers are heat-treated at higher temperatures, amorphous (SiC_xO_y) phase in the fibers crystallizes to β-SiC where the evolution of SiO and CO gases occur [52-56]. The SiO gas reacts with the free carbon and produces SiC and CO. As a consequence, SiC grain size increases. The fibers show severe degradation in tensile strength as a result of the structural destruction caused by the release of these gases and the growth of SiC grains [49, 50].

A reduction in oxygen content is effective in improving the thermal stability at high temperatures. A radiation curing method using an electron beam has been developed in order to synthesize SiC-based ceramic fibers with low oxygen content [17-18]. Such fibers reveal lower oxygen and excess carbon contents. SiC-based ceramic fibers are classified according to heat resistance range where Si-C-O and Si-Ti-C-O fibers are effective below 1500 K, while Si-C and Si-Zr-C-O [57] fibers are effective in the temperature range between 1500-1800 K [58].

Although structural properties of SiC-based fibers and their corresponding woven fabrics are known such as their modulus, strength, oxidation behavior under different atmospheric conditions and temperatures, there exists very limited knowledge about their interaction with EM waves [59, 60].

2.7.2. Alumina Fibers

Synthetic oxide fibers except for glass fibers were first produced in the early 1970s. These fibers are known to be the most widely used filamentary reinforcement for light alloys. Following the production of small-diameter

continuous alpha-alumina fibers, these fibers began to be incorporated into metal matrix composites. The composites which are produced using these fibers show great improvements in stiffness and creep resistance when compared to the unreinforced ones; however, their high cost and brittleness limit their usage [41, 61]. Physical properties of some representative α-alumina fibers are shown in Table 2.2.

Table 2.2 Properties and compositions of some widely used commercial α-alumina based fibers [61].

Fiber Type	**Trade Mark**	**Composition (wt. %)**	**Diameter (μm)**	**Density (g/cm^3)**	**Strength (GPa)**	**Strain to failure (%)**	**Young's modulus (GPa)**
α-Al_2O_3	FP	99.9 Al_2O_3	20	3.92	1.2	0.29	414
	Almax	99.9 Al_2O_3	10	3.6	1.02	0.3	344
	610	99 Al_2O_3 0.3 SiO_2 0.7 Fe_2O_3	10-12	3.75	2.6	0.7	370

α-alumina fiber which is used in this study (Almax®) was produced first in the early 1990s by Mitsui Mining [62]. It is composed of almost pure α-alumina and has a diameter of 10 μm. The fiber has a low density of 3.60 g/cm^3. The Almax fiber consists of grains around 0.5 μm in size; however, the fiber exhibits a large amount of intragranular porosity [63]. This indicates rapid grain growth of α-alumina grains during the fiber fabrication process without elimination of porosity and internal stresses. The fiber exhibits linear elastic behavior at room temperature in tension and brittle failure. This fiber is seen to be chemically stable at high temperatures in air; however its isotropic fine grained microstructure led to easy grain sliding and creep limiting its application as reinforcement for ceramic structures.

High creep resistance implies to the production of almost pure α-alumina fibers, yet obtaining a fine and dense microstructure is quite challenging. Control of grain growth and porosity in the production of α-alumina fibers is obtained by using a slurry consisting of α-alumina particles in an aqueous solution of aluminum salts. These alumina particles act as seeds to lower the formation temperature and rate of α-alumina grains growth. The precursor filament, which is produced by dry spinning, is pyrolysed to result in α-alumina fiber. Flowchart of alumina fiber synthesis is presented in Figure 2.13.

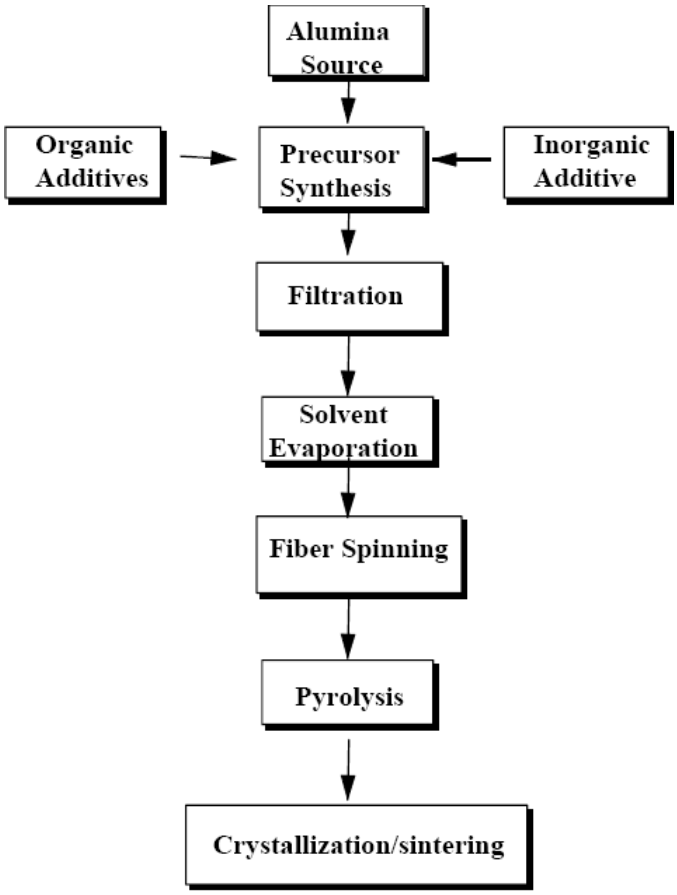

Figure 2.13 Flowchart of alumina fiber synthesis [42].

CHAPTER 3

EXPERIMENTAL PROCEDURE

3.1. Materials and Treatments

The materials used in the present study were SiC-based (Tyranno®, Ube Industries, Co., Ltd., Yamaguchi, Japan) and alumina (Almax®, Mitsui Mining Co., Ltd., Koumachi, Japan) woven fabrics with plain and satin woven types. Even though SiC-based woven fabrics possessed both varieties in chemical composition and in woven type, only woven type was variable in alumina woven fabrics. SiC-based woven fabrics are typically used as reinforcements for high temperature structural ceramic composites due to their high temperature stability and strength with lower creep and grain-growth rate [41, 51, 53]. On the other hand, alumina woven fabrics have major commercial uses in high temperature thermal insulation applications requiring flexible, lightweight and oxidation resistant continuous fibers [41, 42, 61]. Intrinsic properties of both SiC-based and alumina woven fabrics such as their specific modulus and strength, low density and environmental durability related to their structural use are evident [42, 64]. However, there exists very limited knowledge about interaction of EM radiation with SiC-based woven fabrics [59, 60] and according to the best of our knowledge, there is no study available about interaction of EM wave with alumina woven fabrics. The desired property set of lightweight, high environmental durability, low thickness of ceramic woven fabrics and additionally wide electrical resistivity range, 10^{-3} to 10^{4} Ωm [65] of SiC-based woven fabrics draw attention to these materials for EM wave absorbing applications.

Table 3.1 lists basic properties of three different types of SiC-based (S8, PN and ZE8) and two different types of alumina (PA and SA) woven fabrics used in this study as provided by their manufacturers [61, 65]. S8 and PN type woven fabrics show similar chemical compositions (Si, Ti and C content) except that PN possess a carbon-rich layer at its surface. Moreover, their woven types are different; S8 is a satin woven where PN is plain. On the other hand, another satin woven ZE8 reveals higher carbon and silicon content than others; furthermore, it contains zirconium in place of titanium which exists in PN and S8 type woven fabrics. Chemical compositions of alumina woven fabrics (PA and SA) are identical which is almost pure α-alumina. However, their woven types are different; PA is plain woven while SA is satin. Moreover, they have relatively higher densities compared to SiC-based woven fabrics.

Table 3.1 Properties of fibers used in this study.

Code of Woven Fabric	**S8**	**PN (C-coated)**	**ZE8**	**SA**	**PA**
Chemical Composition (wt %)	Si: 50 C: 30 O: 18 Ti: 2	Si: 50 C: 30 O: 18 Ti: 2	Si: 59 C: 38 O: 2 Zr: 1	Al:53 O:47	Al:53 O:47
Woven Type	Satin	Plain	Satin	Satin	Plain
Fiber Diameter (μm)	8.5	8.5	13	10	10
Number of Fibers per Bundle	1600	1600	400	1000	1000
Density (g/cm^3)	2.35	2.39	2.55	3.60	3.60

Used ceramic woven fabrics exhibit 0°/90° bundle orientation, and there are also variations in the woven types, where S8, ZE8 and SA fabrics are satin woven type while PN and PA fabrics are plain woven. Figure 3.1 shows schematic description of the satin and plain woven fabrics.

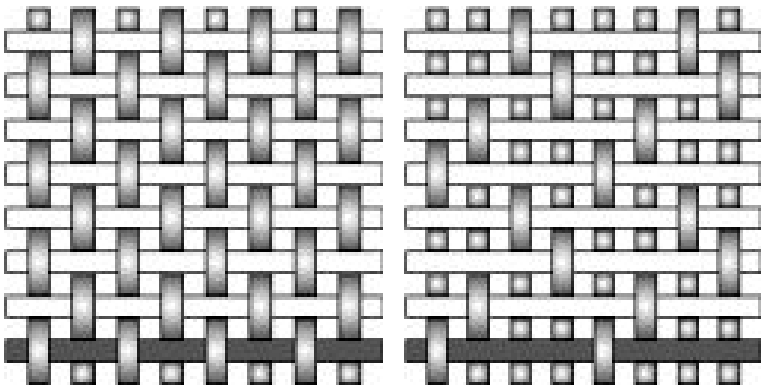

Figure 3.1 Schematic description of (a) plain and (b) satin woven fabrics.

In plain woven fabric 0° fiber bundles pass under and over of each 90° fiber bundle. Because of this structure PN and PA woven fabrics reveal a high level of fiber crimp and possess high symmetry. On the contrary, a harness number exists in satin woven fabrics, which designates the total number of fiber bundles crossed and passed under, before the pattern is repeated. For S8 and ZE8 woven fabrics, the hardness number 8 is added to the designation of the woven fabrics where this number is 5 for SA. S8, ZE8 and SA woven fabrics reveal high degree of surface flatness along with low fiber crimp, and they are relatively tighter compared to PN and PA woven fabrics.

To investigate the EM wave absorption potential of ceramic woven fabrics, 60 x 60 mm square shaped woven fabrics were cut from the as-received woven yarn clothes. In addition to as-received woven fabrics, modified woven fabrics were also tested to determine their EM wave absorption potential. SiC-based woven fabrics were heat-treated in air at 1573 K for 3 hours, and alumina woven fabrics were gold-sputtered. Heat-treatment cycle for SiC-based woven fabrics is schematically shown in Figure 3.2. The aim of this heat-treatment was to modify electrical conductivities of SiC-based woven fabrics and to investigate the effect of heat-treatment on their EM wave absorption potential.

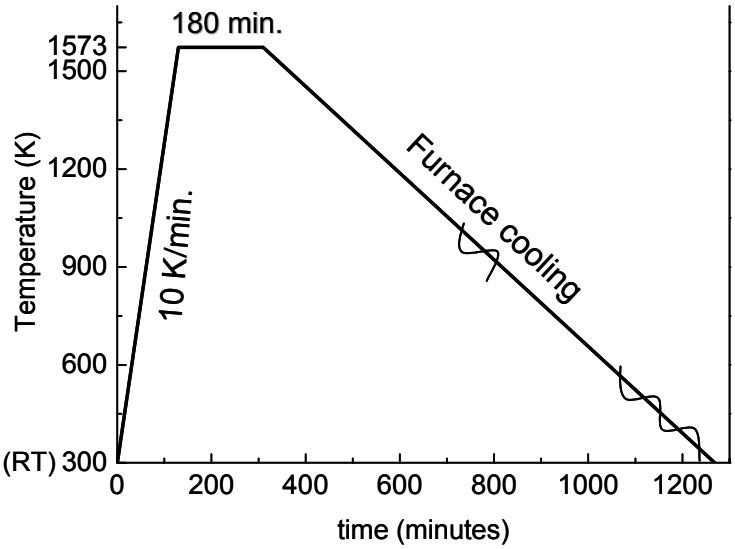

Figure 3.2 Applied heat-treatment cycle.

Surfaces of alumina woven fabrics were coated with gold layer using a standard sputter-coater. 60 x 60 mm square shaped alumina woven fabrics were placed in the chamber of the equipment which operates under vacuum. Applied electric field caused removal of an electron from the argon used as the sputtering gas, making its atoms positively charged. Argon ions were attracted to the negatively charged gold foil, and they knocked out gold atoms from the surface of the gold foil. These gold atoms fell and settled onto the surface of the alumina woven fabric producing a thin gold layer. By this manner, a high conductivity layer was produced on insulating alumina woven fabrics, and effect of this surface modification on the EM wave absorption potential was investigated.

3.2. Characterization of Material Properties

Crystal structures of as-received and modified (either heat-treated or gold-sputtered) SiC-based and alumina woven fabrics were examined using X-ray diffraction (XRD). For crystal structure determination, woven fabrics were fastened

on glass substrates from their edges with the use of double-sided tapes. XRD was performed on an X-ray diffractometer (RINT 2200, Rigaku Corporation, Tokyo, Japan) with Cu Kα radiation in the 2θ range from 20° to 90° with steps of 0.02°.

Microstructural analyses were carried out using scanning electron microscope (SEM) (JSM-6400, Jeol Ltd., Tokyo). Bundles were extracted from the as-received woven fabrics, and then heat-treatment was applied to SiC-based bundles. Tips of the bundles were chopped to create fresh surfaces. Both as-received and heat-treated SiC-based bundles were attached on copper fiber holder with the help of double-sided tape followed by gold coating to eliminate electron charging during examination under SEM. Similar to SiC-based bundles, microstructural analyses of gold-sputtered alumina bundles were performed using SEM.

Following crystal structure determination and microstructural analyses, electrical conductivities of the SiC-based fibers were determined. For this purpose, direct current resistivities of as-received bundles were measured with the help of a DC voltage source. Firstly, bundles were taken from as-received woven fabrics, and both ends were silver-pasted to improve electrical contact. Next, ends of the fiber bundles were connected to a constant voltage source which provided a voltage of magnitude V. The magnitude of the current, I, was recorded at different voltage values for each type of as-received bundle. Average resistances, R, were determined by Ohm's law using Eq. (8) and linear change of measured values with voltage confirmed ohmic contact.

$$V = I * R \tag{8}$$

Resistivities of the bundles, ρ, were calculated using Eq. (9), where l and A are the length and cross-sectional area of a bundle, respectively. Cross sectional areas of the bundles were found out assuming that S8 and PN bundles contain 1600, where ZE8 bundle contains 400 fibers per bundle with known diameters.

$$R = \rho \frac{l}{A} \tag{9}$$

Electrical conductivities, σ, of fibers were determined by taking the reciprocal of resistivities. (Eq. (10)).

$$\sigma = \frac{1}{\rho} \tag{10}$$

To determine the electrical conductivities of heat-treated SiC-based fibers, several bundles were extracted from the woven fabrics, and these bundles were placed on alumina substrates where they were heat-treated in air at 1573 K for 3 hours. Following the heat-treatment both ends of the bundles were chopped to create fresh surfaces, prior to the silver pasting. Prepared bundles are demonstrated in Figure 3.3.

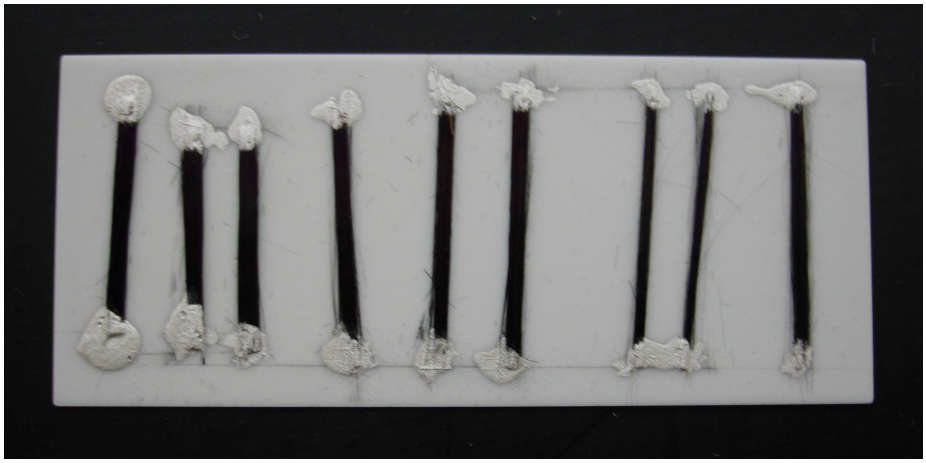

Figure 3.3 Bundle preparation step for electrical conductivity measurement.

Average resistances, R, were measured for each type of heat-treated bundles, and electrical conductivities, σ, of heat-treated fibers were determined by repeating the pre-described procedure.

3.3. Electromagnetic Transmission and Reflection Measurements by Free-Space Method

Reflection loss and transmission loss of ceramic woven fabrics were determined in 17-40 GHz frequency range by free-space method. This measurement technique was preferred over conventional contact type methods as measurement accuracy does not strongly depend on the machining precision of specimens. In addition to this, accurate measurement of EM properties of anisotropic and inhomogeneous media such as ceramics as well as composites can be performed using free-space method without the excitation of higher order modes, which is seldom possible in conventional methods. Furthermore, during the application of the free-space method the measurement is carried out in a nondestructive and contactless manner [15]. The free-space measurement system used in this study is schematically illustrated in Figure 3.4.

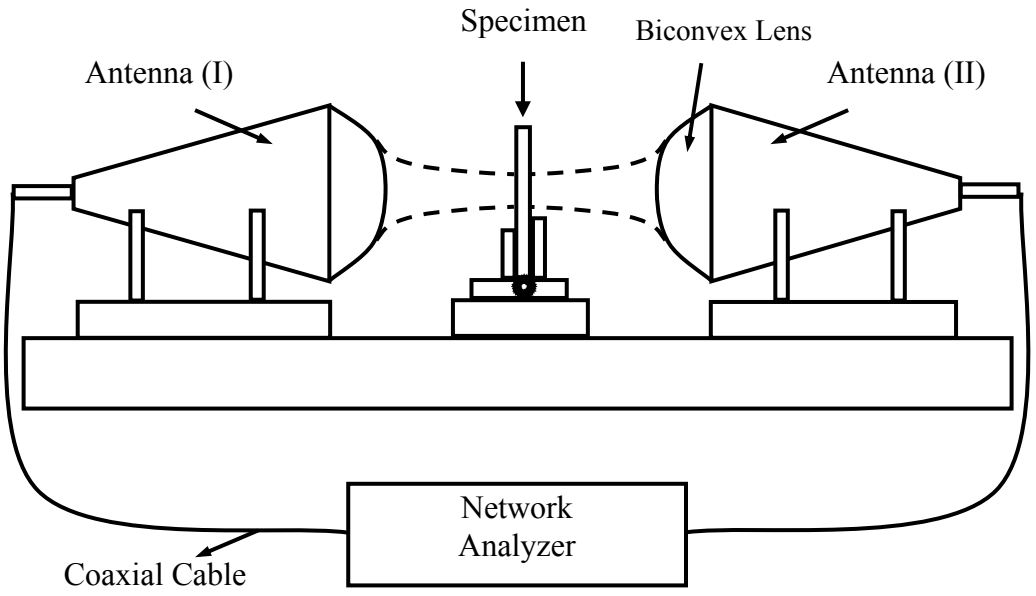

Figure 3.4 Schematic of the free-space measurement system used in this study.

Free-space measurement system was composed of a pair of spot-focusing type horn antennas (transmitting and receiving), a specimen holder and a coaxial cable connected to a HP8722D type network analyzer. Horn antennas were equipped with biconvex polymeric lenses focusing EM waves to the specimen surface with a spot size ~2-3 times wavelength that of the wave under consideration.

Previous to reflection loss and transmission loss determination of ceramic woven fabrics, system was calibrated with TRL (through-reflect-line) calibration [38] in order to minimize measurement inaccuracies. A through standard was configured by keeping the distance between the two antennas equal to twice of the focal distance of the lenses, where no object was present between the antennas during this calibration step. The reflect standards for Antenna I and Antenna II were obtained by placing a metal plate at the focal planes of transmitting and receiving antennas, respectively. The line standard was achieved by separating the focal planes of transmitting and receiving antennas by a distance equal to the quarter of the wavelength at the center of the band under consideration. Time-domain gating was used to minimize the effects of residual mismatches such as source and load impedance mismatch [38] after completion of TRL calibration.

Following the minimization of possible errors in the free-space system with TRL calibration and time-domain gating; woven fabrics, which were attached on square sectioned carton frames (shown in Figure 3.5 and Figure 3.6), were placed into the specimen holder at the center of the two spot-focusing horn antennas.

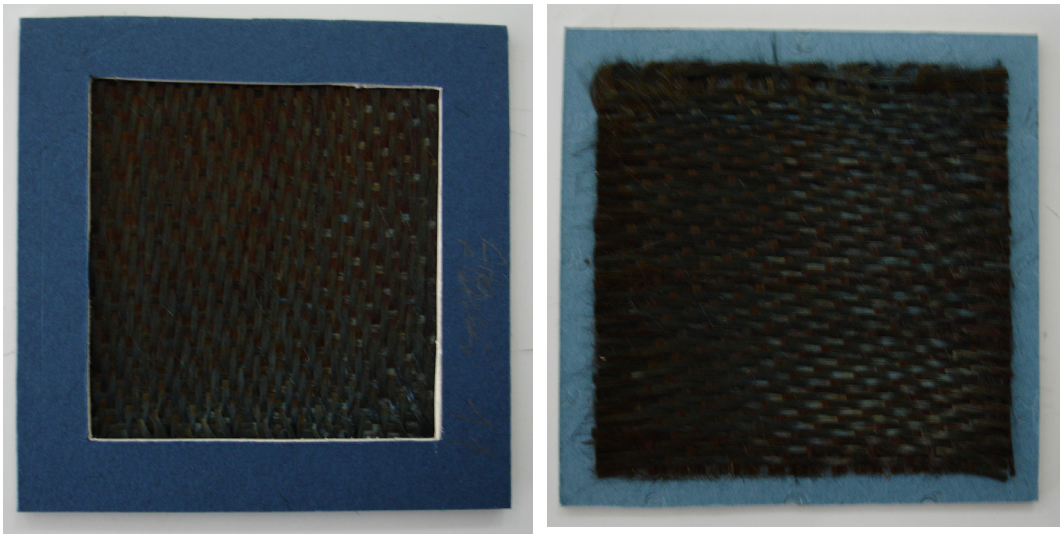

(a) (b)

Figure 3.5 (a) Front (b) back part of carton frames with attached SiC-based woven fabrics.

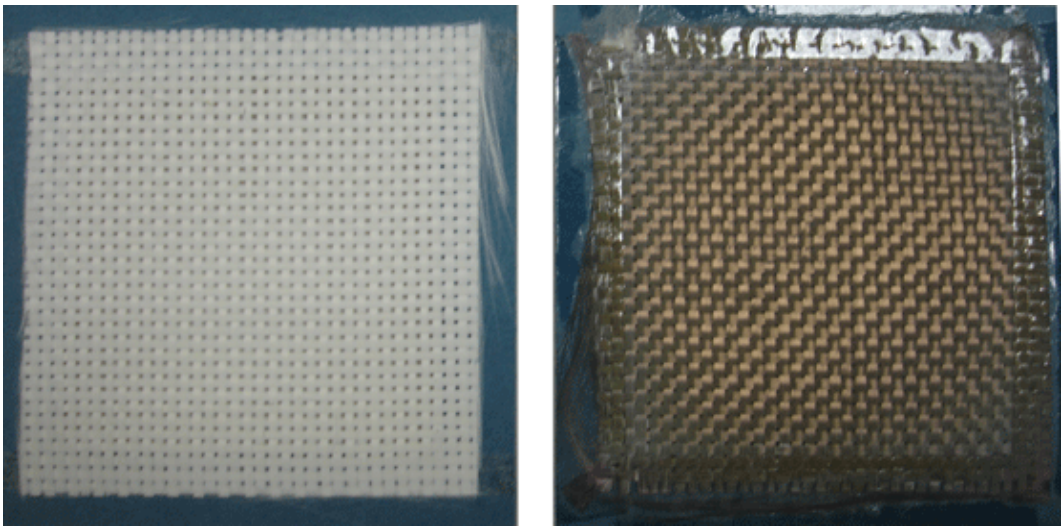

(a) (b)

Figure 3.6 (a) As-received (b) gold-sputtered plain alumina woven fabrics attached on carton frames.

During the measurements, antennas were separated by a distance which was twice of the focal length (330 mm) of the lenses. Horn antenna (I) sent the EM wave onto the specimen surface; the waves which transmitted through the specimen were collected by horn antenna (II), as a result of this S_{21} parameter (transmission loss) was obtained. On the other hand the waves which reflected from the specimen surface were collected by horn antenna (I) at this case S_{11} parameter (reflection loss) was determined. Reflected and transmitted portions of EM wave for single layer ceramic woven fabrics were obtained in the operational frequency range of spot-focusing horn lens antennas (17-40 GHz).

Parameters, which were used to quantify the interaction of EM waves with the woven fabrics, reflection loss, R_{dB} (S_{11}), and transmission loss, T_{dB} (S_{21}), were measured in 17-40 GHz frequency range. Fractions of reflected waves and transmitted waves were calculated using Eq. (11) where P_0, P_R and P_T show measured incident, reflected and transmitted wave powers, respectively.

$$R_{dB} = 10\log\left|\frac{P_R}{P_0}\right|;\ T_{dB} = 10\log\left|\frac{P_T}{P_0}\right| \tag{11}$$

Measurements were also carried out on various double layer combinations of as-received as well as modified (either heat-treated or gold-sputtered) woven fabrics. To construct these combinations; two carton frames with separate woven fabrics were placed at the specimen holder back to back. By this manner double layer combinations having 1 mm spacing (thickness of the carton) between the layers were obtained, and EM wave reflection and transmission losses of these combinations were examined by repeating the above-described procedure.

Firstly, combinations of SiC-based woven fabrics were performed. The first combination set which was made up of as-received SiC-based woven fabrics is given in Table 3.2. The notation (X─Y) used as the designation of the double layer combinations means that X is the first layer woven fabric on the transmitting antenna (I) side where EM wave pass (─) through the second layer woven fabric (Y) received by the receiving antenna (II).

Table 3.2 Double layer combinations of as-received SiC-based woven fabrics.

#	Combination	#	Combination	#	Combination
1	S8─S8	**4**	PN─S8	**7**	ZE8─S8
2	S8─PN	**5**	PN─PN	**8**	ZE8─PN
3	S8─ZE8	**6**	PN─ZE8	**9**	ZE8─ZE8

The second set of combinations of as-received and heat-treated PN (PN-H), S8 (S8-H) and ZE8 (ZE8-H) woven fabrics were performed following the first set. Table 3.3 summarizes the second set of combinations.

Table 3.3 Double layer combinations of as-received and heat-treated SiC-based woven fabrics.

#	Combination	#	Combination	#	Combination
1	S8─S8-H	**4**	PN─S8-H	**7**	ZE8─S8-H
2	S8─PN-H	**5**	PN─PN-H	**8**	ZE8─PN-H
3	S8─ZE8-H	**6**	PN─ZE8-H	**9**	ZE8─ZE8-H

As the last set EM wave interaction of double layer combinations of heat-treated woven fabrics were examined. The last set of combinations formed by heat-treated woven fabrics is given in Table 3.4.

Table 3.4 Double layer combinations of heat-treated SiC-based woven fabrics.

#	Combination	#	Combination	#	Combination
1	S8-H─S8-H	**4**	PN-H─S8-H	**7**	ZE8-H─S8-H
2	S8-H─PN-H	**5**	PN-H─PN-H	**8**	ZE8-H─PN-H
3	S8-H─ZE8-H	**6**	PN-H─ZE8-H	**9**	ZE8-H─ZE8-H

EM wave absorption potential of single layer and multilayer woven fabrics were calculated after determination of reflection and transmission losses. In terms of conservation of energy, the incident EM radiation energy is either reflected, transmitted or absorbed (dissipated and converted into heat) by a material which is schematically shown in Figure 3.7.

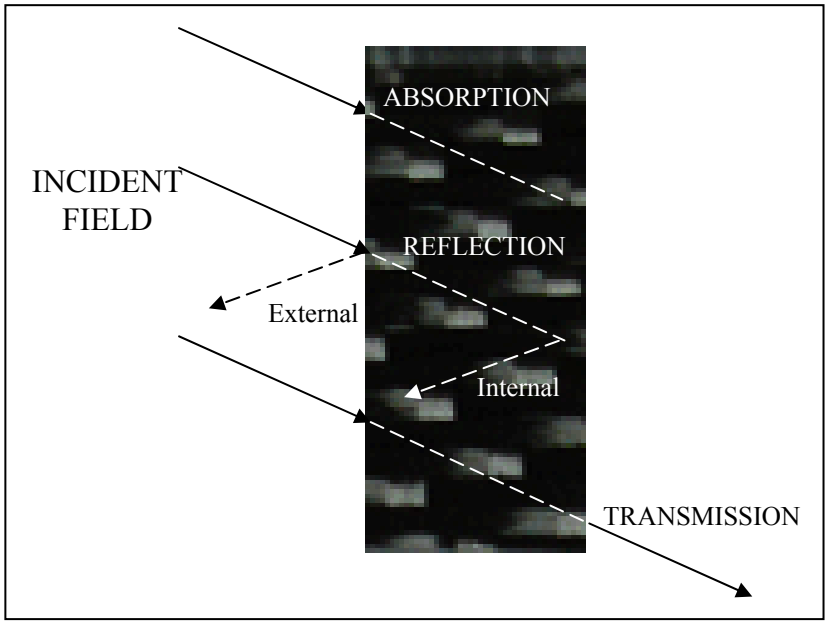

Figure 3.7 Incident wave and material interaction results.

Accordingly, absorption percentage of the woven fabrics and combinations were calculated using Eq. (12) where %R and %T represent reflected and transmitted portion of EM wave, respectively. %R (P_R / P_0) and %T (P_T / P_0) were determined using reflection and transmission losses given in Eq. (11).

$$\text{Absorption Percentage (\%)} = 100 - \%R - \%T \tag{12}$$

Subsequent to determination of reflection and transmission losses as well as absorption potentials of double layer combinations of SiC-based woven fabrics,

some other combinations of alumina and SiC-based woven fabrics were conducted to attain structures with different electrical conductivity layer sequences and to investigate the effect of this arrangement on the resulting EM wave interaction. Table 3.5 shows the first set of combinations composed of as-received woven fabrics.

Table 3.5 Double layer combinations of as-received woven fabrics.

#	Combination	#	Combination
1	PA─S8	**4**	SA─S8
2	PA─PN	**5**	SA─PN
3	PA─ZE8	**6**	SA─ZE8

The second set of combinations was performed with as-received alumina and heat-treated SiC-based woven fabrics to investigate the effect of using lower conductivity second layer on the EM wave absorption potential. This combination set is given in Table 3.6.

Table 3.6 Double layer combinations of as-received alumina and heat-treated SiC-based woven fabrics.

#	Combination	#	Combination
1	PA─S8-H	**4**	SA─S8-H
2	PA─PN-H	**5**	SA─PN-H
3	PA─ZE8-H	**6**	SA─ZE8-H

Combinations containing gold-sputtered alumina woven fabrics were conducted after determining EM wave interaction of combinations of as-received alumina woven fabrics. This set where surface modified alumina woven fabrics were used as

the first layer and as-received SiC-based woven fabrics as the second layer are shown in Table 3.7.

Table 3.7 Double layer combinations of gold-sputtered alumina and as-received SiC-based woven fabrics.

#	**Combination**	#	**Combination**
1	Gold-sputtered PA─S8	**4**	Gold-sputtered SA─S8
2	Gold-sputtered PA─PN	**5**	Gold-sputtered SA─PN
3	Gold-sputtered PA─ZE8	**6**	Gold-sputtered SA─ZE8

As the last set, EM wave interactions of double layer combinations completely composed of modified woven fabrics were examined. This set, which was formed by gold-sputtered alumina and heat-treated SiC-based woven fabrics, is given in Table 3.8.

Table 3.8 Double layer combinations of gold-sputtered alumina and heat-treated SiC-based woven fabrics.

#	**Combination**	#	**Combination**
1	Gold-sputtered PA─S8-H	**4**	Gold-sputtered SA─S8-H
2	Gold-sputtered PA─PN-H	**5**	Gold-sputtered SA─PN-H
3	Gold-sputtered PA─ZE8-H	**6**	Gold-sputtered SA─ZE8-H

Following the determination of reflection and transmission losses, absorption percentages of all combinations were obtained by repeating the pre-described methodology.

CHAPTER 4

RESULTS AND DISCUSSION

This chapter includes the general characterization (crystal structure determination, microstructural analysis and electrical conductivity measurements) of SiC-based and alumina woven fabrics and also results on their interaction with EM radiation. Basic material properties of ceramic woven fabrics were characterized by X-ray diffraction (XRD), scanning electron microscopy (SEM) and electrical conductivity measurement (for SiC-based woven fabrics only). Furthermore, EM wave absorption potential of single and double layer ceramic woven fabrics was determined by free-space method. Following sections express results and discussion about these investigations.

4.1. General Characteristics of Ceramic Woven Fabrics

Crystal structures of as-received and modified (either heat-treated or gold-sputtered) SiC-based and alumina woven fabrics were examined using XRD. Figure 4.1 shows the XRD patterns of as-received and heat-treated S8 type ceramic woven fabrics. In as-received condition, three peaks at 2θ values of 35.9°, 60.2° and 71.8° belonged to β-SiC, and these peaks showed some broadening indicating that the fibers are in nano-crystalline state [55]. Same β-SiC peaks were also observed in heat-treated S8 type woven fabric; however, they were narrower due to coarsening of β-SiC crystallites after heat-treatment. In addition to β-SiC, an extra phase SiO_2 (low-cristobalite) was identified in the diffraction pattern of heat-treated woven fabric. Sharp diffraction peak with 2θ= 22.0° corresponds to the major peak of SiO_2. Detection of SiO_2 phase pointed out the oxidation of the S8 type woven fabric with

heat-treatment. Under equilibrium conditions quartz (SiO_2) is the stable phase at room temperature; however, in the present case cooling from heat-treatment temperature, 1573 K, was not slow enough for reconstructive phase transitions from high temperature stable phase, cristobalite, to quartz. As a result of this, displacive transition brought out distortion of cristobalite and existence of low-cristobalite at room temperature [66].

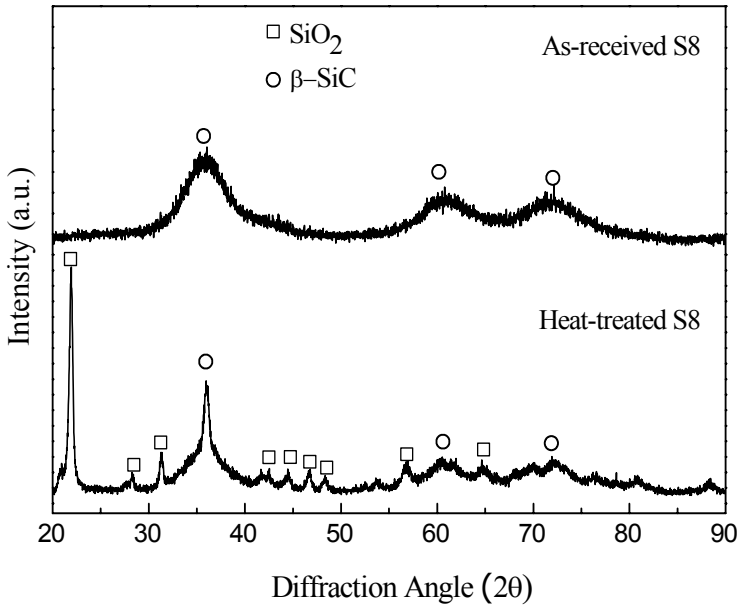

Figure 4.1 XRD spectra of as-received and heat-treated S8 type woven fabrics.

Both in the as-received and heat-treated states, PN woven fabrics revealed similar characteristics with that of S8 type woven fabric. XRD patterns of PN type ceramic woven fabrics are demonstrated in Figure 4.2. In as-received condition β-SiC phase was observed. Following the heat-treatment, SiC peaks became narrower, and SiO_2 (low-cristobalite) peaks were detected. Chemical composition of PN woven fabric is identical to that of S8 woven fabric except that PN possesses a carbon-rich layer at its surface; as a consequence of this, similarity in the XRD patterns of PN and S8 woven fabrics is expected.

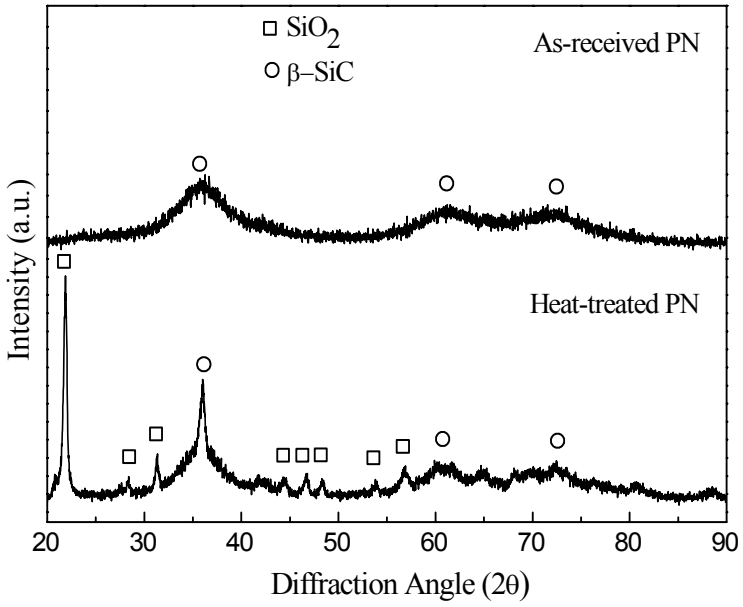

Figure 4.2 XRD spectra of as-received and heat-treated PN type woven fabrics.

Figure 4.3 shows the XRD patterns of as-received and heat-treated ZE8 type ceramic woven fabrics. In as-received ZE8 woven fabric, β-SiC peaks were narrower compared to S8 and PN type woven fabrics showing that ZE8 fibers were highly crystalline in the as-received state [55]. Variations in peak broadening of woven fabrics are related to their production route, especially to their curing temperature. In this type of ceramic fabric slight narrowing was observed in β-SiC peaks subsequent to heat-treatment, and a sharp low cristobalite peak was observed at $2\theta = 22.0°$ which was the evidence of oxidation.

XRD patterns of as-received and gold-sputtered PA type alumina woven fabrics are shown in Figure 4.4. In both conditions, only α-Al_2O_3 peaks were detected. Additional gold peak was not observed in the modified woven fabrics most probably due to nanometer order thickness of the gold surface layer. SA type woven fabric revealed identical XRD pattern to that of PA type woven fabrics.

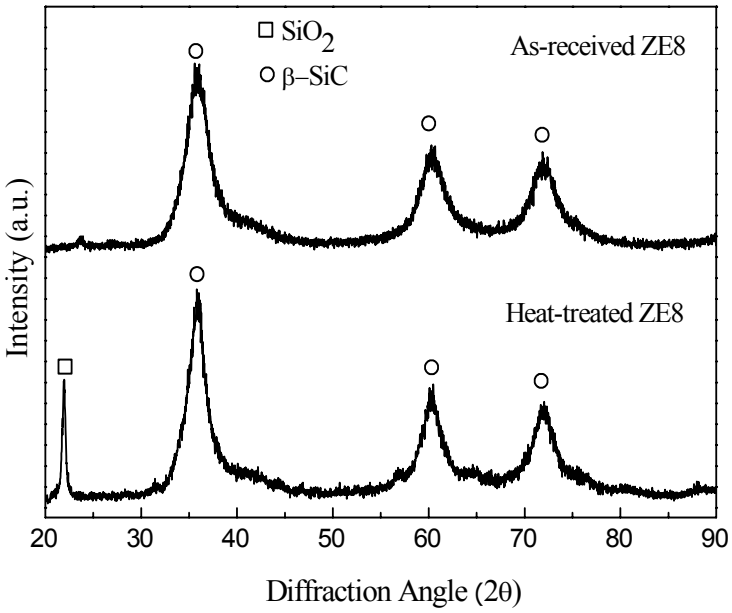

Figure 4.3 XRD spectra of as-received and heat-treated ZE8 type woven fabrics.

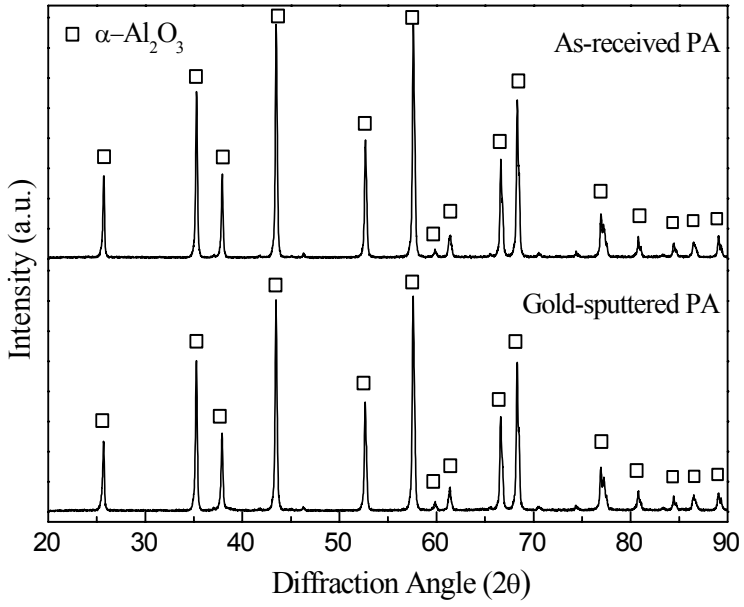

Figure 4.4 XRD spectra of as-received and gold-sputtered PA type woven fabrics.

Following the crystal structure determination of the as-received and heat-treated woven fabrics, their morphologies were investigated using SEM. Figure 4.5 (a) shows SEM micrographs of fibers extracted from S8 type woven fabrics. Fibers revealed a smooth surface. Continuous oxide layer was observed on the surfaces of the fibers of heat-treated S8 type fabrics (Figure 4.5 (b)). Both the SiO_2 film and the fiber core had a smooth and pore-free appearance indicating passive-oxidation of fibers [58]. In case of active oxidation, fibers generally reveal a dual structure with extremely large grains on the surface and small grains in the core [67]. In some regions, the continuity of oxide layer was lost most probably due to specimen handling including chopping of the fibers to observe the fracture surface.

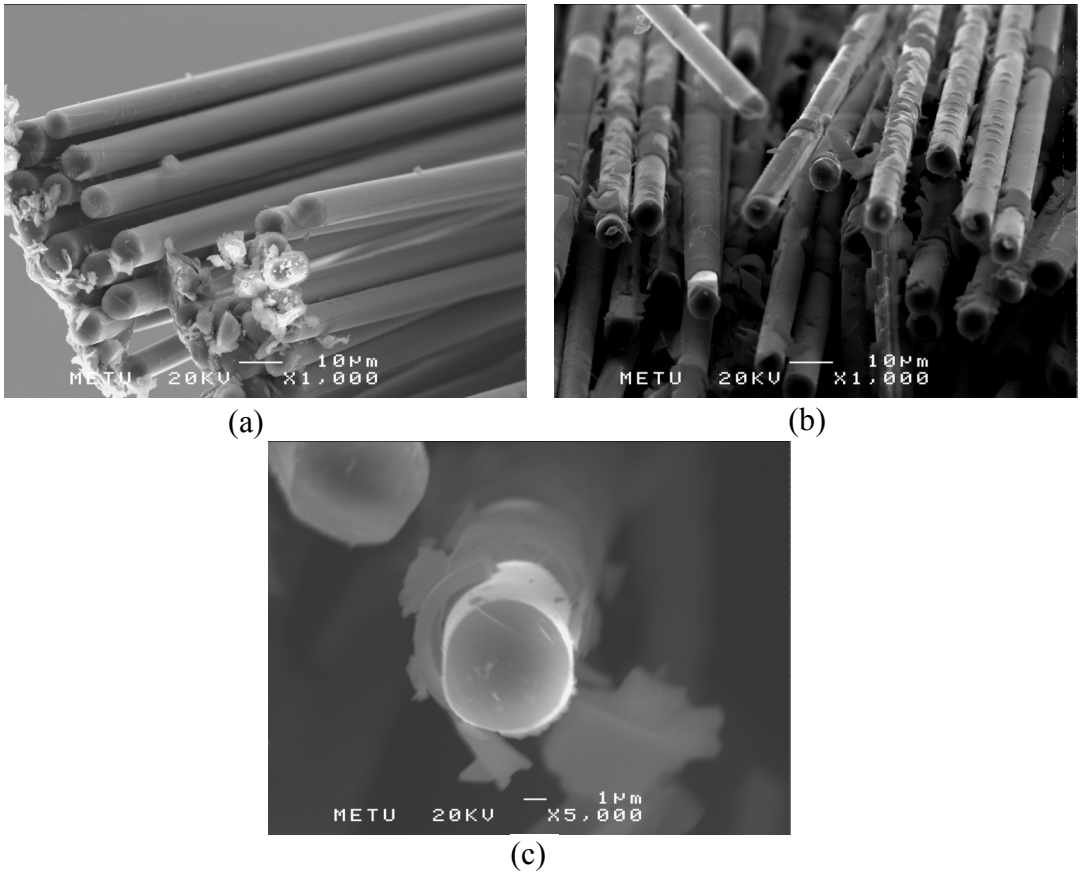

(a) (b)

(c)

Figure 4.5 SEM micrographs of (a) as-received and (b, c) heat-treated SiC-based fibers extracted from S8 type woven fabrics at x1000 and x5000 magnifications, respectively.

Figure 4.5 (c) shows the micrograph of heat-treated S8 type fibers at x5000 magnification. According to this micrograph, thickness of the oxide layer around the fiber was determined to be ~1 μm.

Morphology and structure of as-received and heat-treated fibers extracted from PN type woven fabrics are shown in Figure 4.6. Micrographs of PN fiber revealed similar characteristics with that of S8 type both in the as-received and heat-treated states. A smooth surface was observed in as-received state (Figure 4.6 (a)), while a continuous oxide layer was seen in heat-treated state (Figure 4.6 (b)). Similar to heat-treated S8 fiber, silica layer on the surface of PN fiber was about ~1 μm thick according to SEM observation (Figure 4.6 (c)).

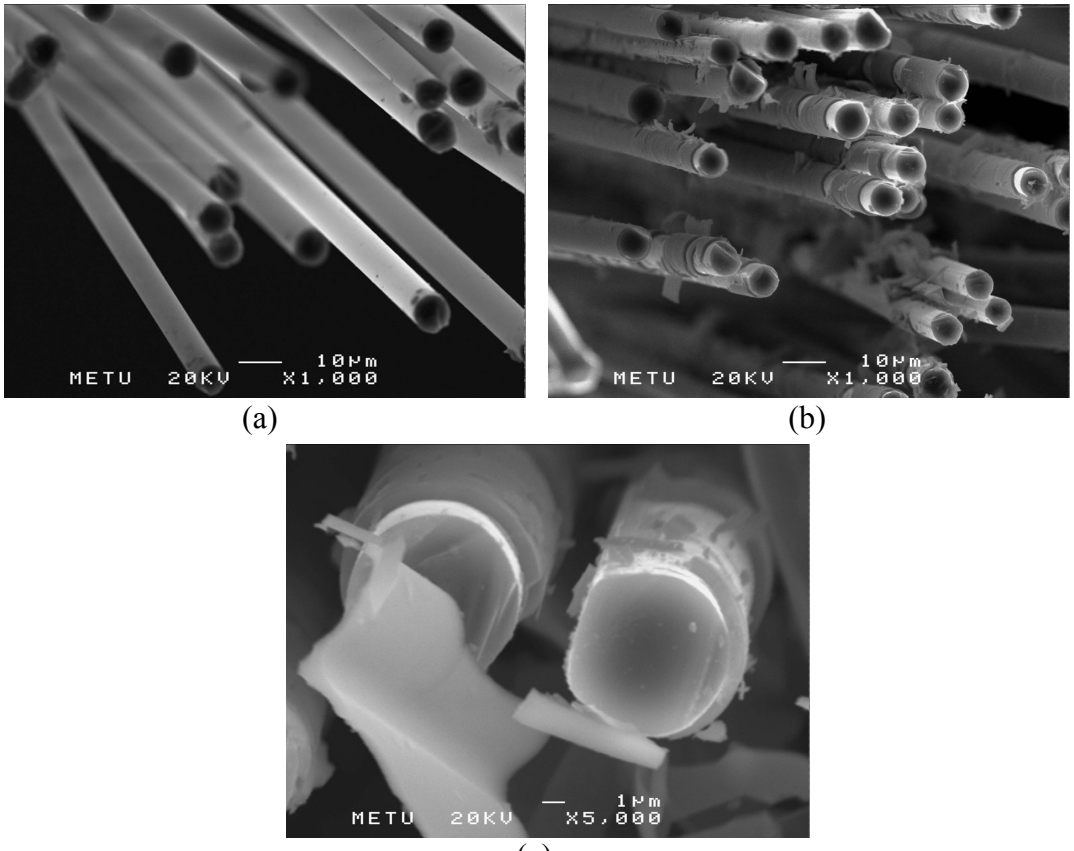

(a) (b)

(c)

Figure 4.6 SEM micrographs of (a) as-received and (b, c) heat-treated SiC-based fibers extracted from PN type woven fabric at x1000 and x5000 magnifications, respectively.

Micrographs of as-received and heat-treated fibers extracted from ZE8 type woven fabrics are shown in Figure 4.7 (a) and (b), respectively. In case of heat-treated ZE8 fibers, a clear continuous oxide layer did not exist around the fibers (Figure 4.7 (a)), where detailed observations revealed that oxidation of the fibers could be observed at localized regions indicated by arrows in Figure 4.7 (b). ZE8 type woven fabric is described as heat resistant by the manufacturer [65], and experimental results verify this behavior. It is considered that the excellent heat stability of the ZE8 fiber is due to the presence of zirconium (Zr) in its chemical structure. In the formed crystal lattice Zr atom bonds to eight oxygen atoms forming a thermally stable structure [68].

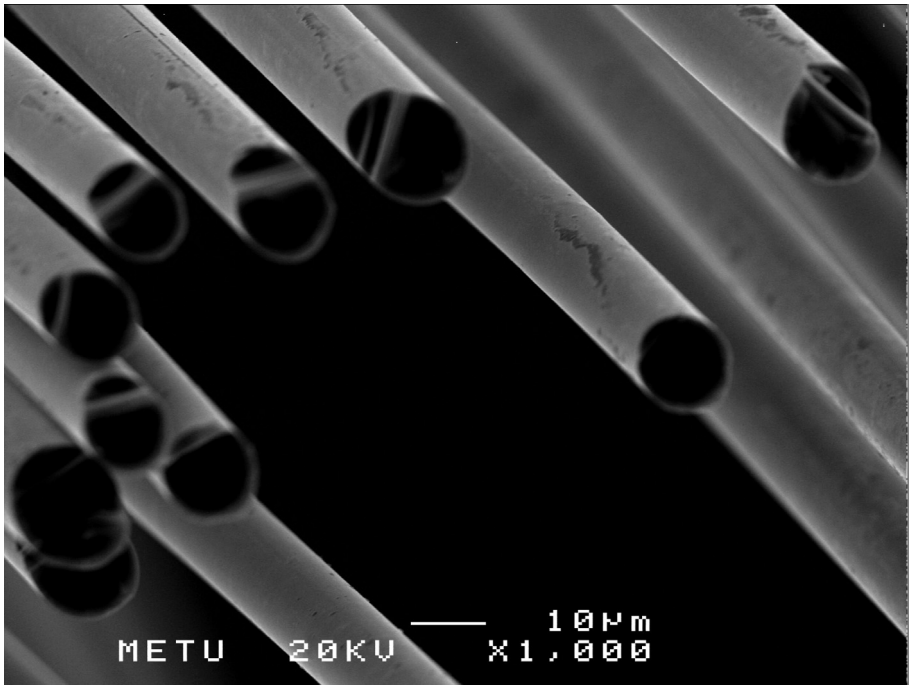

(a)

Figure 4.7 SEM micrographs of (a) as-received and (b) heat-treated SiC-based fibers extracted from ZE8 type woven fabrics.

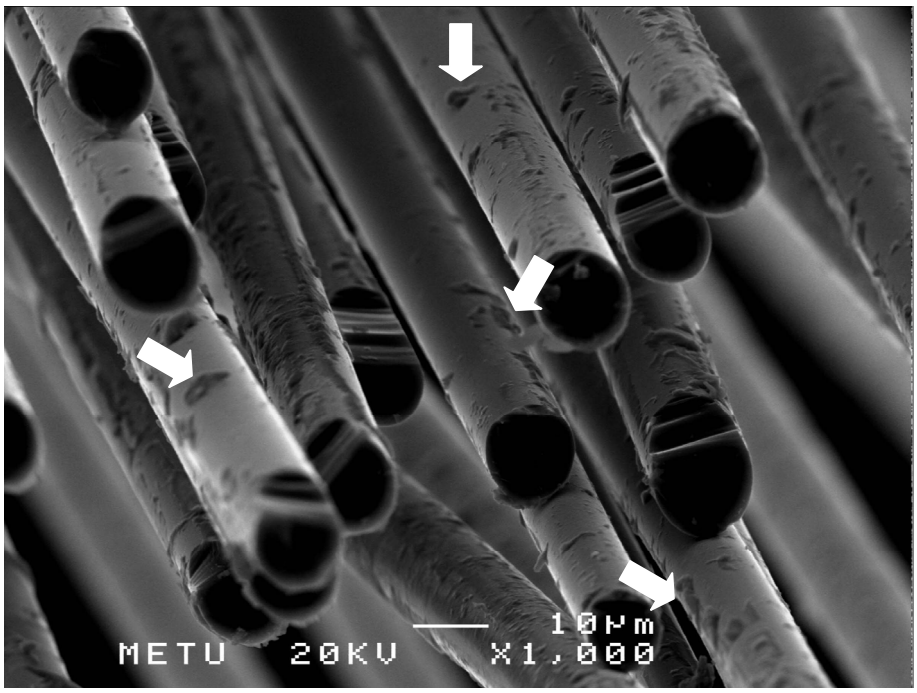

(b)

Figure 4.7 (cont) (b) heat-treated SiC-based fibers extracted from ZE8 type woven fabrics.

Similar to SiC-based bundles, microstructural analysis of gold-sputtered alumina bundles were performed using SEM. Since alumina woven fabrics were electrically insulative, microstructural analysis under SEM was not performed for as-received alumina fibers due to charge-up. Micrographs of gold-sputtered PA type alumina bundles at two different magnifications are shown in Figure 4.8 (a) and (b). Although gold peak was not identified in XRD, energy dispersive spectroscopy (EDS) result (Figure 4.8(c)) revealed the gold peak on the surface of the woven fabrics.

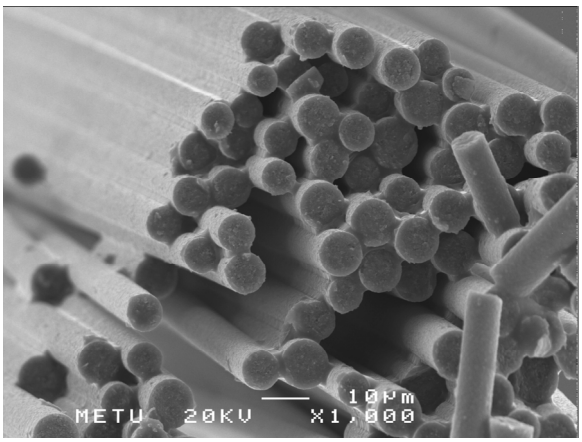

(a)

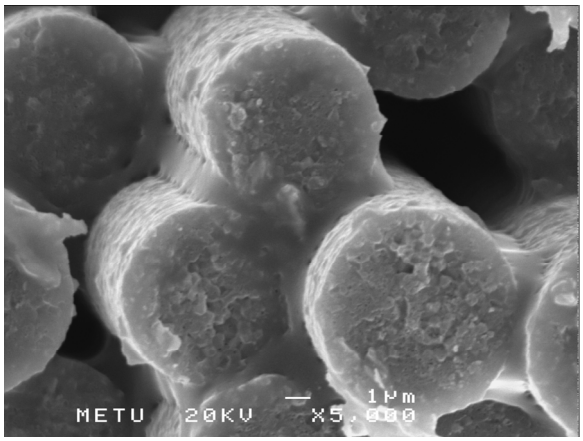

(b)

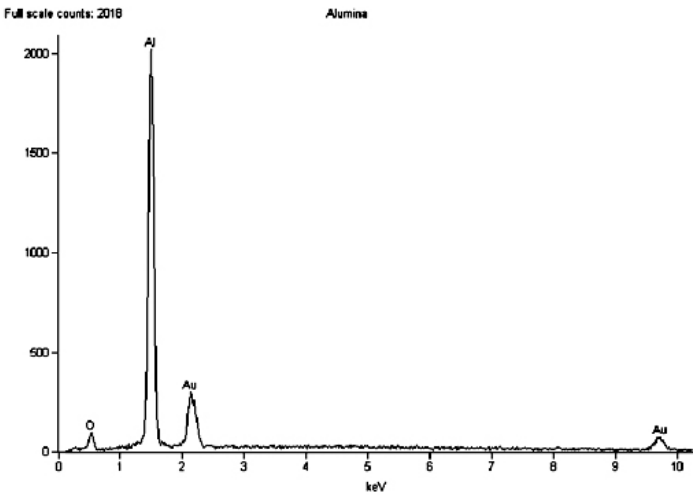

(c)

Figure 4.8 (a), (b) SEM micrographs of gold-sputtered PA type alumina fibers at x1000 and x5000 magnifications, respectively, (c) EDS result of gold-sputtered alumina fibers.

Following the crystal structure determination and microstructural analysis, electrical conductivity measurements were performed on SiC-based fiber bundles extracted from the woven fabrics both in as-received and heat-treated states. Measured electrical conductivities of as-received and heat-treated SiC-based ceramic fibers are given in Table 4.1. As-received ZE8 fiber revealed the highest electrical conductivity among others, which can be explained by its higher Si and C content compared to those of the other two fiber types. High amount of free carbon aggregates in this fiber is also effective in its high electrical conductivity. Although PN and S8 fibers have similar chemical compositions, carbon coating around the PN fiber increases its electrical conductivity compared to that of S8 type fiber.

Table 4.1 Electrical conductivity measurement results of investigated fibers.

Fiber Condition	Fiber Type	DC Conductivity (S/m)
As-received	S8	33.6
	PN	131.8
	ZE8	226.5
Heat-treated	S8	2.8
	PN	0.1
	ZE8	25.8

According to Table 4.1, it is clear that electrical conductivities of fibers decrease significantly following the heat-treatment. Formation of oxide layer around the fibers, disappearance of free carbon aggregates in all fibers at above 773 K and also the subsequent breakdown of fiber microstructure after the heat treatment could be the possible reasons of the decrease in the electrical conductivity. As indicated earlier, PN fiber has a carbon-coated surface which increases its electrical conductivity compared to S8 fiber having similar chemical composition. Carbon is an excellent electrical conductor, and loss of carbon film on PN fiber due

to heat-treatment reduced the electrical conductivity of this fiber significantly. Consequently, S8 and PN fibers revealed similar electrical conductivities after heat-treatment. ZE8 fiber possessed highest electrical conductivity in as-received state and it conserved this tendency after heat treatment acquiring the highest conductivity value among the heat-treated fibers. Instead of an explicit continuous oxide layer existence of isolated oxidized regions could have resulted in the lower electrical conductivity decrease in ZE8 type fiber.

Basic properties of the as-received and heat-treated woven fabrics were investigated and discussed in this section. In the following section results of interaction of SiC-based woven fabrics with EM radiation are examined.

4.2. Interaction of Ceramic Woven Fabrics with Electromagnetic Radiation

Interactions of single and multilayer ceramic woven fabrics with EM radiation were determined in terms of reflection loss (S_{11}) and transmission loss (S_{21}) and also presented as corresponding absorption percentages. In this section firstly, single layer SiC-based ceramic woven fabric EM absorption potentials are investigated. Following this, absorption potentials of the various double layer combinations of as-received and heat-treated woven fabrics are discussed.

4.2.1. SiC-based Woven Fabrics

4.2.1.1. Single-Layer SiC-based Woven Fabrics

Reflection and transmission losses of single layer ceramic woven fabrics were measured in 17-40 GHz frequency range using free-space method. Reflection loss (S_{11}) is defined as reflection of EM energy back into the source side [4] and is represented in decibels (dB). Conversion from dB values to fractions of reflected and transmitted waves were explained in “Experimental Procedure” chapter (page 44). Decreasing reflection loss (increasing negative dB) indicates that reflected

portion of EM wave from the material surface diminishes. With similar manner transmission loss in the following figures shows change in S_{21} (dB) parameter of the specimens under consideration. In this case, decreasing transmission loss (increasing negative dB) indicates that transmitted portion of EM wave from the material surface diminishes.

Changes in reflection losses of as-received SiC-based ceramic woven fabrics are demonstrated in Figure 4.9 as a function of frequency. ZE8 type ceramic woven revealed the highest reflection loss among all as-received woven fabrics at 17-40 GHz frequency range. According to electrical conductivity results, ZE8 fibers revealed the highest electrical conductivity. Increase in electrical conductivity results in increasing reflected fraction from the materials, so reflection loss is strengthened. On the contrary, lower electrical conductivity leads to weakening of reflection from the material surface, and hence lower reflection loss. Electrical conductivity-reflection loss relationship can be explained by follows: EM impedance of the material increases as conductivity decreases. Consequently, the level of impedance mismatch to air becomes lower, and this causes reduction in the reflection loss of the material. As a result of this, it can be stated that electrical conductivity plays a major role in reflection losses of ceramic woven fabrics. Reflection losses of woven fabrics having higher electrical conductivities are strengthened.

Figure 4.10 shows the reflection losses of heat-treated SiC-based woven fabrics. Similar to as-received state, ZE8 type ceramic woven fabric revealed the highest reflection loss after heat-treatment owing to the highest electrical conductivity. PN woven fabric revealed lowest electrical conductivity in the heat-treated state, as a consequence of this, EM reflection from the surface of this woven fabric was weaker, and thereby reflection loss was minimized.

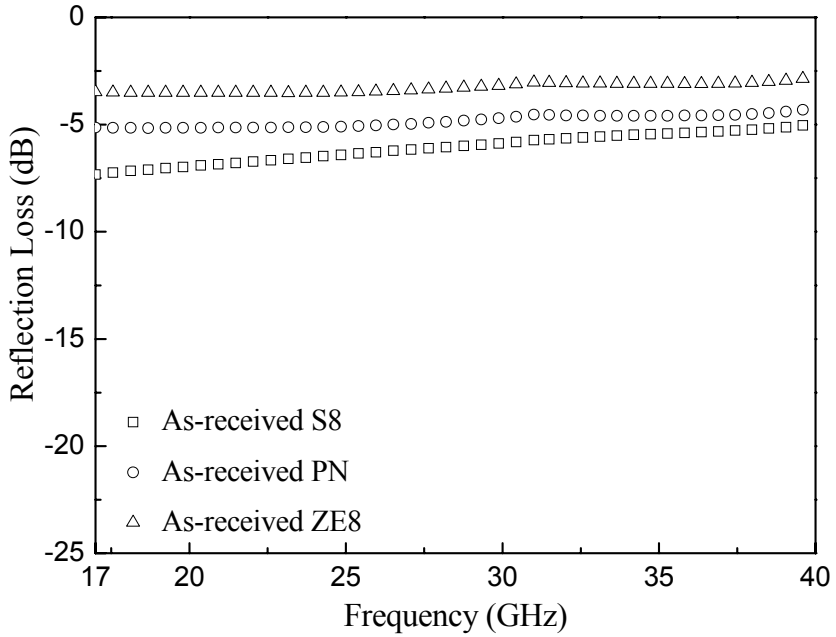

Figure 4.9 Reflection losses of single layer as-received SiC-based woven fabrics.

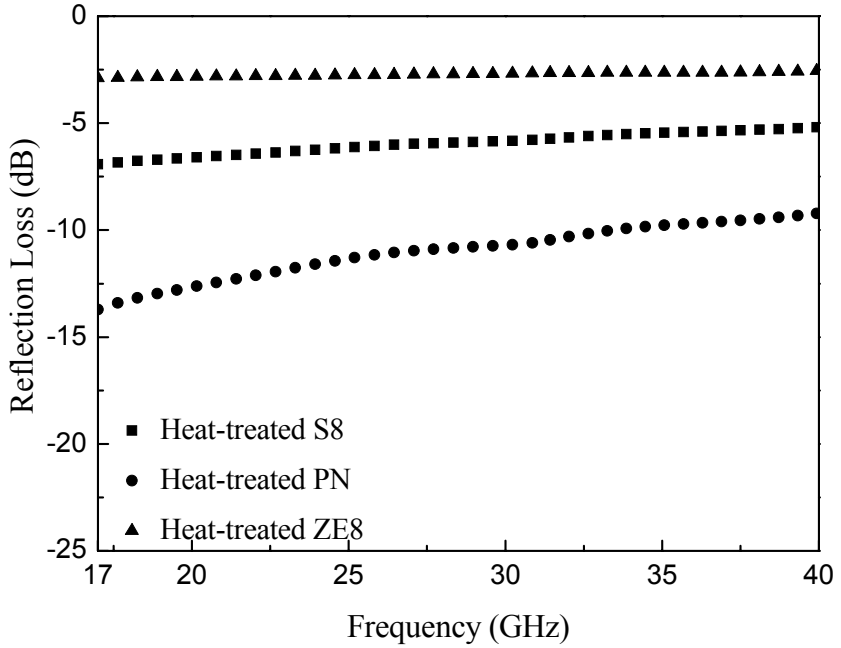

Figure 4.10 Reflection losses of single layer heat-treated SiC-based woven fabrics.

Comparison of reflection losses of as-received and heat-treated single layer SiC-based woven fabrics pointed to the distinct behavior of PN type woven fabric. At low frequencies reflection loss of as-received PN type woven was about -5 dB corresponding to ~31% reflection of EM wave where at similar frequencies reflection loss of heat-treated PN woven fabric decreased to -14 dB with ~3% reflection of EM wave. PN type fabric is composed of carbon coated SiC-based fibers where high conductivity of the carbon yielded higher reflection loss in the as-received condition. However, after heat-treatment in air due to loss of carbon coating and formation of oxide layer, electrical conductivity of the fiber decreased causing a considerable difference between the reflection losses of as-received and heat-treated PN type ceramic woven fabrics.

Transmission losses of as-received and heat-treated single layer SiC-based woven fabrics are plotted in Figure 4.11 and Figure 4.12, respectively, as a function of frequency. Decreasing fraction of transmitted wave through the material corresponds to higher negative dB values. Transmission losses in both as-received and heat-treated woven fabrics revealed slight frequency dependence.

ZE8 type woven fabric in both as-received and heat-treated conditions revealed the lowest transmission. Largest difference in transmitted portions was observed in as-received and heat-treated PN type woven fabrics as in the case of their reflection losses. Moreover, as a general tendency, it was observed that woven fabrics that reflect EM wave more exhibit lower transmission (higher reflection loss corresponds to lower transmission loss).

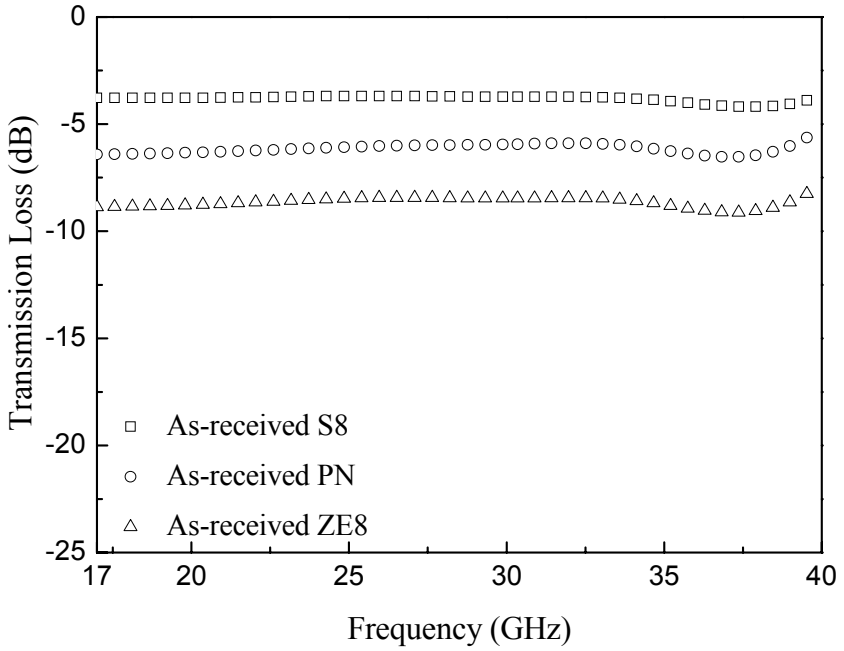

Figure 4.11 Transmission losses of single layer as-received SiC-based woven fabrics.

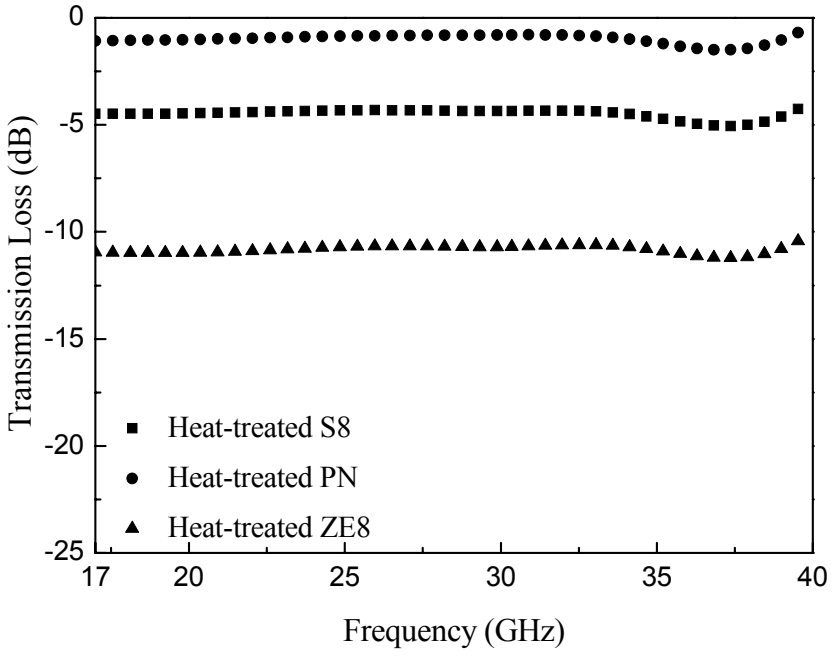

Figure 4.12 Transmission losses of single layer heat-treated SiC-based woven fabrics.

Reflected and transmitted fractions of EM wave were calculated using transmission and reflection losses of woven fabrics, and absorption percentages were determined accordingly. These calculations were explained in detail in the "Experimental Procedure" chapter (page 46). Table 4.2 shows absorption percentages (%) of single layer SiC-based woven fabrics at selected frequencies. Absorption percentages in both as-received and heat-treated states were lower than 50% for all woven types. This result demonstrates the fact that none of the ceramic woven types is applicable in commercial EM wave absorbing materials in single layer form, where typically required absorption level is more than ~95%.

Table 4.2 Absorption percentages of single layer ceramic woven fabrics.

Frequency (GHz)	**Absorption (%)**					
	As-received S8	Heat-treated S8	As-received PN	Heat-treated PN	As-received ZE8	Heat-treated ZE8
20	37.9	42.3	46.2	15.3	42.2	39.8
25	34.3	38.4	44.3	10.6	41.0	38.6
30	31.6	37.2	40.5	8.3	37.5	37.7
35	30.5	37.6	41.2	13.3	37.5	37.4
40	25.1	28.2	32.0	10.5	30.8	34.4
Average	*31.9*	*36.7*	*40.8*	*11.6*	*37.8*	*37.6*

4.2.1.2. Double-Layer SiC-based Woven Fabrics Combinations

To achieve better EM wave absorption potential, various double layer combinations of as-received and heat-treated SiC-based woven fabrics were constructed. Combinations were investigated in three main groups:

i) Combinations of as-received woven fabrics.

ii) Combinations of heat-treated woven fabrics.

iii) Combinations of as-received and heat-treated woven fabrics.

4.2.1.2.1 Double-Layer Combinations of As-received Woven Fabrics

As the first case, combinations of as-received woven fabrics were attempted. S8 woven fabric was used as the first layer of the combination, and one of the as-received SiC-based woven fabrics was placed behind the first layer. Figure 4.13 shows the reflection losses of combinations of as-received S8 with other as-received wovens.

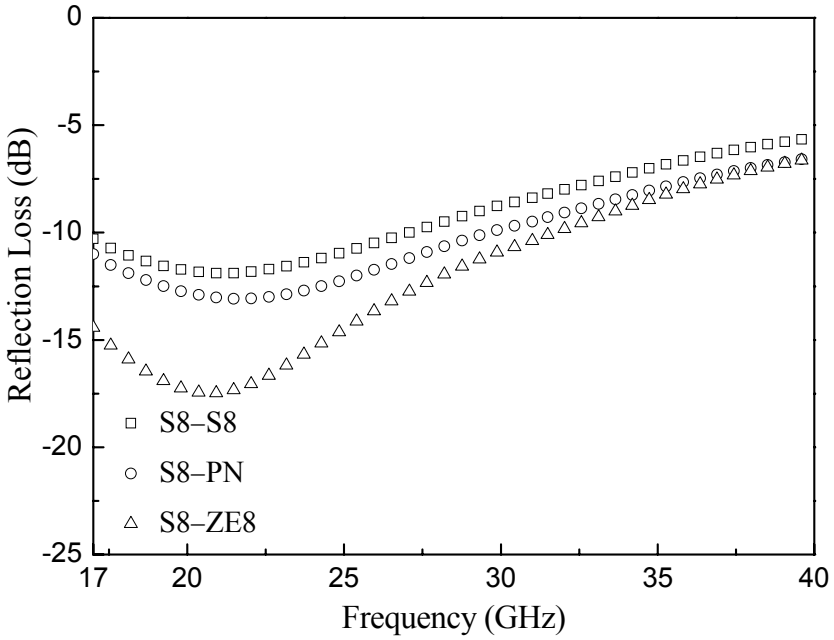

Figure 4.13 Reflection losses of double layer combinations of S8 with other as-received woven fabrics.

All of the combinations showed a minimum at lower frequencies near 20 GHz, and reflection loss was strengthened as frequency increased. Near these minima the reflected portions of the EM wave were as low as ~6% (~-12 dB) for S8─S8, ~5%

(~-13 dB) for S8─PN and ~2% (~-18 dB) for S8─ZE8 combinations. When average reflected portions through 17-40 GHz frequency range were calculated, obtained results were ~12% (~-9 dB) for S8─S8, ~11% (~-10 dB) for S8─PN and ~9% (~-12 dB) for S8─ZE8 combinations. From these average values, it can be concluded that placing lower conductivity woven fabric in front of a high conductivity woven fabric, causes reduction in reflection loss. S8 woven fabric revealed lowest conductivity among other as-received woven fabrics, and placing PN woven fabric behind it weakened the reflection loss. For another case in place of PN, insertion ZE8 woven fabric behind the S8 woven fabric reduced the reflection loss more than the other combinations.

Transmission losses of combinations containing as-received S8 with other as-received woven fabrics are given in Figure 4.14. It was observed that transmission get weaker as frequency of the EM wave increases.

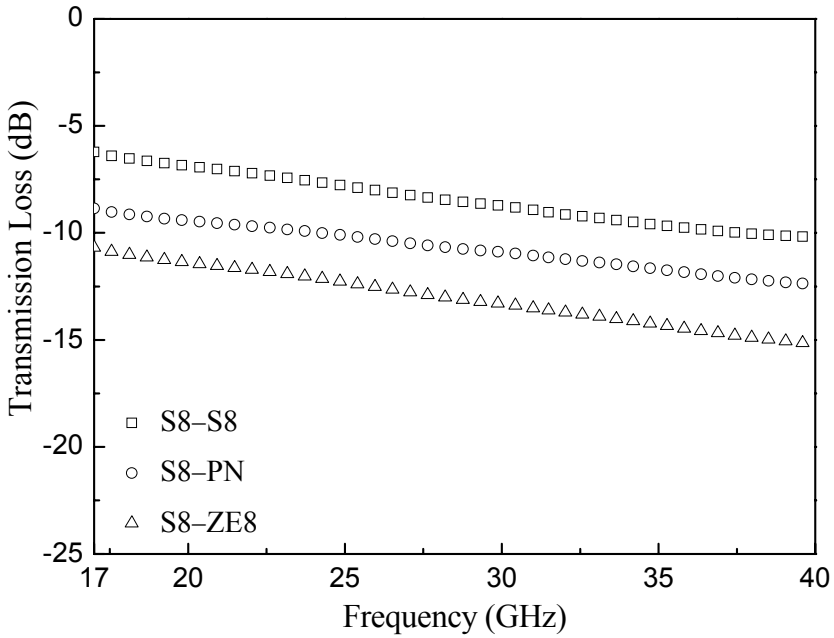

Figure 4.14 Transmission losses of double layer combinations of S8 with other as-received woven fabrics.

Highest transmission was detected for S8─S8 combination, where average transmitted portion of this combination was about ~14% (~-8 dB) over the measured frequency range. On the other hand, S8─ZE8 combination revealed the lowest transmission transmitting ~5% (~-13 dB) of the incident EM wave on average. Among the combinations where S8 woven fabric was used as the first layer, combination of ZE8 (highest conductivity fabric among others) as the second layer caused reduction in transmission. On the contrary, S8 (lowest conductivity woven fabric) as the second layer was responsible for the highest transmission in double layer S8 woven fabric combinations. Absorption potentials of aforementioned combinations are seen in the Figure 4.15.

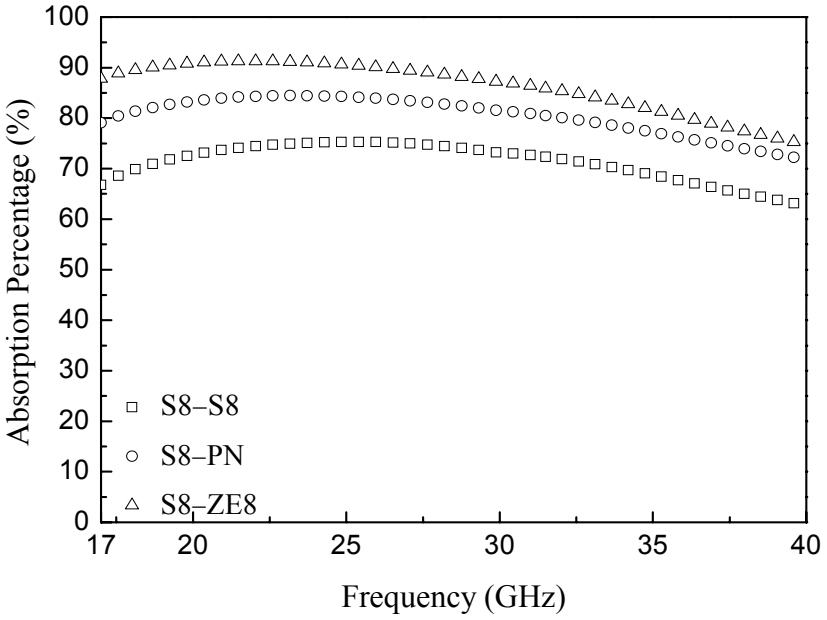

Figure 4.15 Absorption percentages of double layer combinations of S8 with other as-received woven fabrics.

S8─ZE8 combination resulted in more than ~90% absorption up to 26 GHz with the reduced reflection and transmission fractions. For this combination first

layer S8 woven fabric reduced reflection at air-low conductivity layer interface, along with EM wave transmitted through the system, where most of it reflected from the surface of the second layer. From this observation it can be said that low conductivity first layer behaved as absorbing layer while high conductivity second layer behaved as reflective layer bounding EM energy within the material system.

As the result of low→high electrical conductivity layer combinations, relatively higher absorption potentials were achieved. In this respect, highest conductivity mismatch between S8 and ZE8 woven fabrics resulted in maximum absorption potential with an average of ~86% in 17-40 GHz frequency range. From Figure 4.15, it was also concluded that other two combinations containing S8 woven fabric as the first layer also resulted in reasonably high average absorption potentials, ~70% and ~80% for S8─S8 and S8─PN combinations, respectively.

In case of PN usage as the first layer, reflection losses of combinations seemed to be frequency independent. Figure 4.16 shows reflection losses of double layer combinations of PN with other as-received woven fabrics.

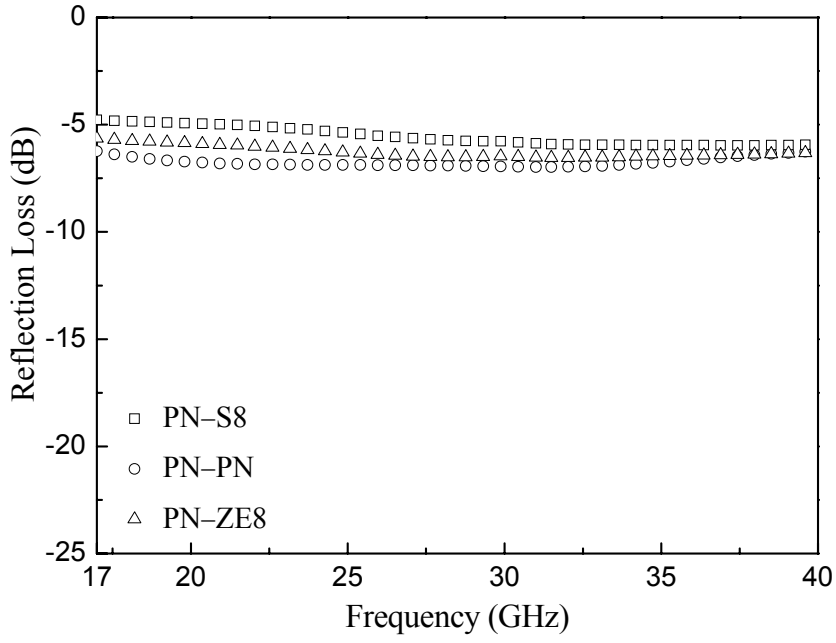

Figure 4.16 Reflection losses of double layer combinations of PN and other as-received woven fabrics.

In case of these combinations, there were no minima as in the case of the combinations of as-received S8 woven fabrics. Reflection losses of these combinations were quite similar where average reflected portions were ~21% (~-7 dB) for PN─PN, ~28% (~-6 dB) for PN─S8 and ~24% (~-6 dB) for PN─ZE8 combinations. PN revealed higher electrical conductivity, and as a result of this, usage of this woven fabric as the first layer increased the reflection losses. Reflection loss of PN─S8 combination was higher than that of PN─ZE8 where PN─ZE8 was a low→high electrical conductivity layer combination, while PN─S8 revealed high→low layer sequence.

Transmission losses of double layer combinations of PN type woven fabric are presented in Figure 4.17. Transmission of combinations decreased as frequency increased. PN─PN combination transmitted ~4% (~-14 dB) of the EM wave, where PN─S8 and PN─ZE8 combinations transmitted ~9% (~-11 dB) and ~2% (~-16 dB) on average, respectively. Higher electrical conductivity of the second layer was effective in suppressing the transmission loss. As the electrical conductivity of the second layer woven fabric increased, transmission weakened as in the case of PN─ZE8 combination.

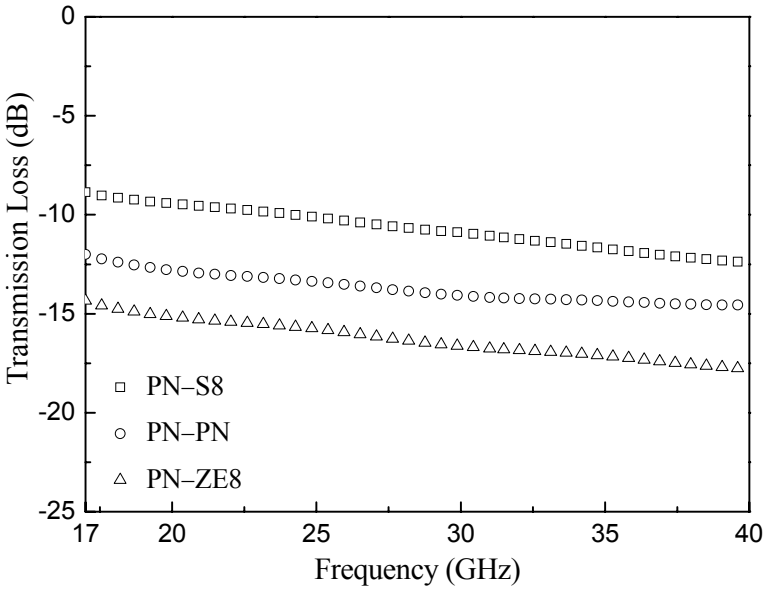

Figure 4.17 Transmission losses of double layer combinations of PN with other as-received woven fabrics.

Absorption potentials of double layer combinations of as-received PN woven fabrics are shown in Figure 4.18. PN─PN and PN─ZE8 combinations revealed similar absorption percentages (higher than ~70%) with respect to frequency, whereas PN─S8 combination exhibited lower due to increased reflection and transmission losses of this double layer combination.

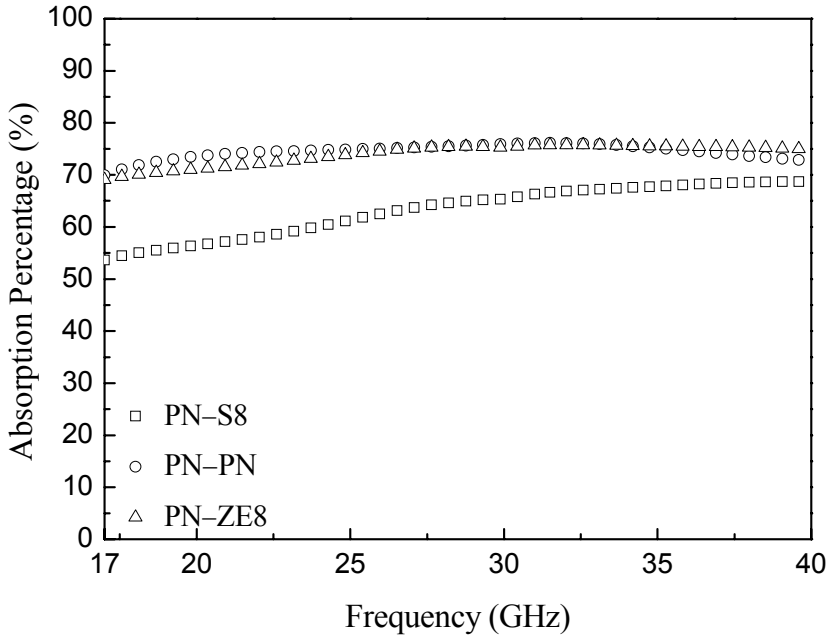

Figure 4.18 Absorption percentages of double layer combinations of PN type woven fabric.

As the last set of double layer combinations that were composed of as-received SiC-based woven fabrics, combinations of as-received ZE8 woven fabric were examined. Figure 4.19 shows the reflection losses of these combinations where similar loss values were observed over the frequency range under consideration. It was observed that reflection losses show slight frequency dependence. In these combinations EM wave first encountered the high conductivity layer ZE8 (most conductive layer among as-received woven fabrics); as a result of this, most of the incident wave reflected from the first layer without finding the opportunity to

transmit through the second layer. In all these combinations, at least ~35% (~-5 dB) of the incident EM wave reflected from the material system.

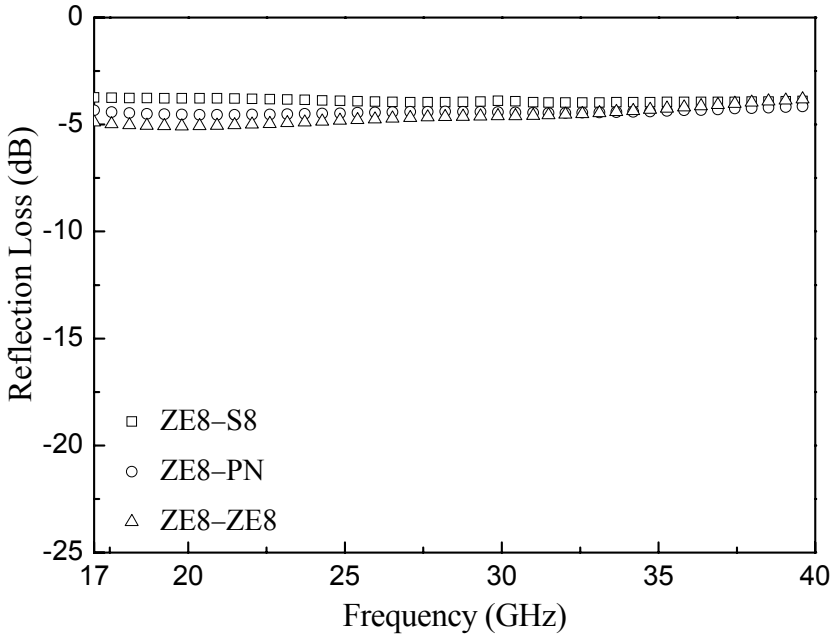

Figure 4.19 Reflection losses of double layer combinations of ZE8 and other as-received woven fabrics.

Figure 4.20 shows transmission losses of double layer combinations of ZE8 type woven fabric. Similar to other combinations, transmission weakened with increasing frequency. ZE8─S8 combination transmitted more EM energy than others due to the usage of low conductivity S8 woven fabric as the second layer. On the other hand, since high conductivity ZE8 woven fabric was used as the first layer, transmitted portions of the EM waves for these combinations were lower when compared to combinations which contained PN and S8 woven fabrics as the first layer. Average transmissions of the combinations were ~1% (~-20 dB) for ZE8─ZE8, ~2% (~-16 dB) for ZE8─PN and ~5% (~-13 dB) for ZE8─S8.

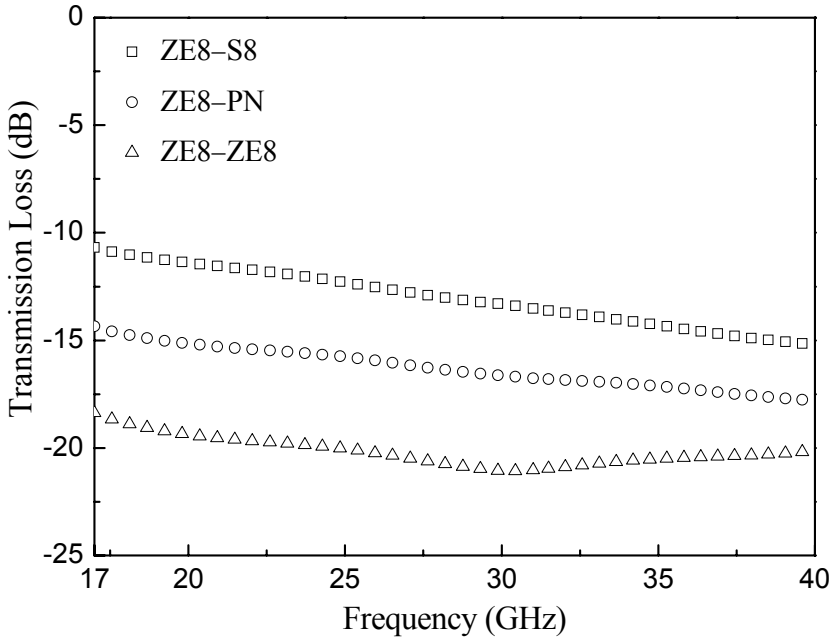

Figure 4.20 Transmission losses of double layer combinations of ZE8 with other as-received woven fabrics.

Absorption potentials of combinations of as-received ZE8 woven fabrics are compared in the Figure 4.21. Although transmission were quite low for these combinations due to the high reflection losses they revealed, overall absorption potentials of the combinations were lower than ~70% along 17-40 GHz frequency range.

When combinations of as-received woven fabrics are considered, better absorption potentials were achieved with the combinations in which S8 type woven fabric was used as the first layer. Since S8 type woven fabric had the lowest electrical conductivity in as-received condition, placing a higher conductivity layer after this woven fabric improved EM wave absorption with reduced reflection loss. Woven type was also another important factor which had influence on the EM wave absorption potential of the woven fabrics. S8 is a satin woven fabric, and accordingly it reveals a smoother surface. As a consequence of this, internal

reflection was eliminated, and with reduced reflection EM wave absorption potential of the combinations has been improved.

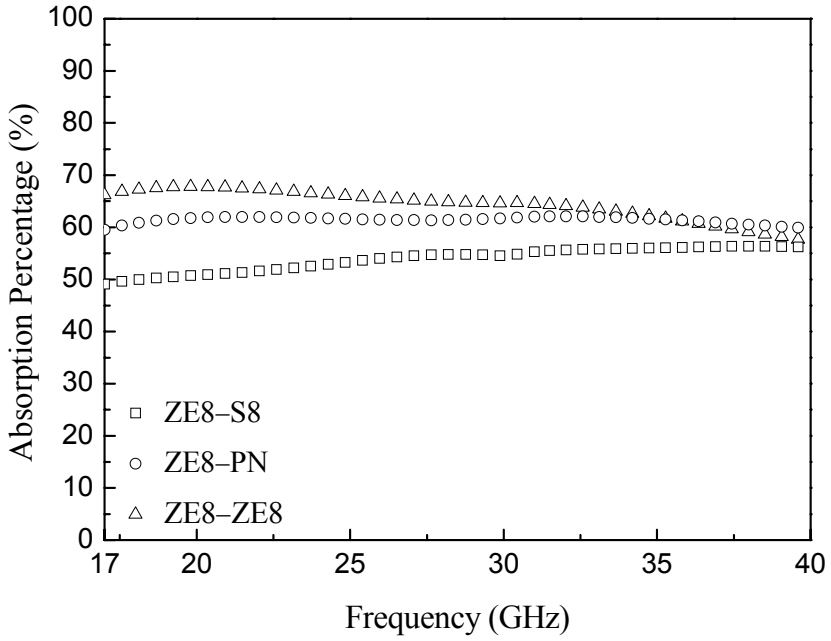

Figure 4.21 Absorption percentages of double layer combinations of ZE8 with other as-received woven fabrics.

4.2.1.2.2 Double-Layer Combinations of As-received and Heat-treated Woven Fabrics

In the second set of the experiments, EM wave interactions of combinations of as-received and heat-treated SiC-based woven fabrics were investigated. Figure 4.22 demonstrates reflection losses of the first investigated combination, heat-treated S8 and as-received woven fabrics. These combinations revealed minima at the low frequency and where the minimum of the S8-H─S8 combination was observed at ~22 GHz. Reflection losses at the minima were quite low; however, strengthened as frequency increased. At the minimum point of S8-H─S8

combination, reflected portion of the EM wave decreased up to ~11% (~-10 dB). At lower frequencies near 17 GHz, reflected fraction decreased up to ~6% (~-12 dB) for both S8-H─PN and S8-H─ZE8 combinations. It was determined that electrical conductivities of all woven fabrics diminished after heat-treatment. As a result of this, placing as-received woven fabrics at the back of the heat-treated woven fabrics always revealed low→high electrical conductivity layer combination. Increasing conductivity mismatch between the woven fabrics weakened reflection loss as in the case of the combinations of heat-treated S8 with as-received ZE8 woven fabrics.

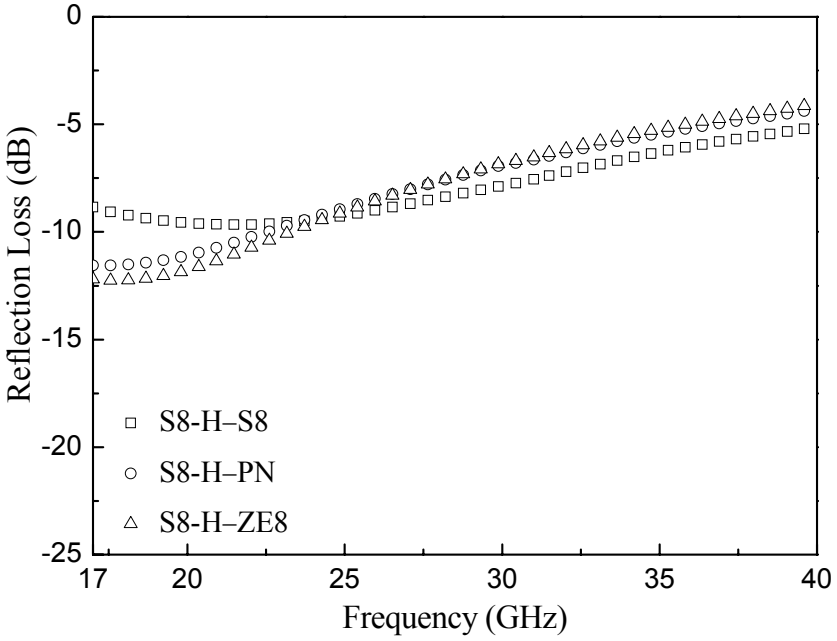

Figure 4.22 Reflection losses of double layer combinations of heat-treated S8 and as-received woven fabrics.

Figure 4.23 shows the transmission losses of combinations of heat-treated S8 with as-received woven fabrics. Among them, combination of S8 woven fabric transmitted more EM energy (on average ~11% (~-10 dB) of the incident energy) compared to other combinations of high conductivity second layers, PN and ZE8.

Average transmitted portions for S8-H─PN and S8-H─ZE8 combinations were ~6% (~-13 dB) and ~3% (~-15 dB), respectively through 17-40 GHz frequency range. This shows that electrical conductivity of second layer is very effective in determining the transmission fractions of the combinations. Increase in the conductivity of the second layer reduces the transmission of the double layer system.

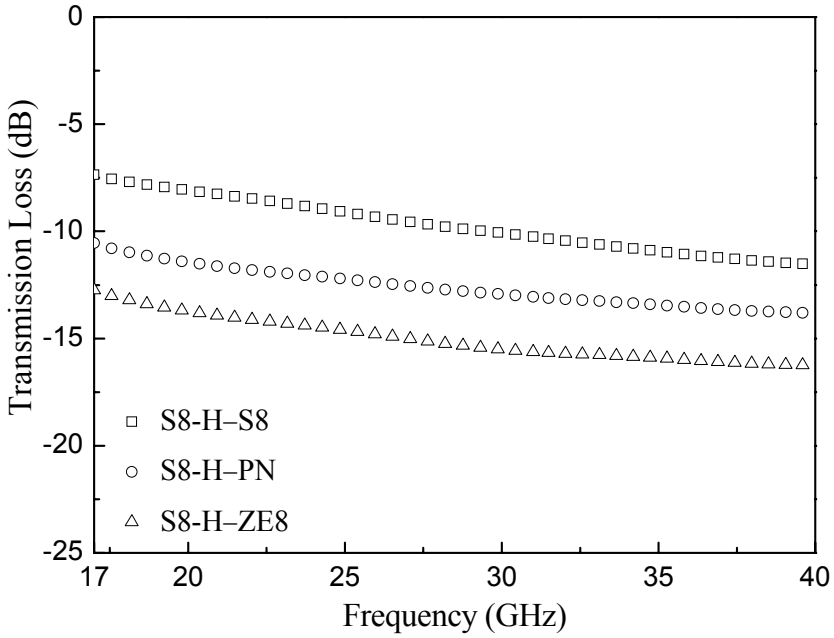

Figure 4.23 Transmission losses of double layer combinations of heat-treated S8 with as-received woven fabrics.

Absorption percentages of these combinations are shown in Figure 4.24. Highest absorption percentage was achieved for the combination of satin woven fabrics (S8-H─ZE8 combination). Absorption potential of this combination reached up to ~90%, where S8-H─PN combination revealed a maximum of ~85%, and S8-H─S8 combination remained in the vicinity of ~75% absorption. Highest absorption potential of S8-H─ZE8 combination can be explained by the highest conductivity mismatch between the layers of heat-treated S8 and as-received ZE8 woven fabrics and also their satin woven types. Absorption potentials of these combinations

decreased with frequency due to increase in their reflection loss at higher frequencies.

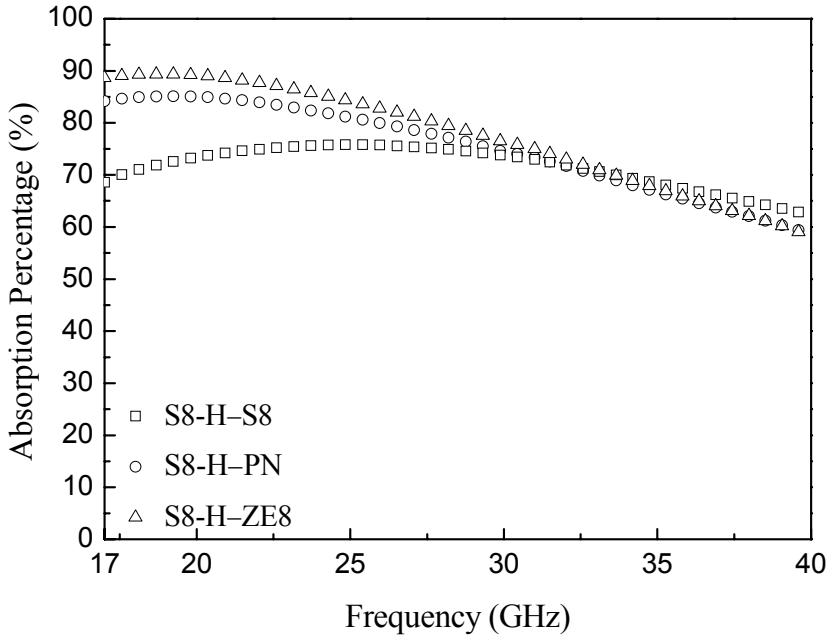

Figure 4.24 Absorption percentages of double layer combinations of heat-treated S8 with as-received woven fabrics.

Figure 4.25 and Figure 4.26 demonstrate the reflection and transmission losses for the combinations of heat-treated PN with as-received woven fabrics, respectively. Low→high electrical conductivity layer combinations were achieved when heat-treated PN was used as the first layer. In case of reflection loss, PN-H─PN and PN-H─ZE8 combinations revealed similar gradually changing trends, while PN-H─S8 combination showed a clear minimum near 25 GHz which reduced its average reflection loss. Reflected portion of EM wave at this minimum decreased up to ~1% (~-20 dB) where average reflection was ~8% (~-13 dB) at 17-40 GHz range. PN-H─PN and PN-H─ZE8 combinations revealed higher reflection losses where their average reflections were ~15% (~-8 dB) and ~12% (~-9 dB),

respectively. PN-H─S8 combination reflected less EM energy when compared to other combinations although electrical conductivity mismatch between the layers were lowest. This can be related to the high crimp structure of PN woven fabric, where reflected portion of EM wave from the second layer can easily transmit through the gaps of this structure; resulting in strengthened overall reflection loss.

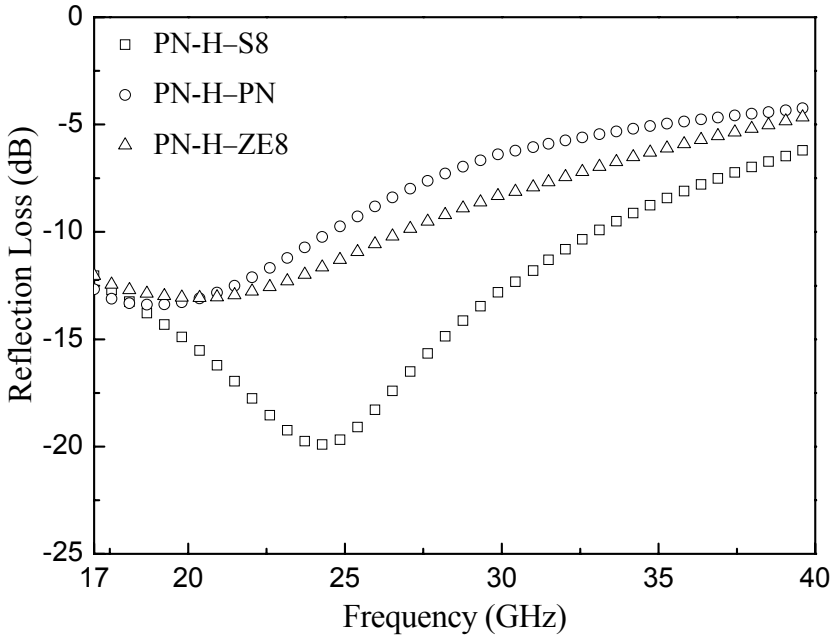

Figure 4.25 Reflection losses of double layer combinations of heat-treated PN and as-received woven fabrics.

When transmission losses of these combinations were investigated, it was observed that lowest conductivity second layer S8 brought up highest transmission which was about ~29% (~-5 dB). On the contrary, highest electrical conductivity second layer ZE8 resulted in lowest transmission which was about ~10% (~-10 dB) for PN-H─ZE8 combination (Figure 4.26).

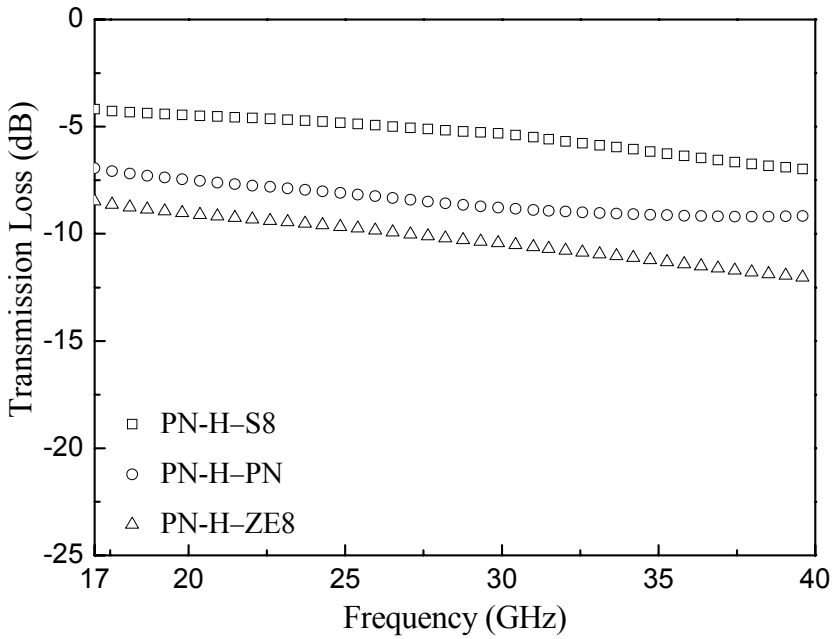

Figure 4.26 Transmission losses of double layer combinations of heat-treated PN with as-received woven fabrics.

Absorption percentages of these combinations are shown in Figure 4.27. Best absorption potential (reaching up to ~80% at lower frequencies) was recorded for PN-H─ZE8 combination due to highest electrical conductivity mismatch between heat-treated PN and as-received ZE8 woven fabrics. In case of PN-H─S8 combination frequency dependence was less dominant, and average absorption was ~63%, which is related to its highest transmission among that of the others. PN-H─PN combination revealed higher absorption potential at lower frequencies, yet it decreased with frequency reaching an average of ~66%.

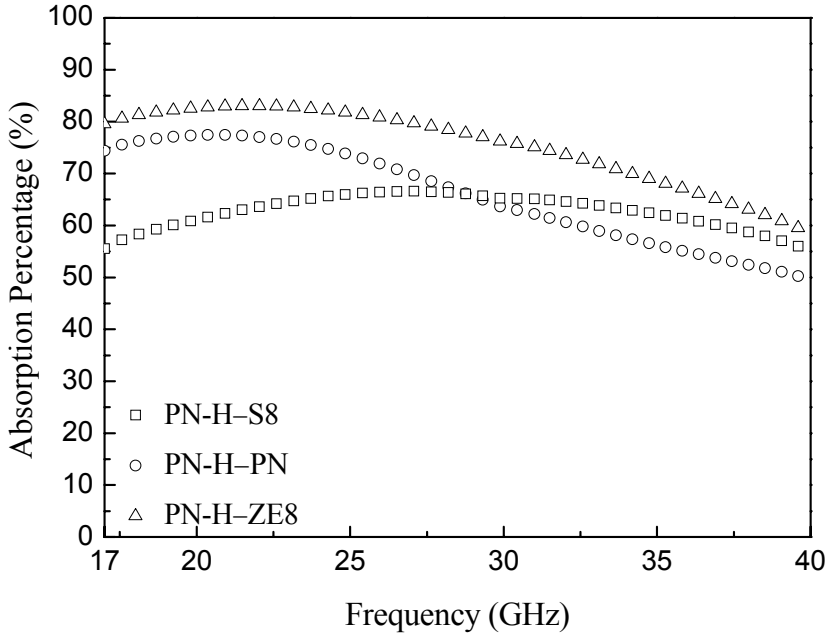

Figure 4.27 Absorption percentages of double layer combinations of heat-treated PN with as-received woven fabrics.

As the last case of this section, combinations of heat-treated ZE8 and as-received woven fabrics were conducted. Figure 4.28 demonstrates reflection losses of these combinations where losses are seen to be frequency independent. Heat-treated ZE8 woven fabric possessed highest electrical conductivity after heat-treatment, and usage of this woven fabric as the first layer strengthened the reflection loss. Combinations of this woven fabric reflected at least ~51% (~-3 dB) of the incident EM radiation.

Transmission losses of double layer combinations of heat-treated ZE8 with as-received woven fabrics are shown in Figure 4.29. Highest electrical conductivity of the first layer (heat-treated ZE8) led to lower transmission for these combinations. Average transmittances for ZE8-H─ZE8 and ZE8-H─PN combinations were ~1% (~-20 dB), whereas it was ~2% (~-17 dB) for ZE8-H─S8 combination. Low conductivity layer S8 strengthened transmission of ZE8-H─S8 combination. Observed low transmission values of these combinations makes them candidate materials for commercial EM interference shielding applications.

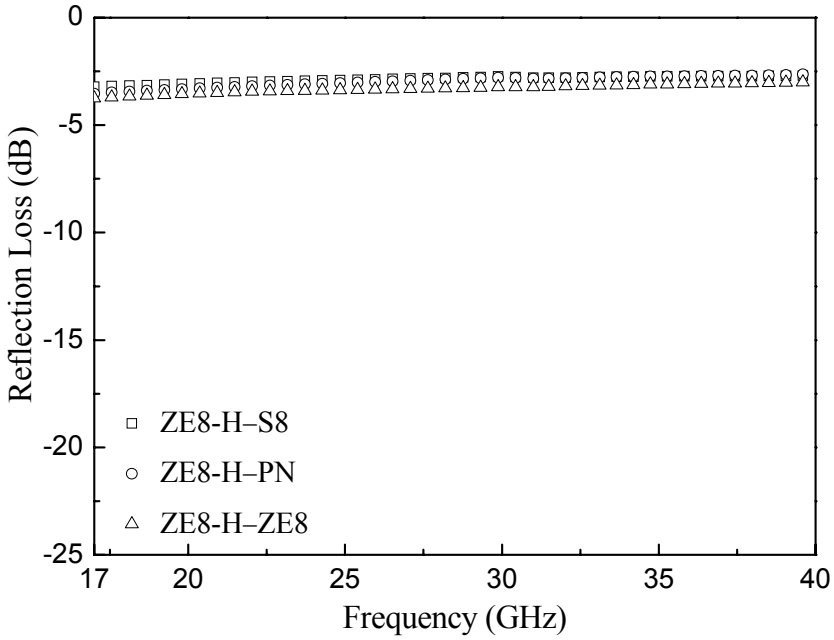

Figure 4.28 Reflection losses of double layer combinations of heat-treated ZE8 and as-received woven fabrics.

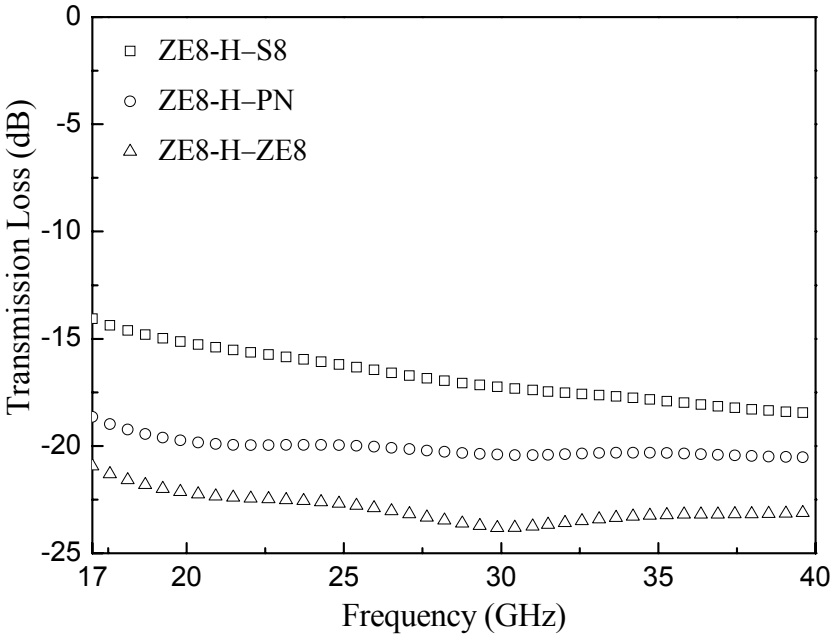

Figure 4.29 Transmission losses of double layer combinations of heat-treated ZE8 and other as-received woven fabrics.

Figure 4.30 shows absorption percentages of double layer combinations of heat-treated ZE8 with as-received woven fabrics. Absorption potentials of these combinations were quite low (below 60%). Although they revealed significantly low transmission, absorption values diminished due to their higher reflection losses.

To sum up this section, as far as combinations of as-received and heat-treated woven fabrics are concerned, better absorption potentials were achieved when heat-treated S8 woven fabric was used as the first layer. This woven fabric has the lower electrical conductivity, and placing high conductivity layers (PN and ZE8) at the back of this woven fabric improved EM wave absorption potential. On the other hand, usage of ZE8 woven fabric as the second layer except for the ZE8-H─ZE8 combination enhanced the absorption potential of the combinations with reduced reflection loss. From this point of view, best absorption potential was achieved with S8-H─ZE8 combination which consisted of satin woven fabrics suppressing internal reflections.

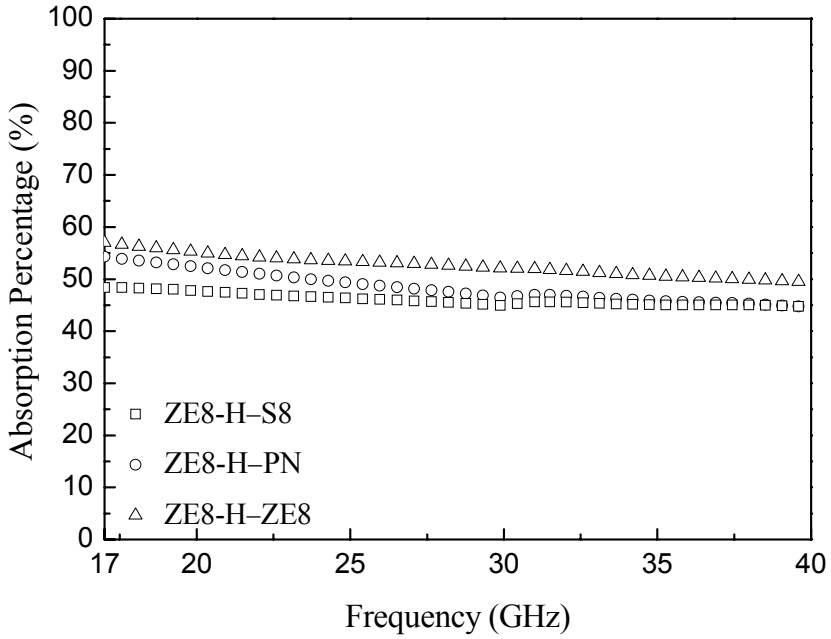

Figure 4.30 Absorption percentages of double layer combinations of heat-treated ZE8 and as-received woven fabrics.

4.2.1.2.3 Double-Layer Combinations of Heat-treated Woven Fabrics

Following to investigations on double layered combinations of two layer as-received as well as front layer heat-treated and other layer as-received woven fabrics; as the last case, double layer combinations of heat-treated woven fabrics were examined.

Reflection losses of combinations of heat-treated S8 with other heat-treated woven fabrics are demonstrated in Figure 4.31. Reflection loss of S8-H─PN-H combination was higher than that of S8-H─S8-H, where S8-H─ZE8-H combination revealed the lowest reflection loss. Although heat-treated S8 and heat-treated PN had similar electrical conductivities, higher reflection loss of S8-H─PN-H combination compared to that of S8-H─S8-H can be attributed to the woven type of PN rather than its electrical conductivity. Since PN is a plain woven fabric revealing a high crimp structure, its reflection (both externally and internally) is higher than those of the other woven types. Average reflected portions of the incident EM wave were ~15% (~-8 dB) and 20% (~-7 dB) for S8-H─S8-H and S8-H─PN-H combinations, respectively, at 17-40 GHz frequency range. A minimum was observed for S8-H─ZE8-H combination, which decreased its reflection loss below to -13 dB (~5% reflection), where average reflection of the combination was ~11% (~-10 dB). As-described in the previous sections, low→high electrical conductivity layer combination weakened the reflection loss as in the case of S8-H─ZE8-H combination.

Transmission losses of these combinations are shown in the Figure 4.32. Average transmissions were ~10% (~-10 dB) for S8-H─S8-H, 26% (~-6 dB) for S8-H─PN-H and ~2% (~-17 dB) for S8-H─ZE8-H combination. Decrease in electrical conductivity of the second layer resulted in higher transmission as in the case of aforementioned combinations. In this context, the combination of heat-treated PN woven fabric revealed highest transmission, this situation was also related to woven type of PN.

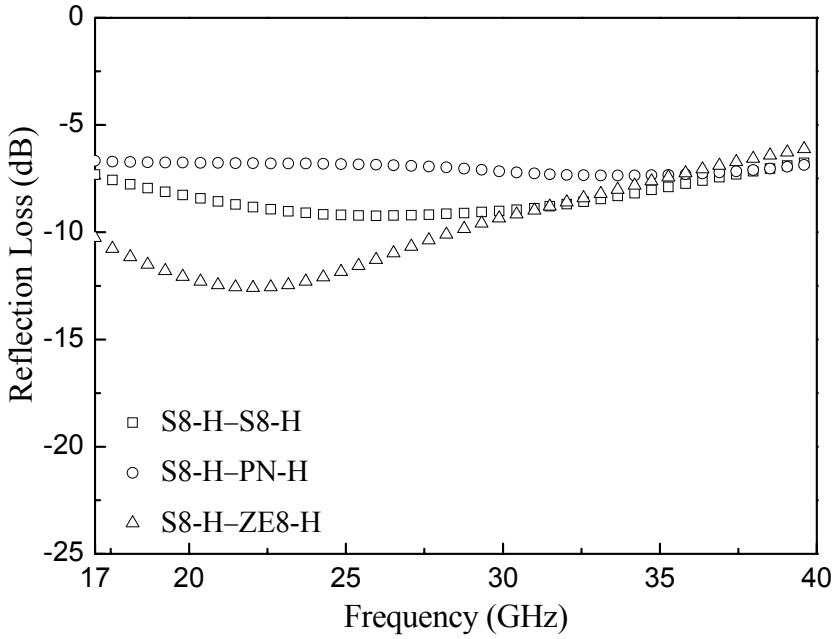

Figure 4.31 Reflection losses of double layer combinations of heat-treated S8 and other heat-treated woven fabrics.

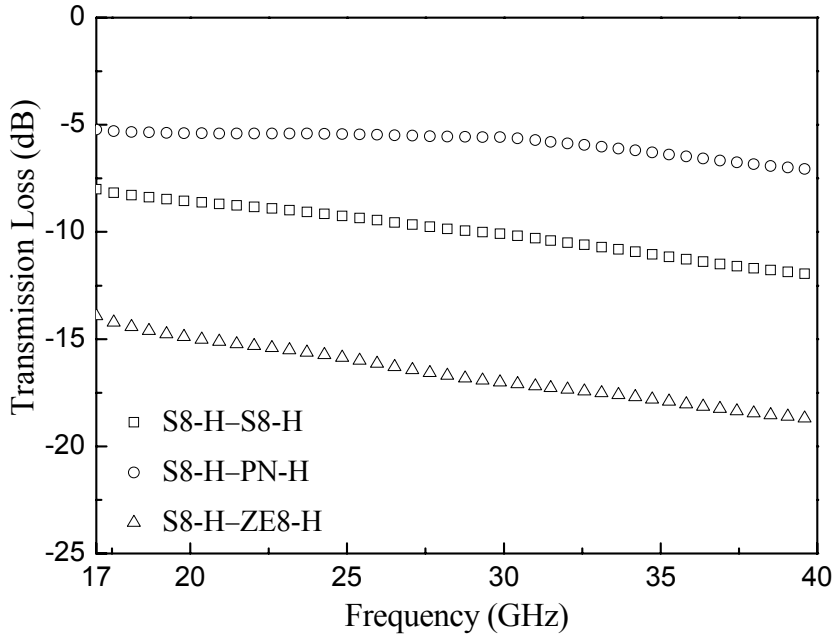

Figure 4.32 Transmission losses of double layer combinations of heat-treated S8 and other heat-treated woven fabrics.

Frequency dependence of absorption percentages are given in Figure 4.33 for these combinations. S8-H─PN-H combination revealed almost ~50% absorption at 17-40 GHz frequency range due to its higher reflection and transmission. Average absorption of S8-H─S8-H combination was higher than ~70%. Due to reduced reflection and transmission, absorption percentage of S8-H─ZE8-H combination reached to above ~90% at 19-26 GHz frequency range where its average absorption was ~86% through 17-40 GHz range.

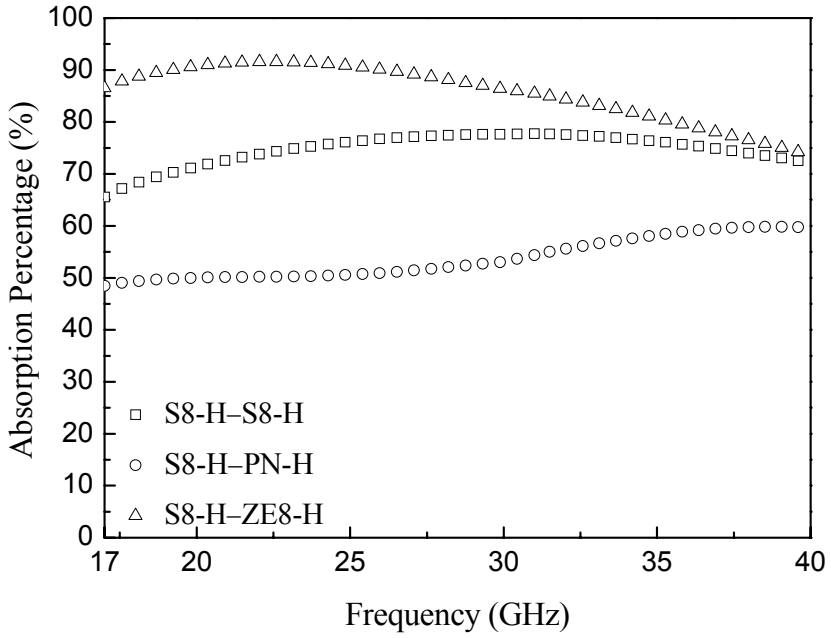

Figure 4.33 Absorption percentages of double layer combinations of heat-treated S8 with other heat-treated woven fabrics.

Figure 4.34 shows the reflection losses of combinations of heat-treated PN as the first layer. Reflection loss of combination of heat-treated PN with heat-treated ZE8 was higher than that of the others (almost ~13% (~-9 dB) of the incident wave reflected), although low→high conductivity layer sequence was satisfied. Due to existence of gaps in the high crimp structure of PN, reflected portion of EM wave

from the second layer could pass from the gaps and reach the receiving antenna side resulting in strengthened reflection loss. Heat-treated ZE8 woven fabric revealed the highest electrical conductivity among heat-treated woven fabrics, leading to the high reflection of PN-H─ZE8-H combination. Similar trends were observed for PN-H─S8-H and PN-H─PN-H combinations. When second layer conductivity increased, reflection loss of the system was strengthened. Another important point was the minima at the reflection loss curves. PN-H─ZE8-H combinations revealed a gradually changing curve, and a shallow minimum was observed near 25 GHz. On the other hand, for PN-H─S8-H and PN-H─PN-H combinations sharper minima were seen at 30 GHz and 33 GHz, respectively, where reflected fraction at these minima decreased up to ~2% (~-17 dB) and ~0.6% (~-22 dB), respectively.

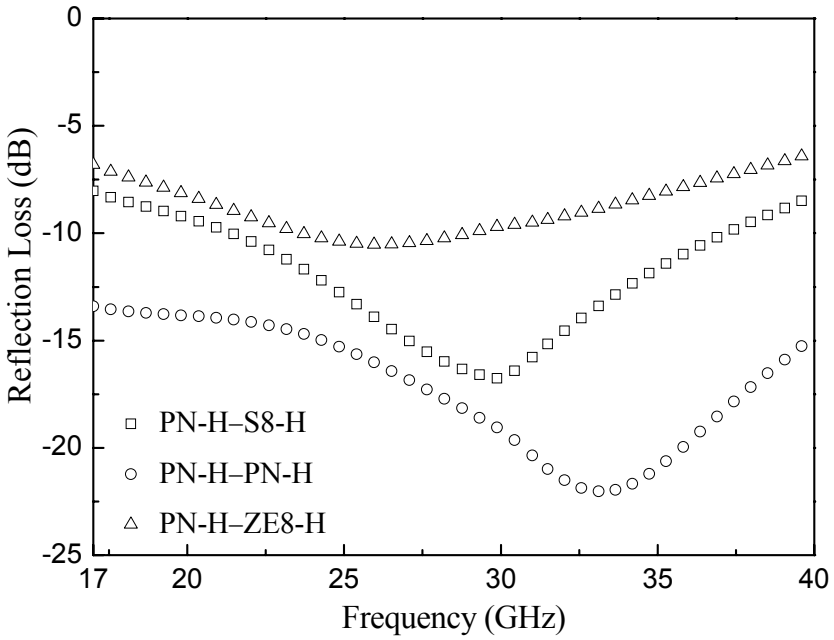

Figure 4.34 Reflection losses of double layer combinations of heat-treated PN and other heat-treated woven fabrics.

Transmission losses of these combinations are shown in the Figure 4.35. The combination of heat-treated PN (having lowest conductivity among heat-treated woven fabrics) as the second layer transmitted most, whereas the combination containing heat-treated ZE8 (having highest electrical conductivity among heat-treated woven fabrics) as the back layer transmitted least of the incident EM energy. Transmission of the combinations slightly depend on frequency change. PN-H─S8-H, PN-H─PN-H and PN-H─ZE8-H combinations revealed average transmission values of ~26% (~-6 dB), ~61% (~-2 dB) and ~6% (~-12 dB), respectively.

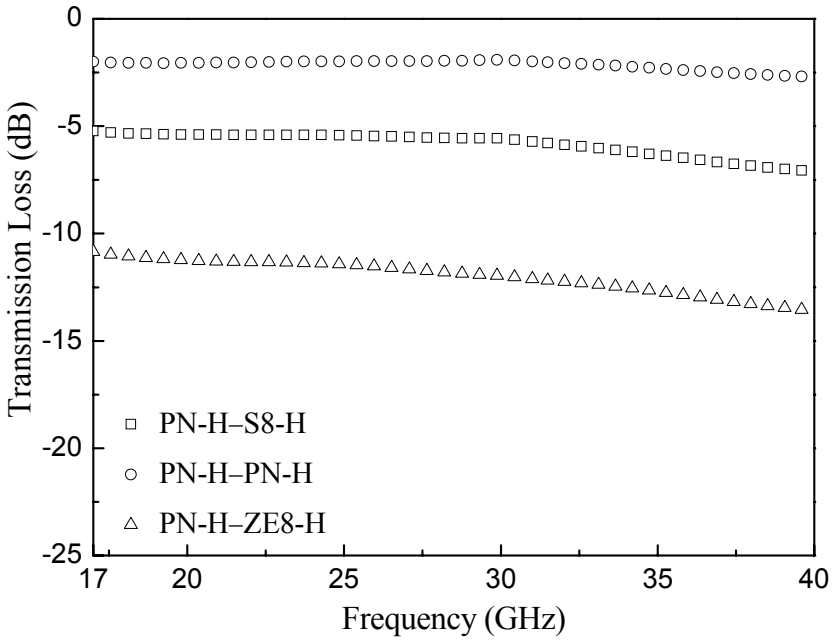

Figure 4.35 Transmission losses of double layer combinations of heat-treated PN and other heat-treated woven fabrics.

Absorption potentials of these combinations are shown in Figure 4.36. PN-H─ZE8-H combination reached up ~85% absorption potential in 25-28 GHz frequency range. On the other hand, absorption potential of PN-H─PN-H combination was quite low due to the existence of lowest electrical conductivity

woven fabrics in double layer form leading to the highest transmission (average ~61% (~-2 dB) which resulted in the lowest absorption amount. On the contrary, PN-H─S8-H combination reached ~70% absorption at 28-35 GHz frequency range due to reduced transmission when compared to PN-H─PN-H combination.

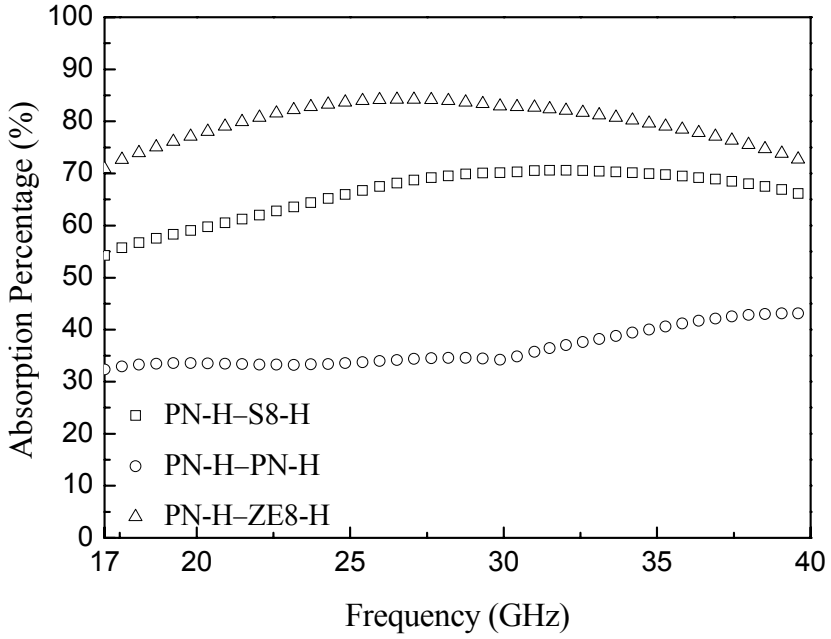

Figure 4.36 Absorption percentages of double layer combinations of heat-treated PN with other heat-treated woven fabrics.

As the last set of combinations composed of heat-treated layers, heat-treated ZE8 woven fabric was used as the first layer. Reflection losses of these combinations were seen to be frequency independent according to Figure 4.37. Average reflection percentages were ~53% (~-3 dB) for ZE8-H─S8-H, ~56% (~-3 dB) for ZE8-H─PN-H and ~50 % (~-3 dB) for ZE8-H─ZE8-H combinations.

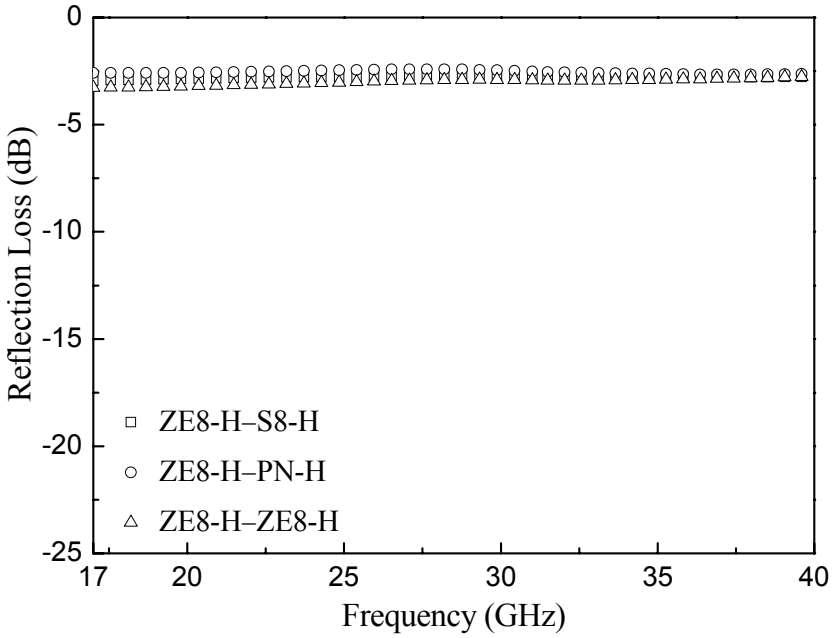

Figure 4.37 Reflection losses of double layer combinations of heat-treated ZE8 with other heat-treated woven fabrics.

Since most of the incident wave reflected from these combinations, transmission fractions of them were relatively low which can be seen in Figure 4.38. ZE8-H─PN-H combination transmitted more (average ~6% (~-12 dB)) due to the lower electrical conductivity of heat-treated PN woven fabric which possessed plain woven type. On the other hand, ZE8-H─S8-H combination transmitted ~2% (~-17 dB) of the incident wave through 17-40 GHz while ZE8-H─ZE8-H transmitted ~0.3% (~-25 dB) only.

Due to significant reflection losses of the combinations that were made up of heat-treated ZE8 as the front layer, average absorption potentials of these combinations were in the vicinity of at most 50% which is shown in Figure 4.39.

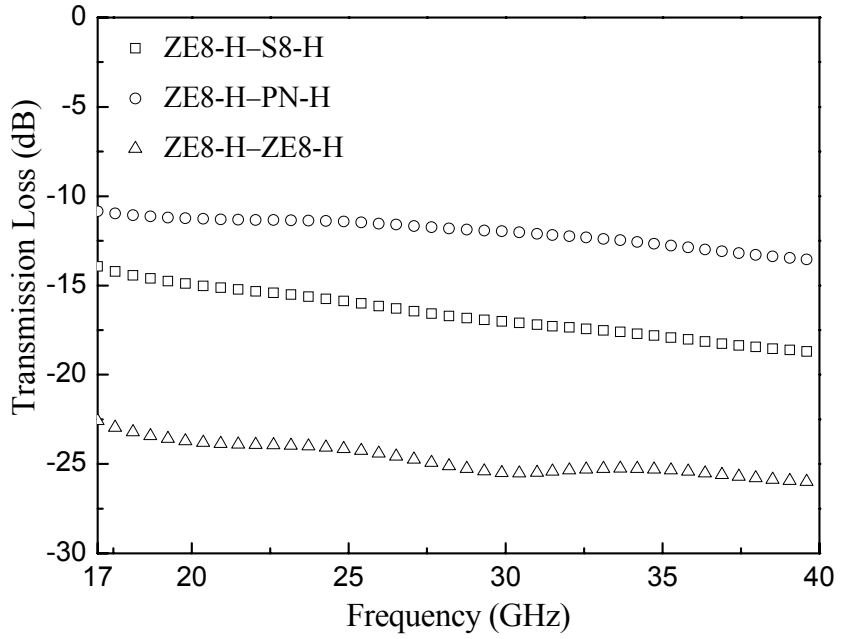

Figure 4.38 Transmission losses of double layer combinations of heat-treated ZE8 with other heat-treated woven fabrics.

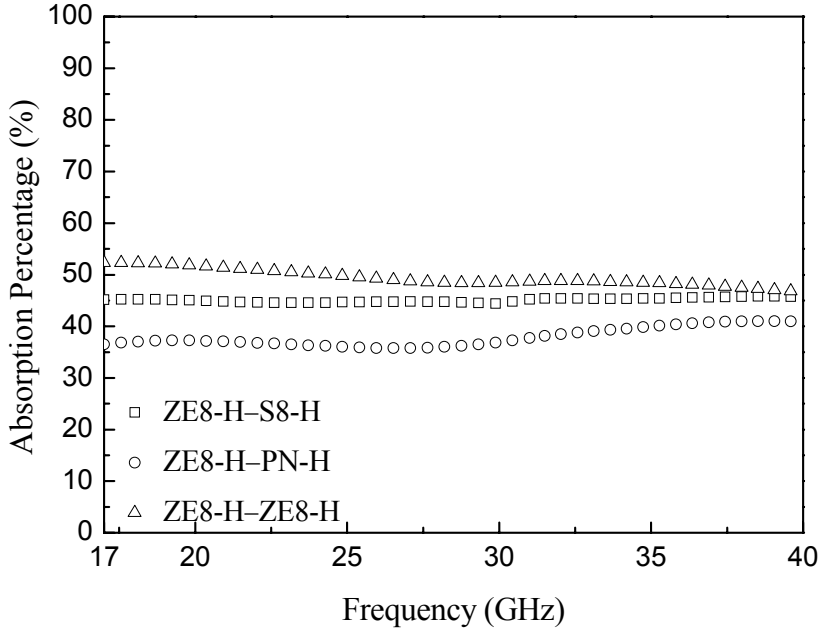

Figure 4.39 Absorption percentages of double layer combinations of heat-treated ZE8 with other heat-treated woven fabrics.

To conclude, when double layer combinations of heat-treated woven fabrics are considered, lower absorption potentials were obtained with heat-treated ZE8 woven fabric as the first layer in relation with its higher electrical conductivity. On the contrary, when heat-treated ZE8 was used as the second layer, absorption potentials were improved since high electrical conductivity mismatch was achieved between the layers of combinations. S8-H─ZE8-H combination revealed the best absorption potential among examined combinations of heat-treated woven fabrics. This potential can be attributed to both satisfying high electrical conductivity mismatch between the layers and satin woven fabric usage.

To sum up, various double layer combinations of SiC-based ceramic woven fabrics showed better EM wave absorption potential than those of single layers. Better absorption potentials were achieved when satin wovens were used in double layer combinations, and high electrical conductivity mismatch was achieved between layers. First layer should have lower electrical conductivity to eliminate higher reflection loss, while second layer should be conductive enough to achieve highest possible electrical conductivity mismatch to reduce transmission simultaneously. Absorption potentials of selected double layer combinations of S8 and ZE8 type woven fabrics are shown in Figure 4.40.

As-received and heat-treated S8 and ZE8 type combinations revealed similar absorption potentials which were higher than 90% in 18.5-26.5 GHz frequency range. This result demonstrates the fact that heat-treatment does not directly result in an improvement in the absorption potential of SiC-based ceramic woven fabrics. Rather than a direct effect, the significance of heat-treatment is to obtain woven fabrics having different electrical conductivities. In this regard, with the proper sequence of woven fabrics (low conductivity layer in front of high conductivity layer), better absorption potentials can be achieved. On the contrary, if a high electrical conductivity layer is placed in front of a low conductivity layer, absorption potential of combinations decreases (Figure 4.40 (open and filled circles)) since a significant portion of the incident EM radiation reflects from the surface before transmitting through the material system. This result demonstrates the fact that sequence of layers in multilayer form has a significant effect in achievable absorption potentials. Finally, high absorption potential (above 85%) of

properly designed double layer combinations of SiC-based ceramic woven fabrics in GHz range renders them attractive as EM wave absorbing material systems.

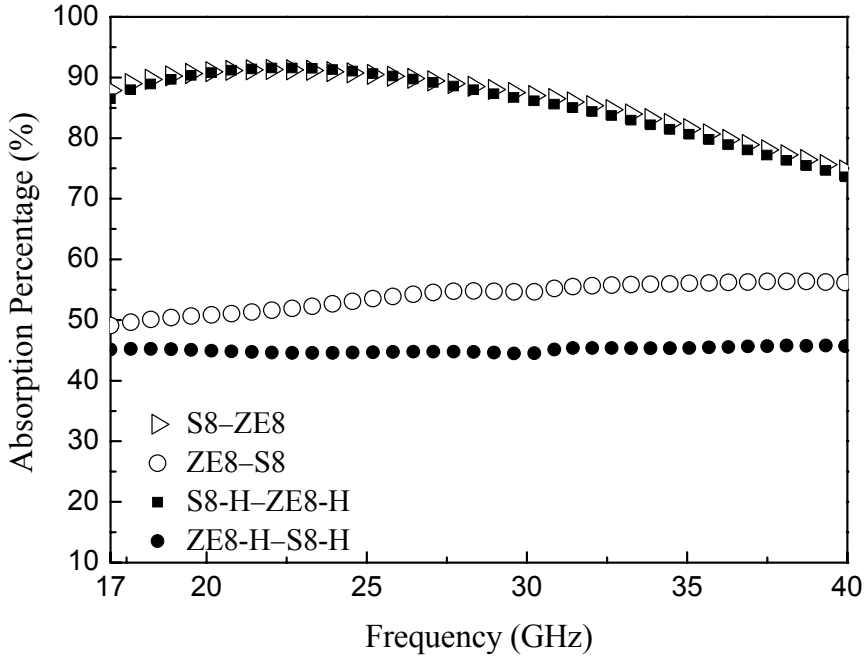

Figure 4.40 Absorption potentials of selected double layer combinations of S8 and ZE8 type woven fabrics.

4.2.2. Alumina Woven Fabrics

In this section, EM wave absorption potentials of single as well as double alumina woven fabrics were investigated.

4.2.2.1. Single-Layer Alumina Woven Fabrics

EM wave absorption potentials of plain and satin alumina woven fabrics were evaluated prior to any surface modification. Reflection losses of these two wovens revealed similar behaviors, which are shown in Figure 4.41. At lower frequencies PA woven fabric reflected ~0.6% (~-22 dB) of the incident EM wave while SA

woven fabric reflected ~0.8% (~-21 dB). Reflections were strengthened at higher frequencies where average reflection for PA and SA woven fabrics became ~1.5% (~-18 dB) and ~2% (~-17 dB), respectively.

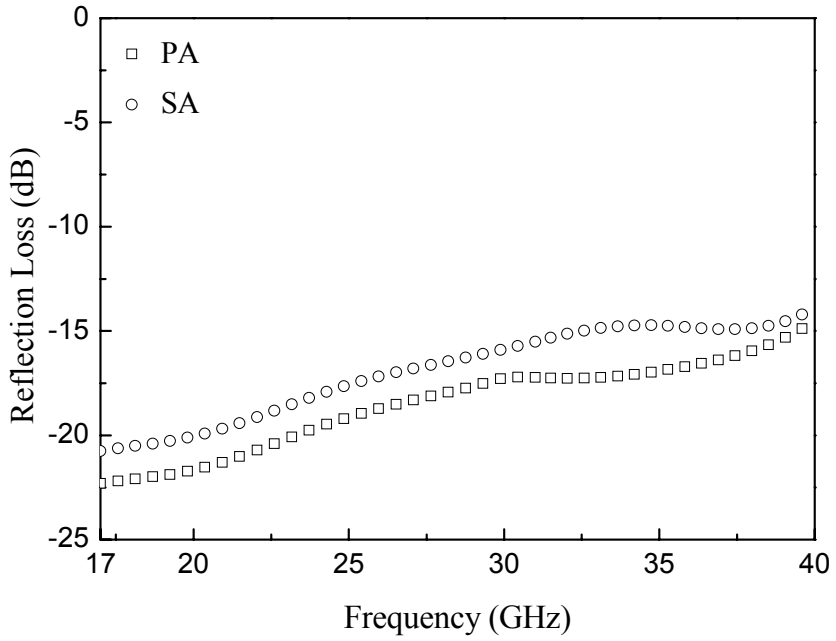

Figure 4.41 Reflection losses of single layer as-received alumina woven fabrics.

Transmission losses of alumina woven fabrics were determined to be frequency independent as shown in Figure 4.42 that are in the vicinity of 0 dB. This indicates that almost all of the EM wave transmitted through alumina woven fabrics. This situation can be attributed to the very low electrical conductivities of alumina wovens.

Absorption potentials of as-received alumina woven fabrics calculated from their reflection and transmission losses were very low (~1%) since most of the EM energy transmitted through the samples.

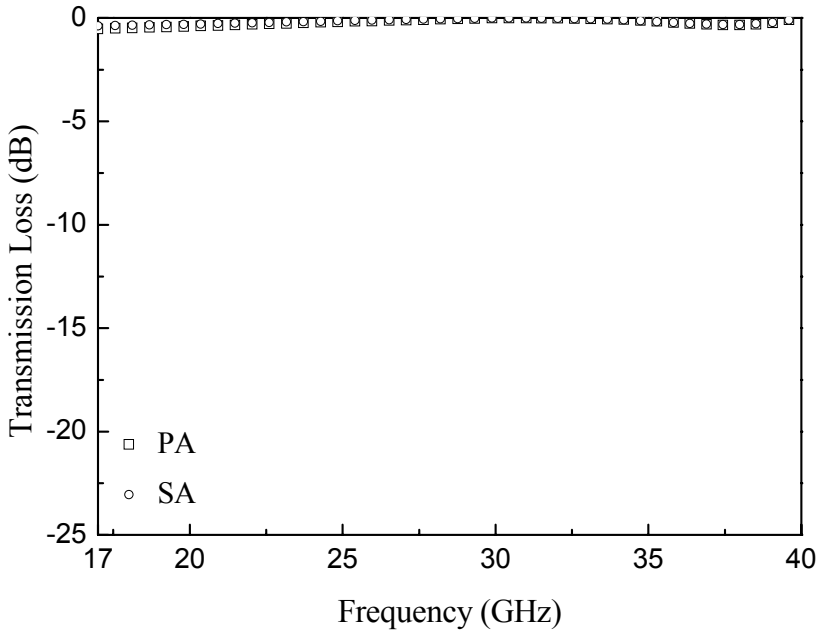

Figure 4.42 Transmission losses of single layer as-received alumina woven fabrics.

Figure 4.43 and Figure 4.44 demonstrate reflection and transmission losses of surface-modified (gold-sputtered) alumina woven fabrics, respectively. It was observed that reflection losses of the woven fabrics were strengthened while transmission were weakened after surface modification. Gold-sputtered SA woven fabric reflected less EM energy at 17-40 GHz frequency range. Average reflection was ~12% (~-9 dB) for satin woven fabric whereas it was ~56% (~-3 dB) for plain. Since plain woven fabric possessed a high level of crimp structure, reflection losses from this woven fabric could have been strengthened. Conductive layer (gold) on the surface of the woven fabrics was thought to be the main reason for increased reflection after modification.

Transmission losses of the gold-sputtered alumina woven fabrics were weakened after surface modification (Figure 4.44). Creating a high conductivity layer on the surfaces of woven fabrics caused reduction in transmission. This effect was more dominant in PA woven fabric where only ~19% (~-7 dB) of EM wave transmitted through the sample. Transmitted portion of EM radiation through SA woven fabric was about ~44% (~-4 dB) on average.

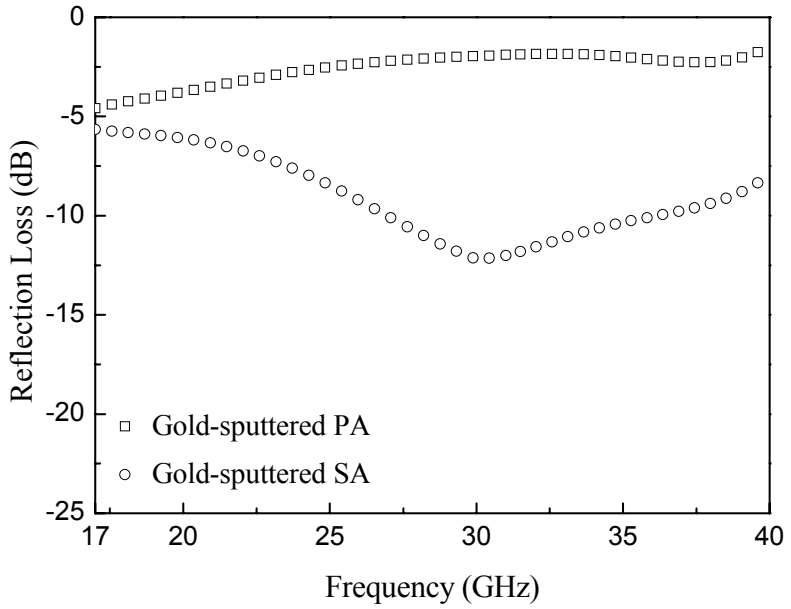

Figure 4.43 Reflection losses of gold-sputtered alumina woven fabrics.

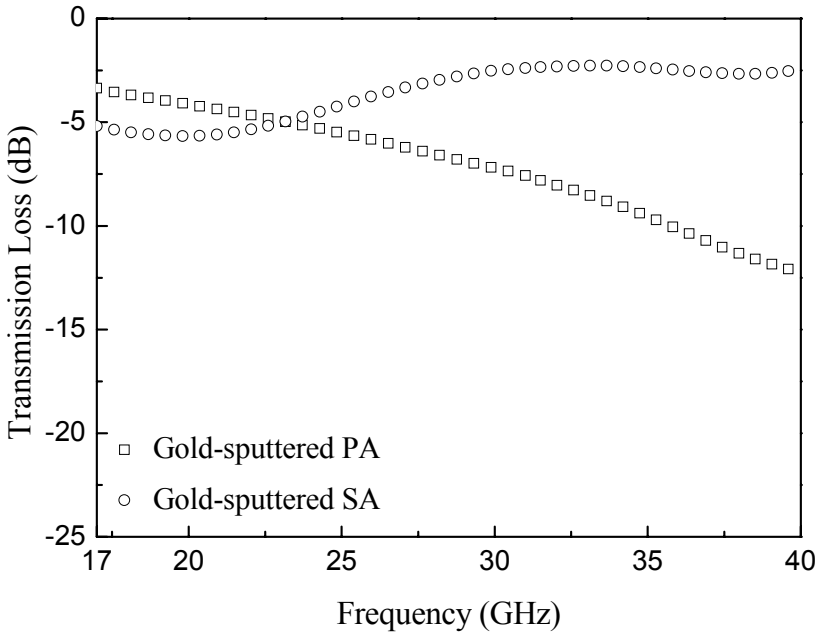

Figure 4.44 Transmission losses of gold-sputtered alumina woven fabrics.

Modification of the surface of electrically insulating alumina woven fabrics with a conductive coating changed their interaction with EM waves resulting in reduced transmission and increased reflection. Absorption potential of single layer gold-sputtered alumina woven fabrics was low in the vicinity of 30-40%; however, it was still better than that of as-received condition owing to reduced transmission after modification.

4.2.2.2. Double-Layer Alumina Woven Fabrics Combinations

EM wave absorption potentials of single layer as-received and surface modified alumina woven fabrics did not seen to be sufficient for their usage as EM wave absorbers in GHz frequency. To achieve better absorption potentials double layer combinations of alumina woven fabrics were conducted.

Self-combinations of as-received alumina woven fabrics revealed similar results to single layer as-received alumina woven fabrics, since most of the EM wave transmitted through the insulative layers. High transmission losses of these combinations resulted in very low absorption potential. However, this situation was different when combinations were composed of surface-modified layers.

Reflection losses of double layered surface-modified woven fabrics are given in Figure 4.45. Reflection loss of gold-sputtered SA woven fabric in self-combination form was low and revealed a minimum at 27 GHz where reflection loss dropped to below -21 dB meaning that at most 0.6% of EM wave reflected from the structure. Self-combination of gold-sputtered PA woven fabric with itself possessed very high reflection loss. Since chemical compositions of alumina woven fabrics and applied surface modifications are identical, the reason of this difference can be attributed to woven type. Due to high level of crimp structure of the plain wovens, reflected portion of the EM wave from the combinations containing plain woven fabrics was higher compared to that of satin woven type.

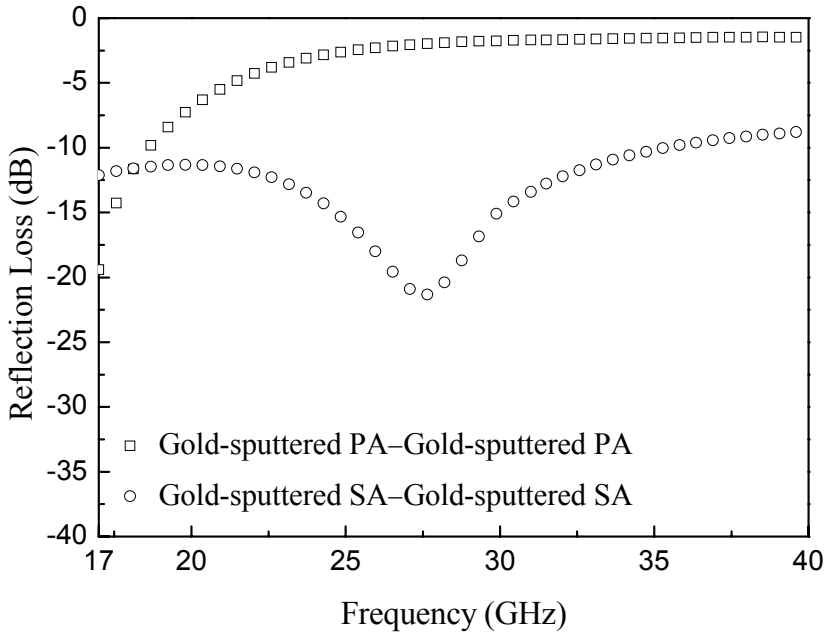

Figure 4.45 Reflection losses of double layered gold-sputtered alumina.

Similar to reflection, transmission of double layered surface-modified SA woven fabric combination was lower, which is shown in Figure 4.46. This combination's transmission was almost independent of frequency in 17-40 GHz range with an average value of ~-22 dB (transmitted portion of the EM wave < 0.6%). In case of combination of plain woven fabric decrease in transmission was more obvious in double layered self-combination.

Due to both reduced reflection and transmission of self-combination of double layered surface modified SA woven fabrics, significantly high absorption potential reaching to ~98% was obtained (Figure 4.47). Average absorption of this combination was ~93% along 17-40 GHz frequency range. On the contrary, related to the higher reflection and transmission of double layered gold-sputtered PA woven fabric self-combination, highest reached absorption potential was ~48%.

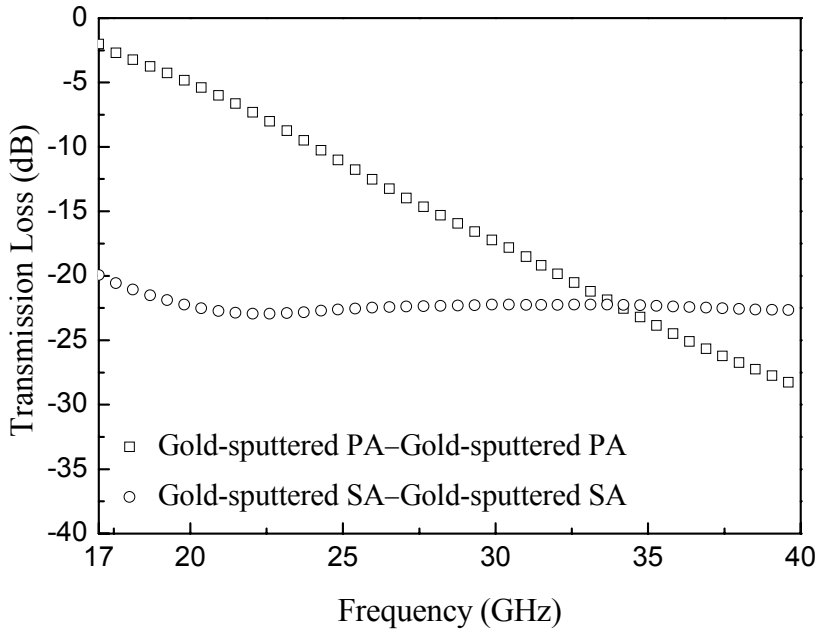

Figure 4.46 Transmission losses of double layered gold-sputtered alumina woven fabrics.

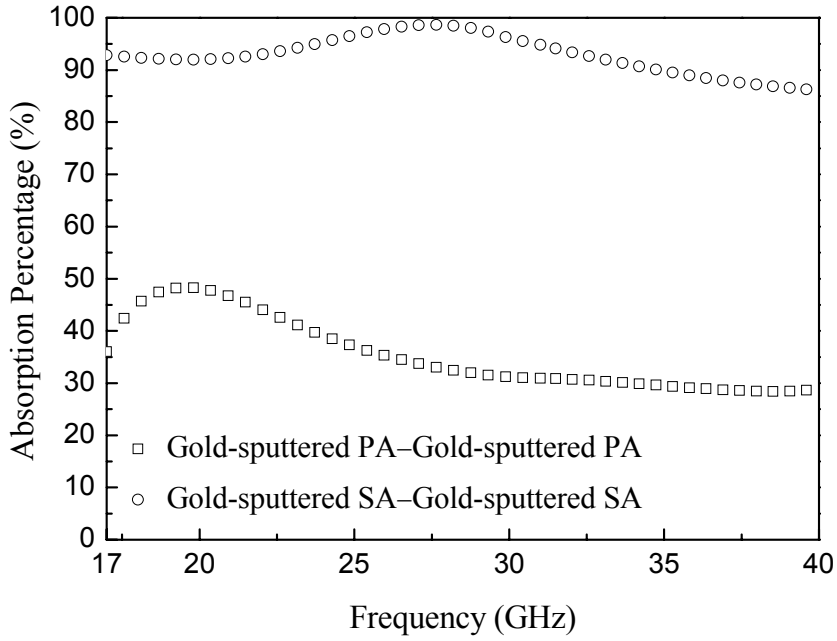

Figure 4.47 Absorption potential of double layered gold-sputtered alumina woven fabrics.

To sum up, absorption potential of as-received and surface-modified alumina woven fabrics was investigated in this section. Single layer as-received and modified alumina woven fabrics can not be used as EM wave absorbers due their insufficient absorbing capability. This situation is also valid for double layer combinations of as-received woven fabrics. Double layered modified SA woven fabric combination achieved significantly high absorption potentials (above 98%) due to reduced reflection and transmission which makes it a powerful candidate material system for EM wave absorption applications in GHz frequency range.

4.2.3. Double-Layer Combinations of Alumina and SiC-based Woven Fabrics

Absorption potentials of alumina and SiC-based woven fabrics were individually investigated up to this section. To achieve different electrical conductivity layer sequences and to investigate the effect of this arrangement on the resulting EM wave interaction, combinations containing alumina and SiC-based woven fabrics were conducted at this section.

4.2.3.1. Combinations of As-received Alumina and SiC-based Woven Fabrics

Reflection losses of combinations where as-received PA woven fabric was used as the first layer are shown in Figure 4.48. In this figure it was observed that high conductivity second layer (SiC-based woven fabric layer) was very effective on the reflection losses of the combinations. Among the as-received SiC-based ceramic fabrics, ZE8 type woven fabric, revealing the highest electrical conductivity, resulted in high reflection loss of the combination where almost ~36% (~-4 dB) of the incident wave reflected. On the contrary, combination of low conductivity S8 woven fabric revealed lowest reflection loss where reflected fraction of the EM wave was ~16% (~-8 dB) on average.

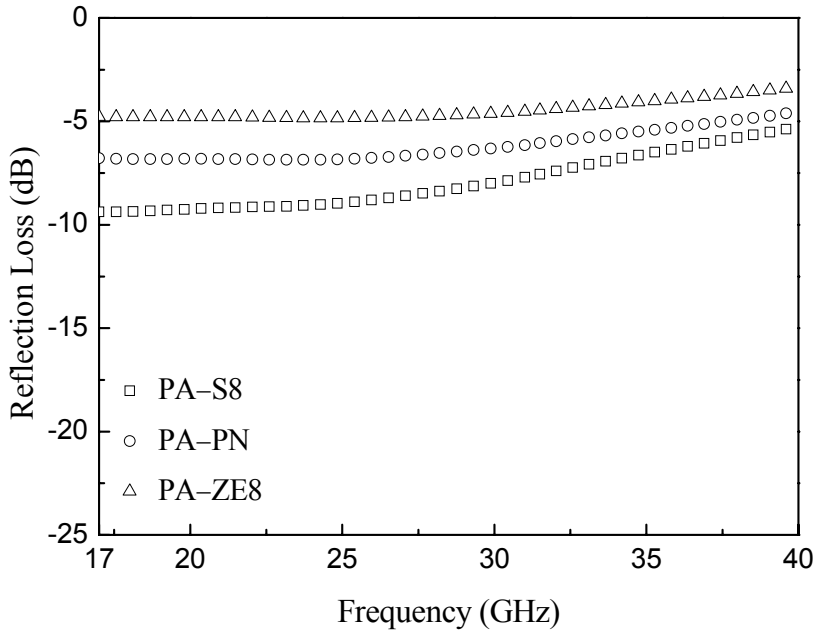

Figure 4.48 Reflection losses of the combinations of as-received PA with SiC-based woven fabrics.

Similar to the reflection loss, second layer which was placed at the back of the alumina plain woven fabric was also effective in transmission losses of the combinations (Figure 4.49). Combinations which showed higher reflection loss revealed lower transmission. Combination of S8 woven fabric transmitted more (~-4 dB = ~42% on average) EM wave compared to the combination ZE8 woven fabric (~-8 dB = ~15% on average). Transmission losses of combinations were seen to be frequency independent as in the case of single layer as-received SiC-based woven fabrics in Figure 4.9. Since alumina plain woven fabric transmitted almost all of the incident EM radiation reaching to the second layer, transmission and reflection losses of the combinations were very similar to that of the single layer as-received SiC-based woven fabric.

Absorption potentials of combinations (Figure 4.50) were below 60% due to high reflection and transmission. Combination of PN woven fabric revealed better absorption potential owing to optimized reflection and transmission compared to other combinations.

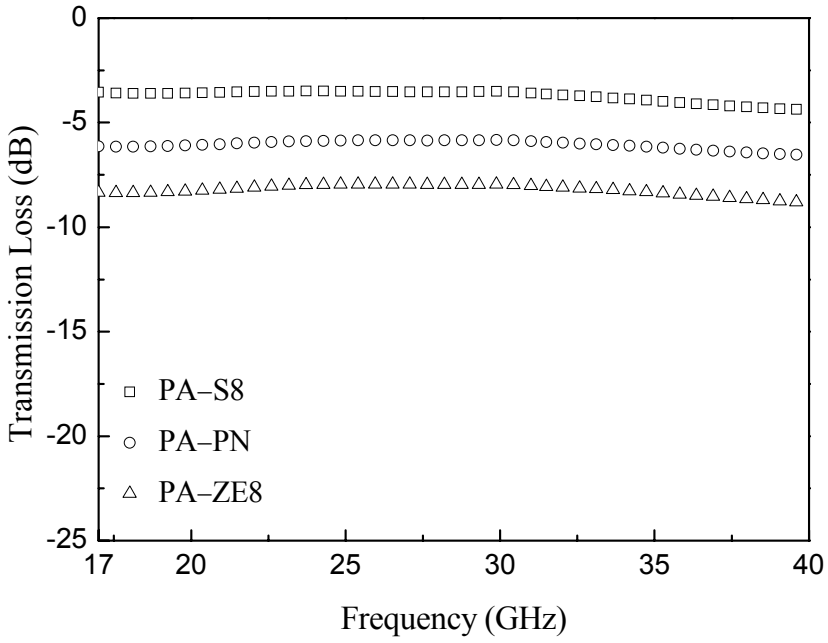

Figure 4.49 Transmission losses of the combinations of as-received PA with SiC-based woven fabrics.

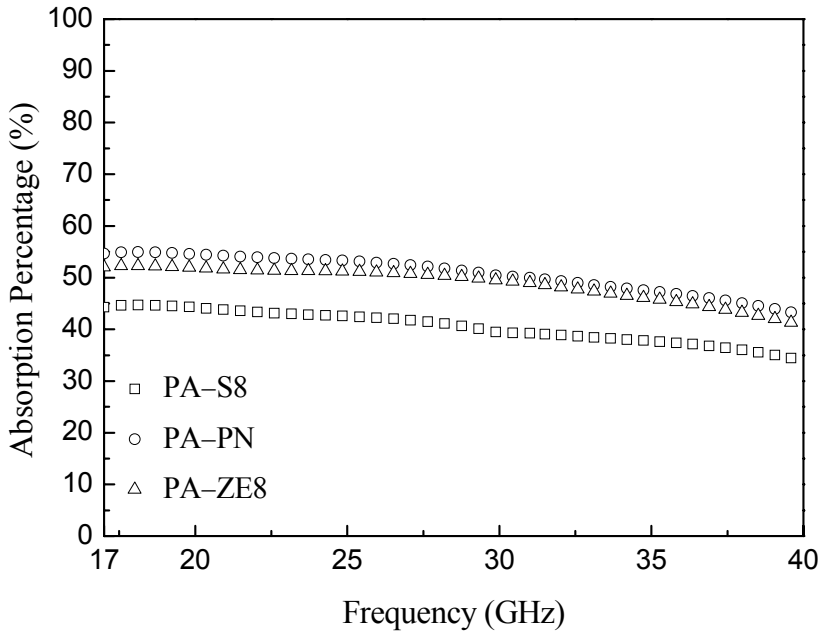

Figure 4.50 Absorption percentages of the combinations of as-received PA with SiC-based woven fabrics.

Absorption potentials of the as-received SA and SiC-based woven fabric double layer combination were investigated after performing as-received PA and SiC-based woven fabric combinations in order to examine whether woven type of alumina fabric was effective in absorption potential of the combinations or not. Reflection and transmission losses of these combinations are presented in Figure 4.51 and Figure 4.52, respectively.

Similar to combinations of alumina plain woven fabric, second layer was effective in both reflection and transmission loss of the double layer structure containing satin alumina woven fabric. Combination of ZE8 woven fabric revealed highest reflection loss where lowest reflection loss belonged to the combination of S8 woven fabric as the second layer. Figure 4.51 is very similar to Figure 4.48. Calculated average reflected portions were ~15% (~-8 dB) for SA─S8, ~25% (~-6 dB) for SA─PN and ~35% (~-5 dB) for SA─ZE8 combination.

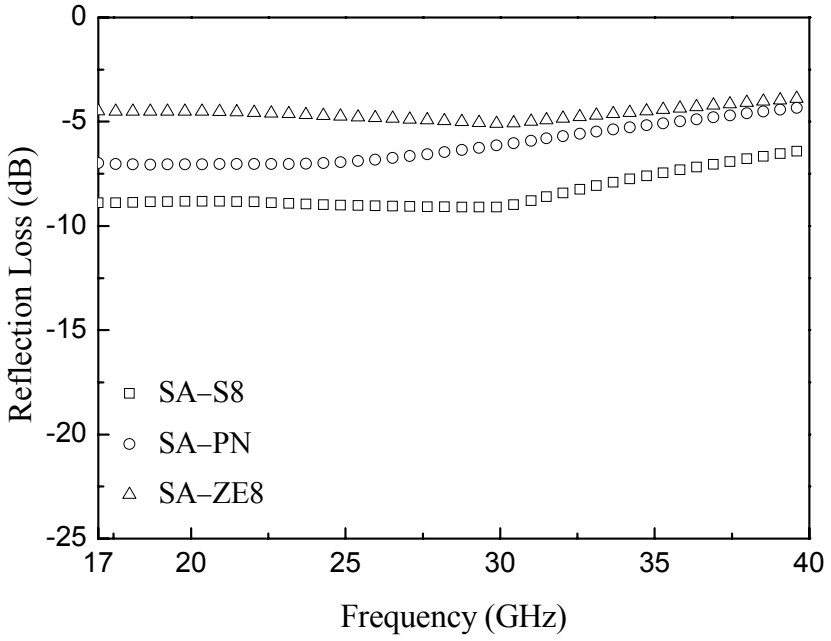

Figure 4.51 Reflection losses of the combinations of as-received SA and SiC-based woven fabrics.

When transmittances of the combinations were investigated, it was observed that the combination of ZE8 woven fabric transmitted least (on average ~-9 dB = ~14%), while the combination of S8 type woven fabric transmitted most (on average ~-4dB = ~ 42%). High electrical conductivity second layer in combinations resulted in higher reflection and lower transmission as in the case of the combination of as-received alumina satin and ZE8 woven fabric. Absorption potentials of these combinations (Figure 4.53) were low (below 60%) similar to the combinations of as-received PA and SiC-based woven fabrics.

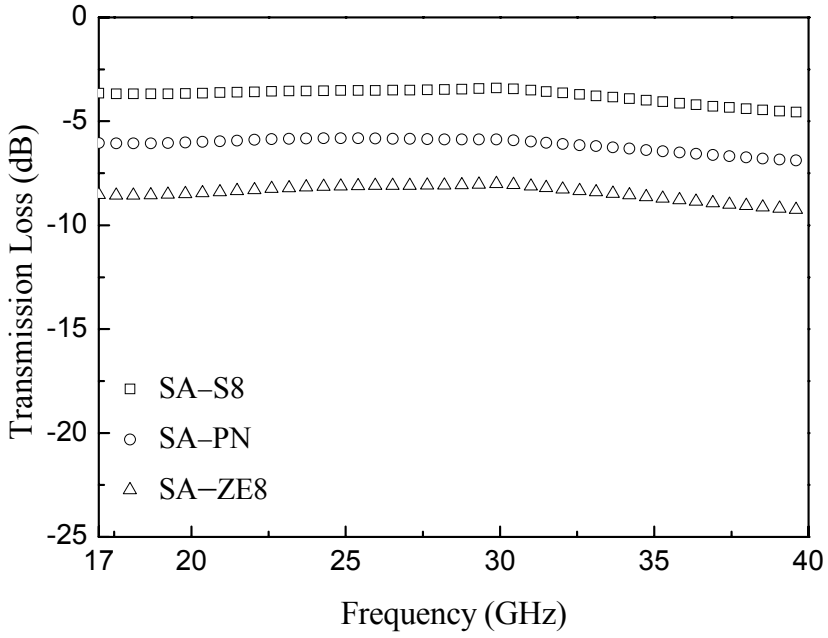

Figure 4.52 Transmission losses of the combinations of as-received SA and SiC-based woven fabrics.

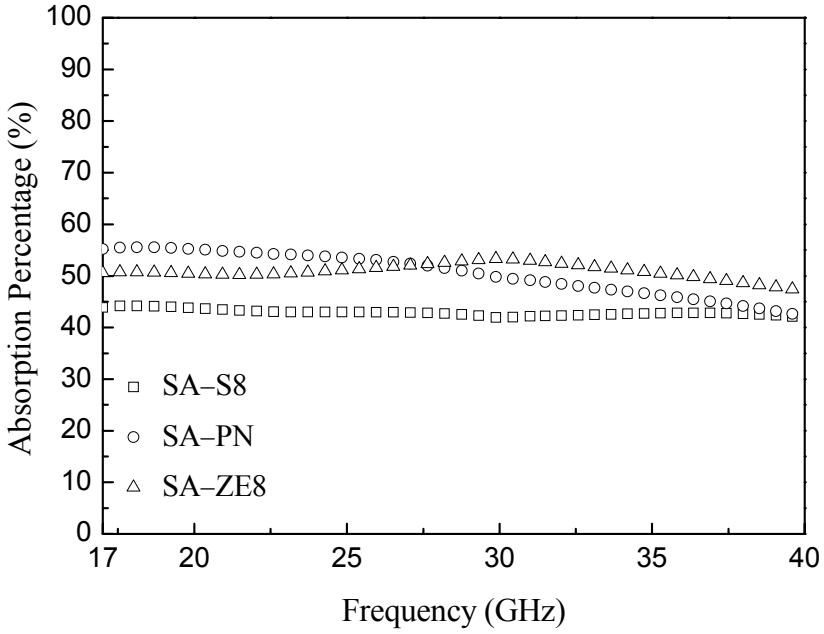

Figure 4.53 Absorption percentages of the combinations of as-received SA and SiC-based woven fabrics.

4.2.3.2. Combinations of As-received Alumina and Heat-Treated SiC Woven Fabrics

As the second set, combinations of as-received alumina and heat-treated SiC-based woven fabrics were examined. Reflection and transmission losses of the combinations are shown in Figure 4.54 and Figure 4.55, respectively. Combination containing heat-treated ZE8 woven fabric revealed the highest reflection loss (on average ~-2dB= ~58% reflection) among the other combinations. It showed an almost frequency independent character. Similar to the pre-described combinations electrical conductivity of the second layer SiC-based woven fabric played a dominant role in the reflection and transmission losses.

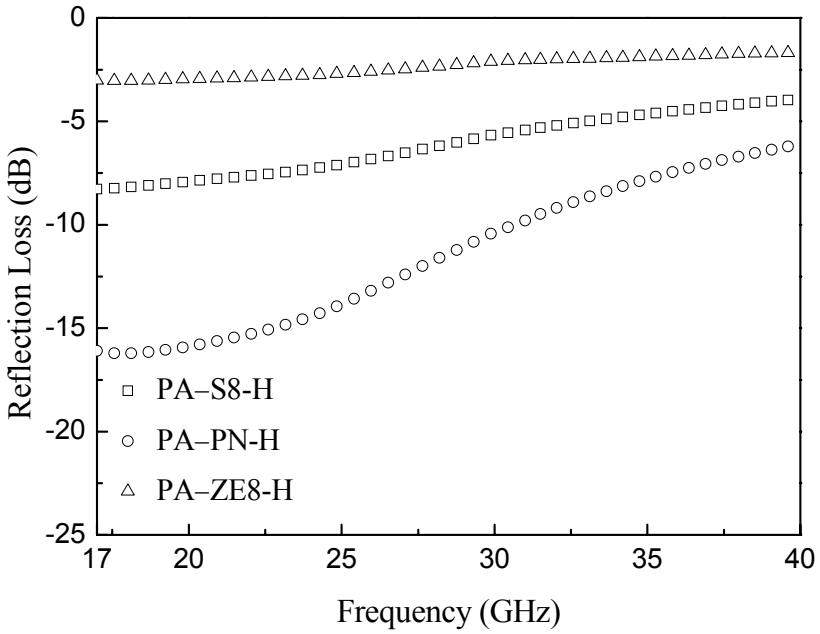

Figure 4.54 Reflection losses of the combinations of as-received PA and heat-treated SiC-based woven fabrics.

Heat-treated PN woven fabric revealed the lowest electrical conductivity in heat-treated state, and combination containing this woven fabric showed the highest transmission and lowest reflection loss as expected (Figure 4.55). Highest transmission of the combination of as-received PA and heat-treated PN woven fabric can be attributed to their woven type and lower electrical conductivities. Plain type of both layers could have resulted in the highest transmission of the combination. ~67% (~-1dB) of the incident EM wave transmitted through this combination where transmission value was only ~8% (~11 dB) for the combination having heat-treated ZE8 woven fabric.

Figure 4.56 shows the absorption potentials of these combinations, where as-received PA and heat-treated PN woven fabric combination revealed quite low absorption percentage, which has resulted from the highest transmission of the combination.

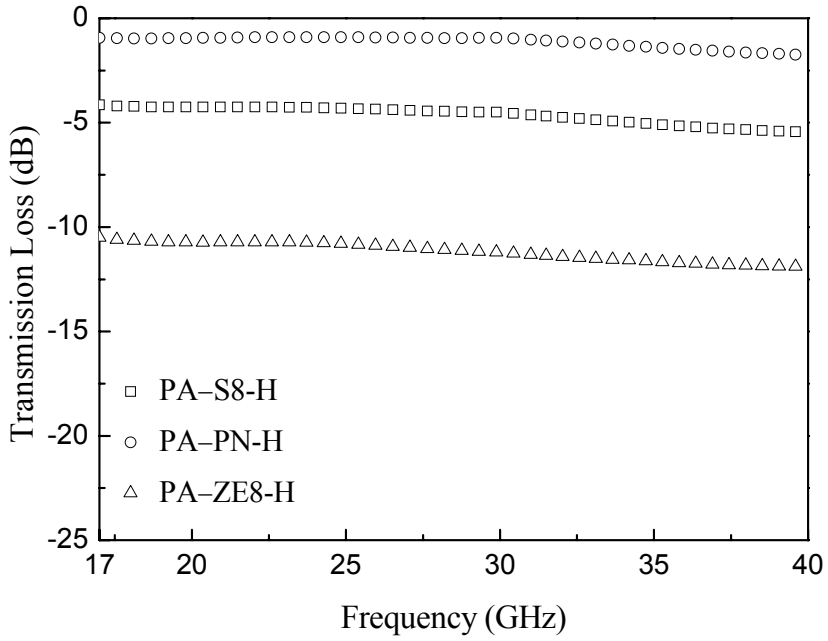

Figure 4.55 Transmission losses of the combinations of as-received PA and heat-treated SiC-based woven fabrics.

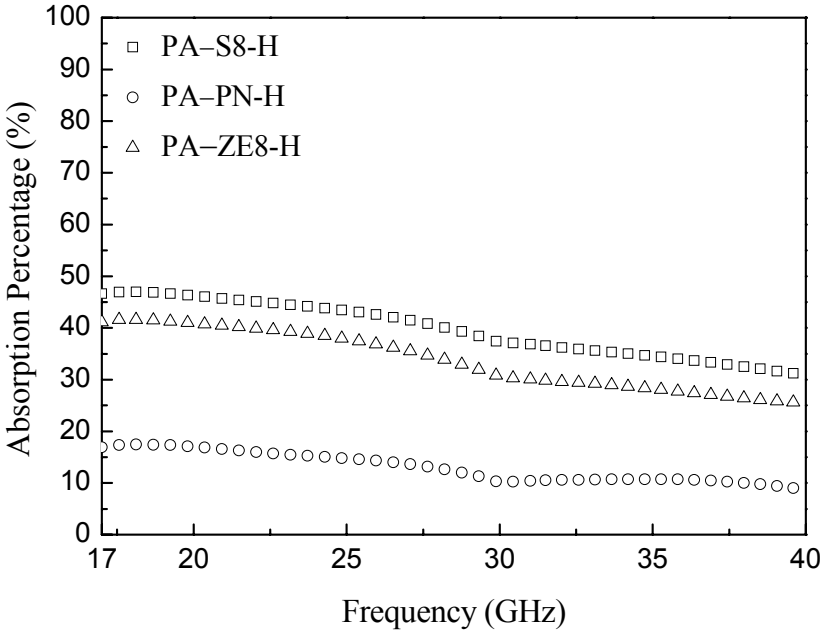

Figure 4.56 Absorption percentages of the combinations of as-received PA and heat-treated SiC-based woven fabrics.

Pre-mentioned combinations were repeated using SA woven fabrics as the first layer of the combination. Figure 4.57, Figure 4.58 and Figure 4.59 demonstrate reflection and transmission losses and absorption percentages of combinations of as-received SA and heat-treated SiC-based woven fabrics, respectively. These figures are similar to that of Figure 4.54, Figure 4.55 and Figure 4.56 which represents EM wave interaction of combinations composed of PA and heat-treated SiC-based woven fabrics. From this point of view, it can be stated that woven type of the first alumina layer, either plain or satin, did not reveal any major effect on reflection and transmission losses and on resulting EM wave absorption potentials of the combinations. Second layer placed at the back of the first layer was very effective on transmission and reflection losses, as a result of this, they were the dominant factor in the absorption potential of the combinations.

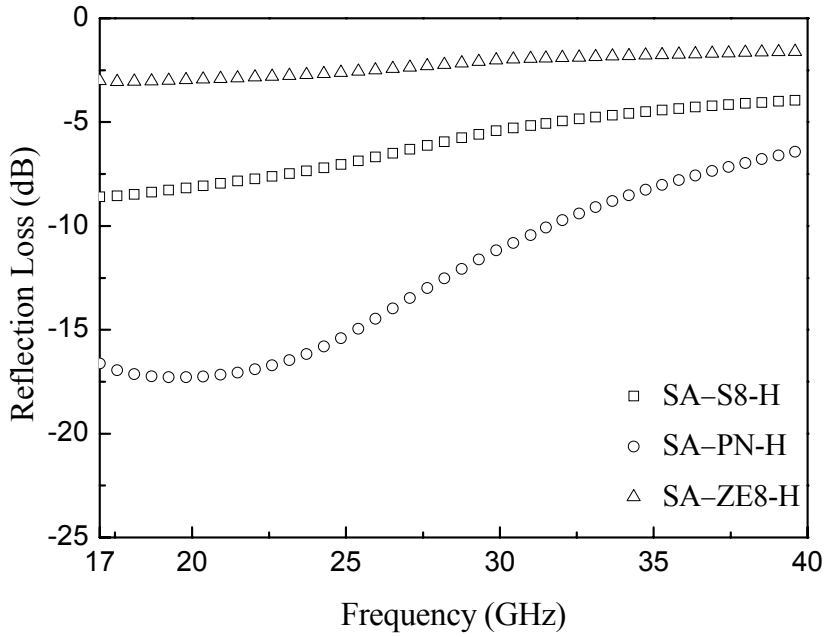

Figure 4.57 Reflection losses of the combinations of as-received SA and heat-treated SiC-based woven fabrics.

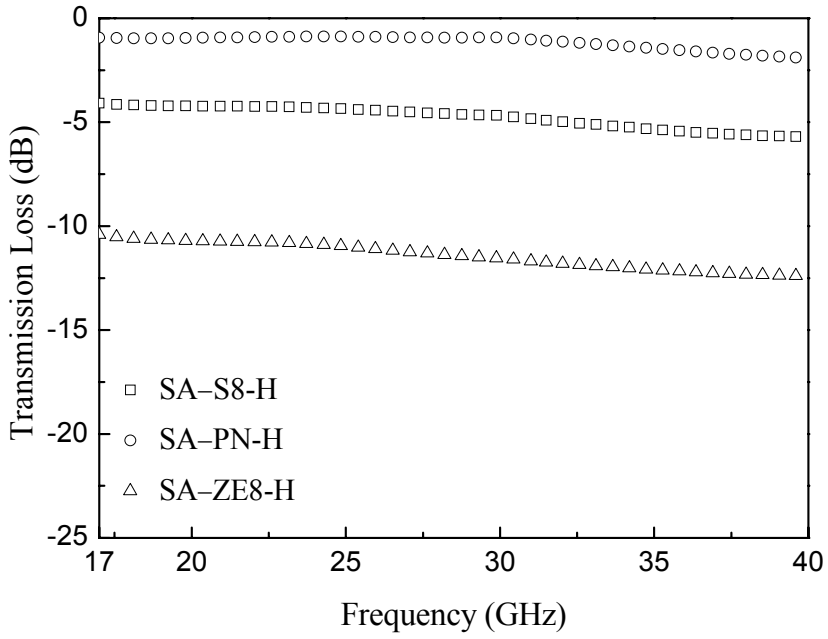

Figure 4.58 Transmission losses of the combinations of as-received SA and heat-treated SiC-based woven fabrics.

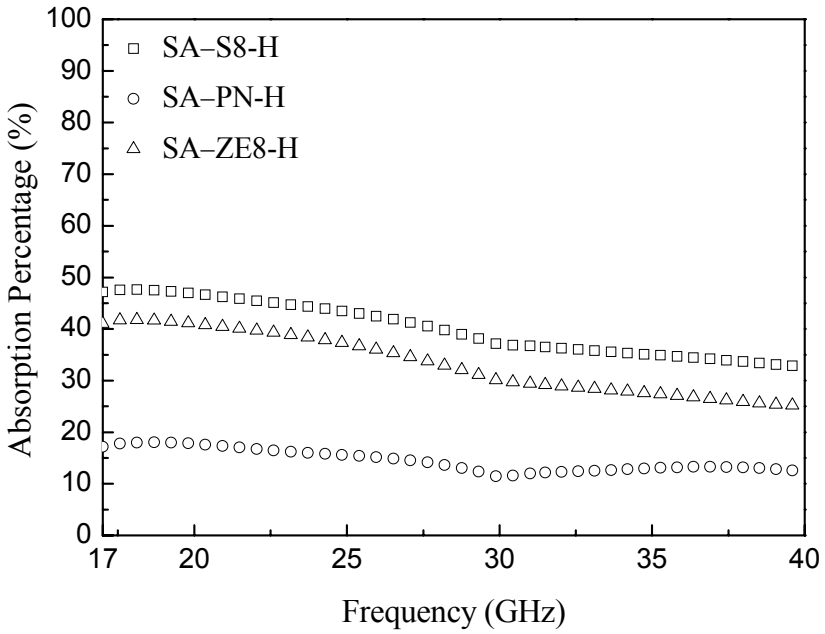

Figure 4.59 Absorption percentages of the combinations of as-received SA alumina and heat-treated SiC-based woven fabrics.

4.2.3.3. Combinations of Surface Modified Alumina and As-received SiC-based Woven Fabrics

In this section, investigations were conducted on double layer combinations containing gold-sputtered alumina woven fabric as the first layer. First of all, combinations of gold-sputtered alumina and as-received SiC-based woven fabrics were carried out. It was observed that all combinations revealed similar reflection losses (Figure 4.60) indicating that second layers (SiC-based woven fabrics) were less effective in this particular case. Reflection losses of these combinations were quite high, ~53% (~-3 dB) of the incident EM wave reflected from gold-sputtered PA─ZE8 combination, and this fraction was ~49% (~-3 dB) and ~43% (~-4 dB) for combinations of PN and S8 woven fabrics, respectively. Although the curves were similar, difference in percentages of reflected portions is related to high decibel levels. At these levels small changes in the curves results in high variance in extracted fraction values. High conductivity gold coating on the surface of the first layer revealed a dominant role on reflection loss of the combinations.

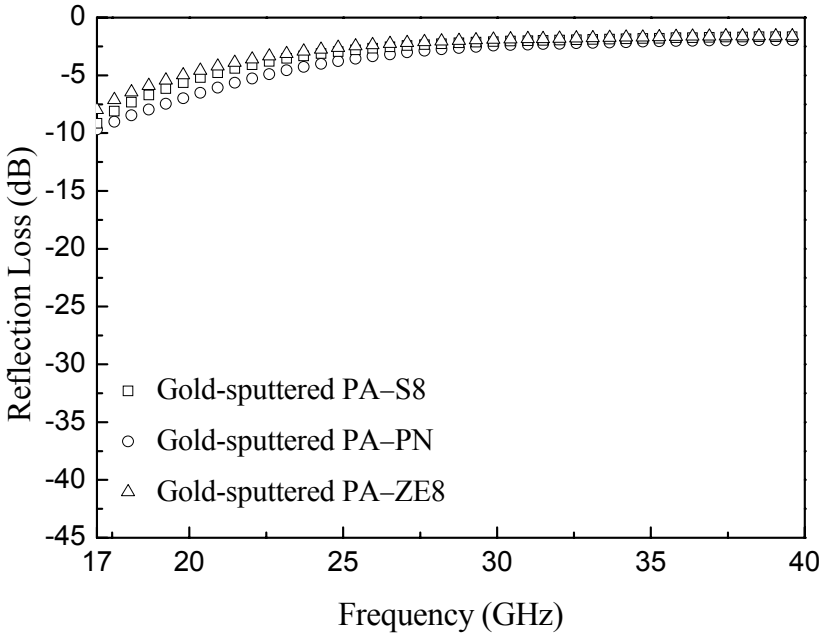

Figure 4.60 Reflection losses of the combinations of gold-sputtered PA and as-received SiC-based woven fabrics.

Transmission losses of these combinations are shown in Figure 4.61. Weakening of transmission with increasing frequency was noticed, and it was observed that second layers were effective in transmissions of the combinations. First layer reflected EM wave as much as it could, and then remaining portion of the radiation passed through the second layer and reached the other side. As a result of this, electrical conductivity of the second layer had an observable influence on the transmission of the combinations. Combination containing ZE8 woven fabric (highest electrical conductivity fabric among as-received SiC-based fabrics) transmitted least of the EM wave having an average of ~2% (~-17 dB) and reached to below ~0.3% (~-25 dB) transmission at higher frequencies. Combination having as-received S8 woven fabric transmitted significantly ~8% (~-11 dB) of the EM wave on average. All combinations revealed significantly low transmission at higher frequencies.

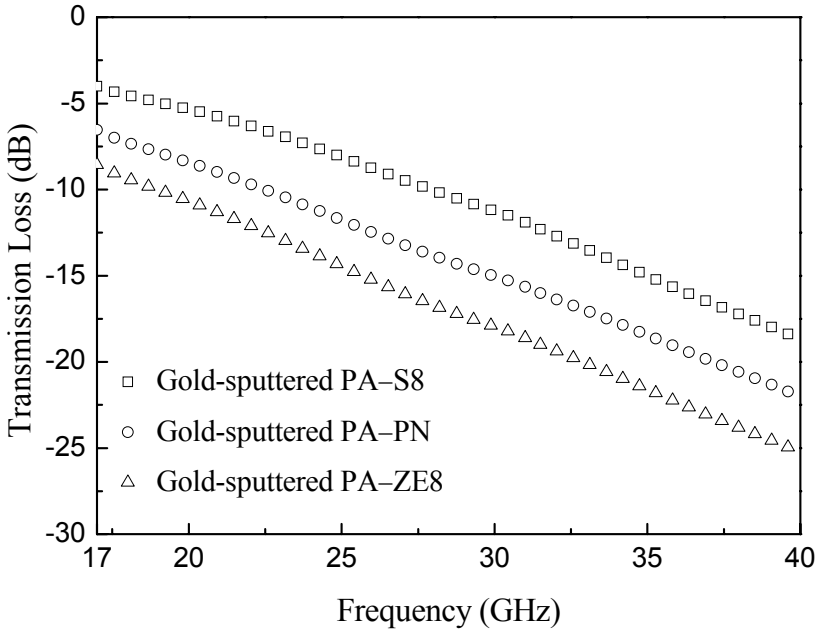

Figure 4.61 Transmission losses of the combinations of gold-sputtered PA and as-received SiC-based woven fabrics.

Combinations containing gold-sputtered PA woven fabrics were more successful in absorbing EM radiation compared to the combinations of as-received alumina woven fabrics, although highest achieved absorption potential was ~70% (Figure 4.62). This value was obtained for combinations having ZE8 and PN woven fabrics at low frequencies owing to the reduced transmission of these combinations.

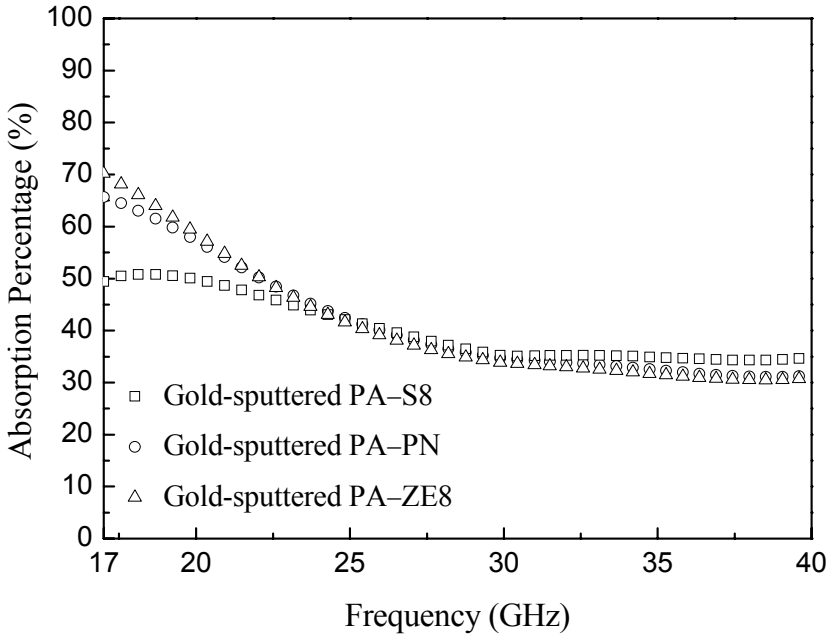

Figure 4.62 Absorption potentials of the combinations of gold-sputtered PA and as-received SiC-based woven fabrics.

Following the examination of gold-sputtered PA woven fabric combinations, new combinations were performed with gold-sputtered satin woven fabrics. In this way, effectiveness of woven type on EM wave absorption potential of the combinations could be discussed.

As the first set, combinations of gold-sputtered SA and as-received SiC-based woven fabrics were conducted. Reflection losses of these combinations are demonstrated in Figure 4.63. Reflection losses of these combinations were quite different than those of the ones with gold-sputtered PA woven fabric as the first

layer. Two basic differences were observed in these curves, the first one was the overall decrease in reflection loss, and the second one was the minima which were observed near 30 GHz. Reflected portion dropped to below ~0.05% (~-33 dB) for combination containing S8 woven fabric, where ~0.5% (~-23 dB) and ~1.3 % (~-19 dB) for combinations having PN and ZE8 woven fabrics, respectively, near to this frequency. In addition to the first layer, second layer (SiC-based layer) was also seen to be effective in the reflection losses, since the combination of high conductivity ZE8 layer resulted in higher reflection losses compared to the other combinations.

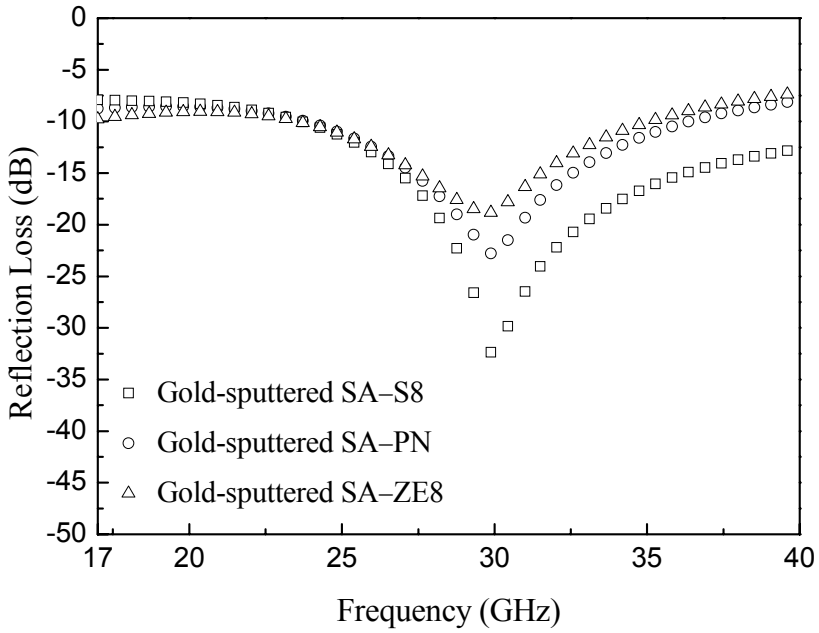

Figure 4.63 Reflection losses of the combinations of gold-sputtered SA and as-received SiC-based woven fabrics.

Combination having the highest conductivity ZE8 woven fabric transmitted least (on average ~5.3% (~-13 dB)) and combination containing lowest conductivity S8 woven fabric transmitted most (on average ~16% (~-8 dB)) according to Figure 4.64.

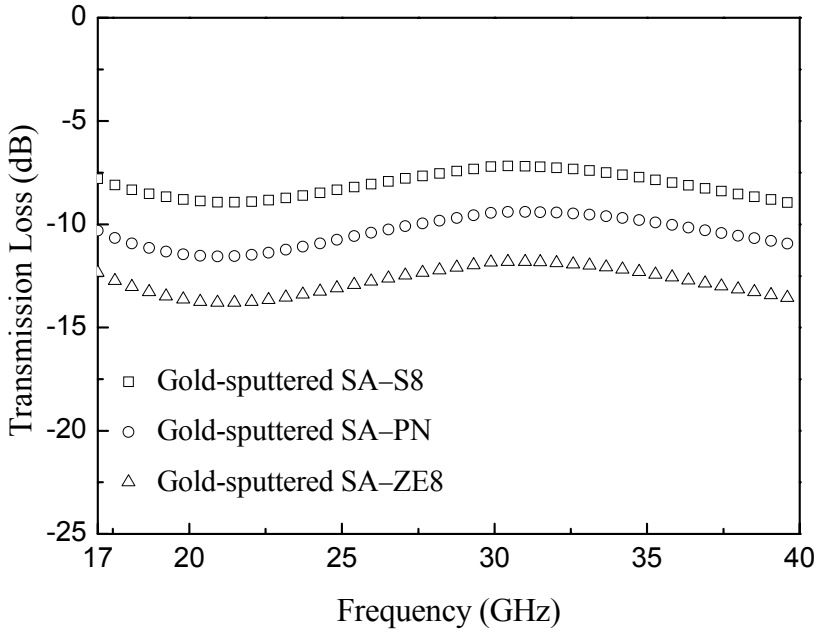

Figure 4.64 Transmission losses of the combinations of gold-sputtered SA and as-received SiC-based woven fabrics.

Higher absorption potentials were achieved in combinations of gold-sputtered alumina satin woven fabrics (Figure 4.65). Calculated highest absorption potentials were on average ~86% for the combination having ZE8 woven fabric, reaching to ~92% at about 30 GHz frequency where a minimum was observed in its reflection loss. Average absorption potential of combination containing PN woven fabric was ~82%, and it was ~78% for the combination of S8 woven type. Relatively high absorption potentials of these combinations were related to reduced reflection loss, which was achieved when gold-sputtered alumina satin woven fabric was used as the first layer. This situation was most probably due to the satin woven type of the first layer having smoother surface which effectively eliminates internal reflections. As a result of this, combinations containing gold-sputtered alumina satin revealed improvement in the EM wave absorption compared to the ones having alumina plain woven fabric.

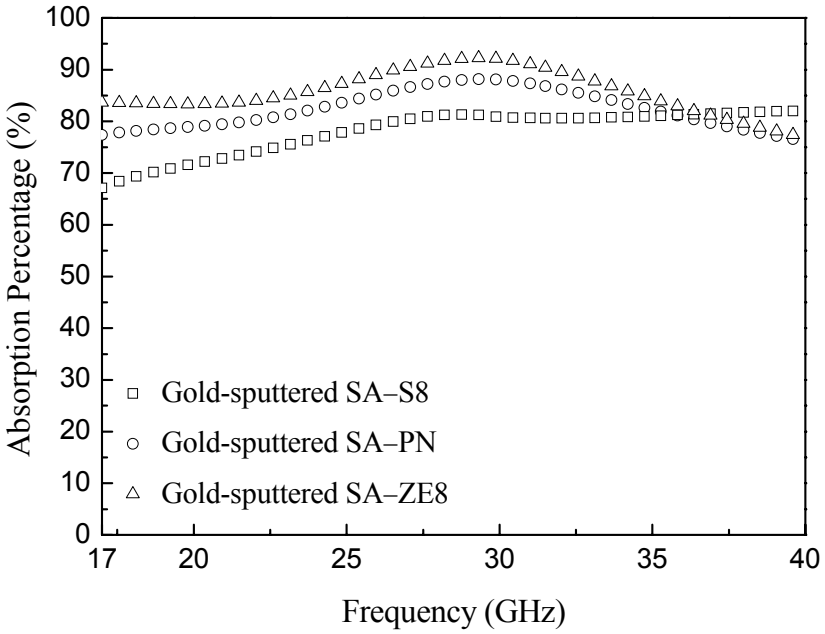

Figure 4.65 Absorption percentages of the combinations of gold-sputtered SA and as-received SiC-based woven fabrics.

4.2.3.4. Combinations of Surface Modified Alumina and Heat-treated SiC-based Ceramic Woven Fabrics

In this part, gold-sputtered alumina and heat-treated SiC-based woven fabric combinations were carried out. Reflection losses of gold-sputtered PA and heat-treated SiC-based woven fabrics (Figure 4.66) were very similar to those of containing as-received SiC-based woven fabrics (Figure 4.60). This result verified the effectiveness of first layer on the reflection losses of the combinations. In these combinations more than ~50% of incident EM wave reflected from the surfaces of the systems.

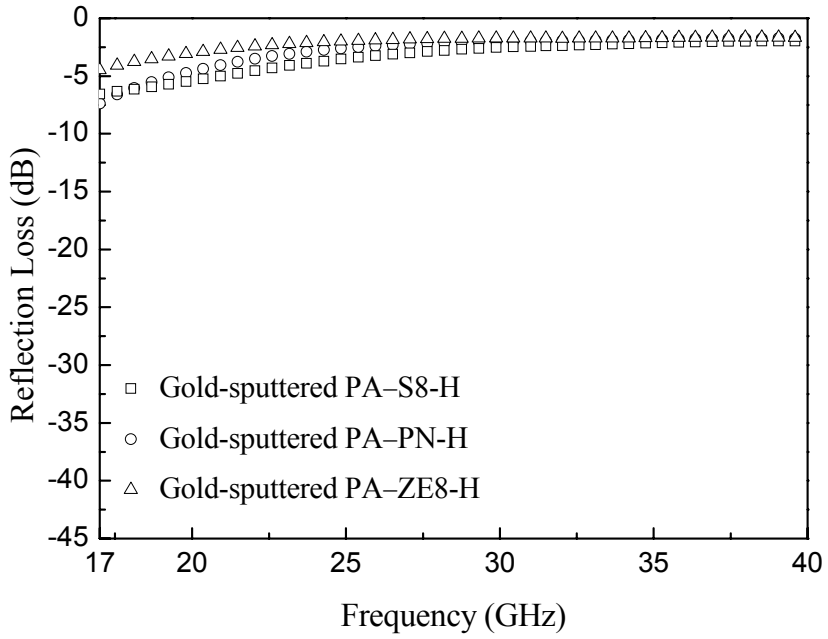

Figure 4.66 Reflection losses of the combinations of gold-sputtered PA and heat-treated SiC-based woven fabrics.

Transmission losses of these combinations are shown in Figure 4.67. Effect of the second layer on transmission was observed. Combination having heat-treated ZE8 woven fabric revealed lowest transmission having an average of ~0.9% (~-20 dB). At high frequencies transmission reduced significantly reaching to ~0.3% (~-25 dB), ~1.2% (~-19 dB) and ~2.7% (~-16 dB) for combinations containing heat-treated ZE8, S8 and PN as the second layer, respectively.

Absorption potentials of these woven fabric combinations are shown in Figure 4.68. It was observed that EM wave absorption capability of these combinations were low (below 60%) due to their high reflection losses.

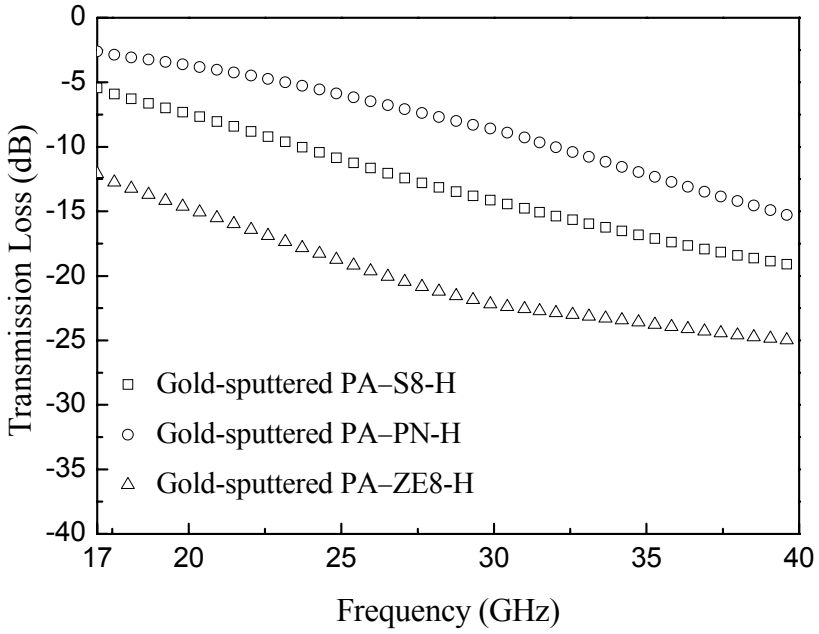

Figure 4.67 Transmission losses of the combinations of gold-sputtered PA and heat-treated SiC-based woven fabrics.

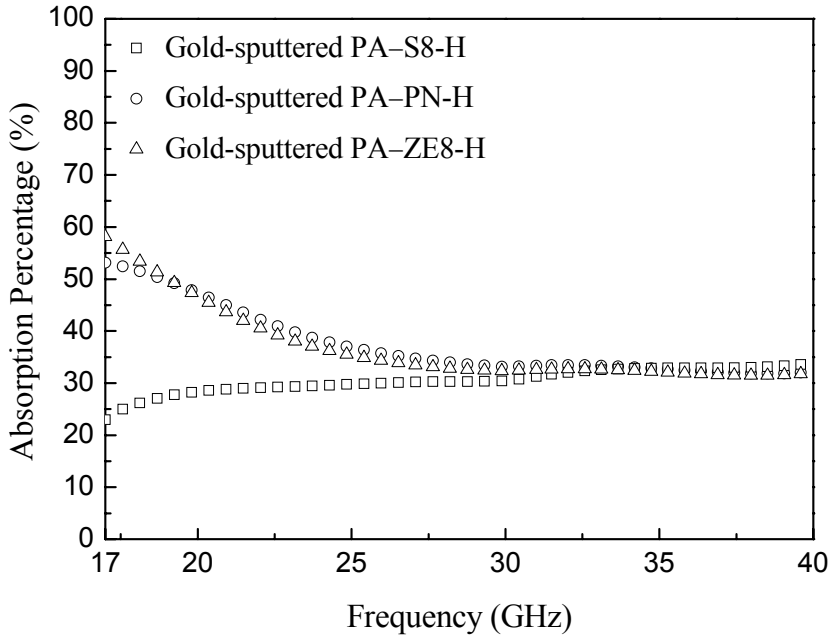

Figure 4.68 Absorption percentages of the combinations of gold-sputtered plain alumina and heat-treated SiC-based woven fabrics.

As the last set of double layer combinations, combinations of gold-sputtered SA and heat-treated SiC-based woven fabrics were conducted. Reflection losses of these combinations are given in Figure 4.69. Similar to combinations of as-received SiC-based woven fabrics, minima were observed at the reflection loss curves. Reflection losses of these combinations were lower than ~-20 dB which means less than ~1% reflection in a certain frequency range between 25 and 28 GHz for the combination containing heat-treated ZE8, where this is in 27-30 GHz range for the combination having heat-treated S8 woven fabric.

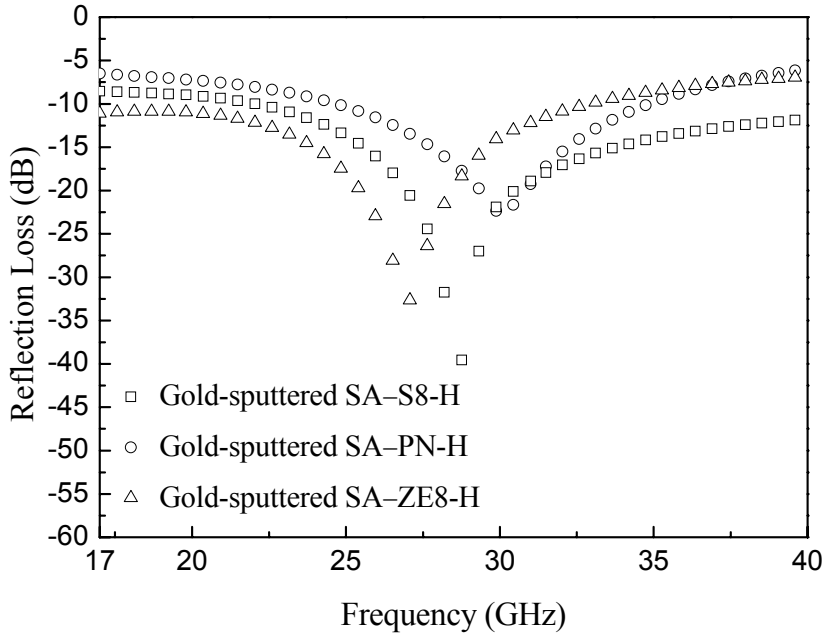

Figure 4.69 Reflection losses of the combinations of gold-sputtered SA and heat-treated SiC-based woven fabrics.

Figure 4.70 shows the transmission losses of these combinations. Transmitted fraction of the combination containing high conductivity heat-treated ZE8 woven fabric was on average ~2.4% (~-16 dB) while it was ~32% (~-5 dB) for the combination having low electrical conductivity heat-treated PN.

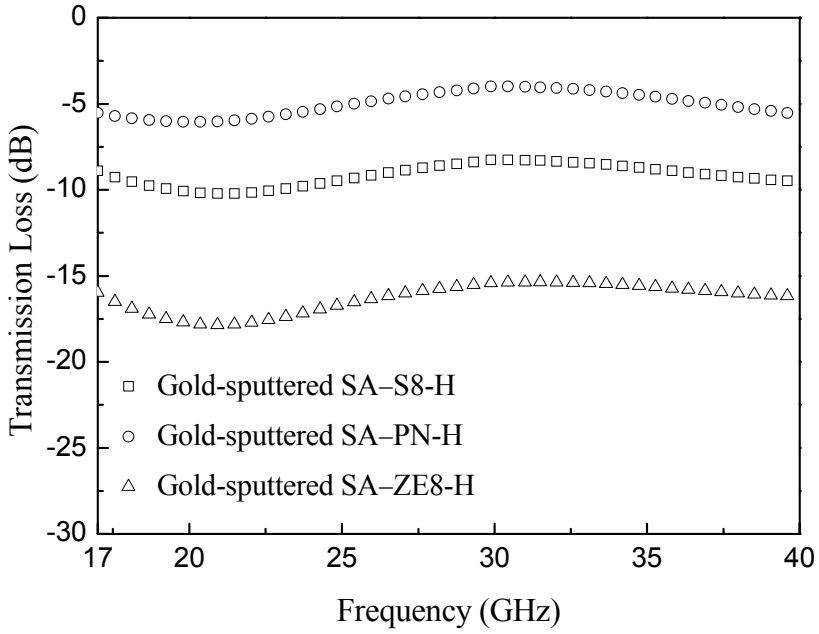

Figure 4.70 Transmission losses of the combinations of gold-sputtered SA and heat-treated SiC-based woven fabrics.

Absorption potentials of these combinations are shown in Figure 4.71 where the highest absorption (on average ~89%) was achieved with combination of heat-treated ZE8 woven fabric. Absorption percentage of this combination was higher than ~90% in 19-31 GHz frequency range reaching to ~97% in 26-28 GHz frequency range.

When gold-sputtered alumina satin was the first layer and absorption potentials of combinations containing as-received (Figure 4.65) and heat-treated (Figure 4.71) SiC-based woven fabrics (as the second layer) were compared, it was observed that the absorption potential of the combination having heat-treated PN decreased significantly compared to that of as-received one. This can be attributed to electrical conductivity decreasing after heat-treatment of PN woven fabric which resulted in higher transmission leading to an overall reduction in EM wave absorption potential of the combination.

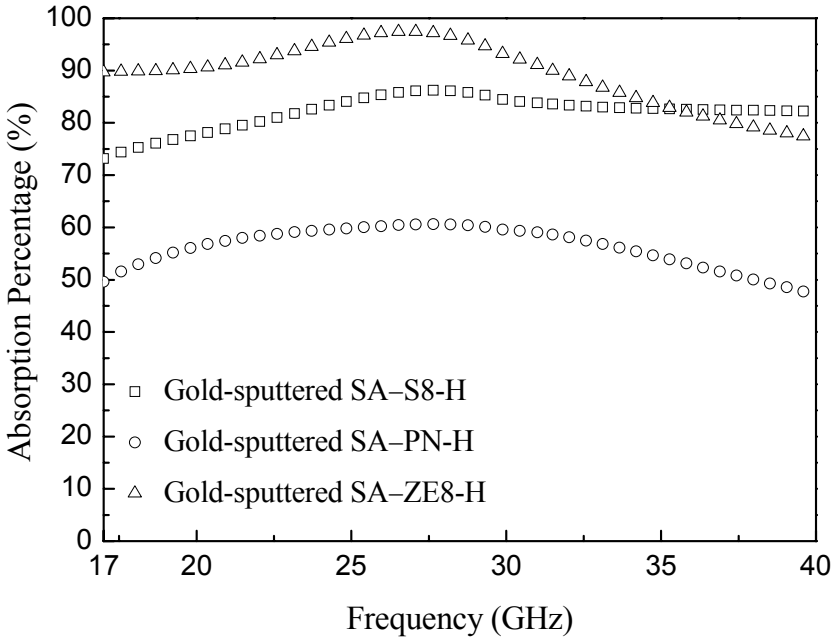

Figure 4.71 Absorption percentages of the combinations of gold-sputtered SA and heat-treated SiC-based woven fabrics.

To conclude, absorption potential of combinations containing alumina and SiC-based woven fabrics were discussed in this section. As-received and modified woven fabrics were placed at the back of each other, and effects of different layer configurations on the resulting EM wave interaction were discussed. When as-received alumina woven fabrics were used as the first layer of the double layer combinations, absorption potential of the structure was mainly controlled by the absorbing capability of second layer, since most of the EM wave transmitted through the first insulating layer reaching to the second one. As a result of this, combinations behaved as if they were formed by the second layer only. Absorption potentials of such combinations were lower than 60% proportional to the absorbing capability of single layer as-received and heat-treated SiC-based woven fabrics. In the other case, where surface modified alumina woven fabrics were used as the first layer, absorption potentials of combinations improved. Combinations having gold-sputtered PA reflected most of the EM wave, therefore, SiC-based layer could only be effective in terms of reducing the overall transmission loss. On the other hand,

usage of modified SA woven fabric as the first layer reduced reflection losses significantly because of its woven type, where effectiveness of the second layer in both transmission and reflection losses was observed. In these combinations highest absorption potentials were achieved when a high conductivity SiC-based woven fabric was used as the second layer. Considerably high absorption potentials of these combinations (>98%) draw attention to these materials for EM wave absorbing applications in GHz frequency range.

CHAPTER 5

CONCLUSION

EM wave absorption potential of single layered and multilayered SiC-based and alumina ceramic woven fabrics were determined in 17-40 GHz frequency range using free-space method. SiC-based ceramic woven fabrics were modified by heat-treatment in air while alumina woven fabrics by gold-sputtering. Effect of these modifications on the EM wave absorption potentials of the ceramic woven fabrics was investigated. Moreover, effect of the sequence of ceramic woven fabric layers having different electrical conductivity, chemical composition and woven type on the resulting interaction with EM radiation has been discussed.

Consequently, following conclusions have been drawn for SiC-based woven fabrics and their double layer combinations:

- Heat-treatment of SiC-based woven fabrics caused reduction in their electrical conductivity due to oxidation of fibers which leads to destruction of fiber structure and disappearance of free carbon aggregates in all fibers. Heat resistant ZE8 type woven fabric was influenced least from the modification, whereas carbon coated PN type vice versa due to the loss of its carbon rich layer after heat-treatment.
- As-received and heat-treated single layer ceramic woven fabrics did not reveal sufficient absorption potential (lower than 50%) for typical applications. Various double layer combinations of ceramic woven fabrics showed better EM wave absorption potential than those of single layers.
- Sequences of woven layers in combinations were effective on the absorption potential of material system, where “low→high” electrical conductivity layer

combinations led to better absorption results than other double layer combinations.

- ❖ Combinations of heat-treated woven fabrics did not directly result in an improvement in absorption potential. Rather than a direct increasing effect on absorption, the function of heat-treatment was to change electrical conductivities of the woven fabrics to achieve low→high electrical conductivity layer combinations.
- ❖ Double layer combinations of satin woven types (ZE8 and S8) revealed promising absorption characteristics compared to other combinations due to their smooth surface properties. S8 and ZE8 woven fabric combinations in as-received and heat-treated states showed higher than 90% absorption potentials in a wide frequency range. High absorption potential of SiC-based ceramic woven fabrics in multilayer arrangement in GHz range renders them powerful candidate materials for EM wave absorbing applications.

For alumina woven fabrics and their double layer combinations, following conclusions have been drawn:

- ➢ As-received plain and satin alumina woven fabrics transmitted most of EM energy resulting in very low absorption potentials. For these woven fabrics reflection loss was strengthened while transmission loss was weakened after surface modification due to the presence of high electrical conductivity gold layer on woven fabrics. Although absorption potential improved after surface modification, it was still not sufficient for commercial applications.
- ➢ Double layer combinations of as-received alumina woven fabrics revealed similar behavior (most of EM energy transmitted) to single layer as-received alumina woven fabric for both plain and satin woven type. In the case of surface modified woven fabrics, double layered alumina satin woven fabric revealed a promising absorption potential which was on average ~93% in 17-40 GHz frequency range.

Conclusions regarding double layer combinations of alumina and SiC-based woven fabrics are summarized below:

- Combinations in which as-received plain/satin alumina woven fabrics were used as the first layer and as-received SiC-based ceramic woven fabrics as the other layer, transmission and reflection losses of the combinations were dominated by high conductivity layer (SiC-based woven fabric). Transmission loss revealed a weakening trend with the conductivity increase whereas reflection loss was strengthened.
- Absorption potential of combinations containing as-received alumina woven fabrics were very similar to that of the single layered as-received SiC-based ceramic woven fabrics which proved that plain and/or satin alumina woven fabric transmitted most of the EM energy with a negligible absorption. This situation was also valid for the combinations of heat-treated SiC-based woven fabrics.
- Combinations of gold-sputtered alumina plain woven fabric revealed very high reflection loss since most of the EM energy was reflected form the gold coated first layer, and this tendency was also related to the increase in internal reflection due to plain type woven fabric. Owing to the highly reflective behavior of the first layer, second layer became inefficient in overall reflection loss while transmission losses of the system were controlled by this layer. Higher electrical conductivity second layer resulted in lower transmission loss and vice versa.
- Combinations of gold-sputtered alumina satin woven fabric revealed better absorption potentials compared to that of plain due to reduced reflection and transmission losses of the systems. SiC-based backing layer was effective on both reflection and transmission losses of these combinations. Increase in the electrical conductivity increase of this layer resulted in higher reflection and lower transmission loss of the combinations.
- Double layer combination of gold-sputtered alumina satin and ZE8 woven fabric revealed promising absorption characteristics compared to other combinations. This combination of as received and heat-treated fabric arrangement showed higher than 95% absorption potential in a wide frequency range. High absorption potential of multilayer alumina and SiC-

based ceramic woven fabrics in GHz range renders them powerful candidate materials for EM wave absorbing applications.

To sum up, following guidelines can be emphasized in light of the results which obtained throughout this study:

- ✓ In multilayer EM wave absorbers, systems containing individual layers with varying electrical conductivities reveal improved EM wave absorbing capability when low→high conductivity layer sequence is achieved. In terms of its operation low conductivity first layer reflects a small portion of the EM wave and transmits the remaining portion through. A higher conductivity second layer bounds the wave between layers and reduces the secondary reflection, consequently due to high conductivity of this layer transmission loss is weakened. As a result of this, higher absorption potentials can be achieved.
- ✓ Usage of an insulative material as the first layer is ineffective for multilayer applications, since this layer behaves as an inert component by transmitting almost all of the EM wave through. On the other hand, utilization of a high electrical conductivity layer is not useful due to the fact that most of the EM wave reflects from its surface.
- ✓ In case of woven fabric usage as an EM wave absorber, satin woven fabrics can be recommended, since smoother surface of these woven fabrics reduces internal reflections and avoids additional transmission losses which are observed in plain woven fabrics due to their high level of surface crimp along with gaps present in the structure.

REFERENCES

[1] A. S. Serway, Physics for Scientists and Engineers, Saunders College Publishing, Orlando, 1990.

[2] M. Kotlarchyk, Electromagnetic Radiation and Interactions with Matter, Wiley, New York, 2002.

[3] E. F. Knott, J. F. Shaeffer, M. T. Tuley, Radar Cross Section, Artech House, Boston, 1993.

[4] P. S. Neelkanta, Handbook of Electromagnetic Materials: Monolithic and Composite Versions and Their Applications, CRC-Press, Florida, 1995.

[5] C. K. Yüzcelik, Radar Absorbing Material Design, Naval Postgraduate School Monterey CA, 2003.

[6] J. Joo, A. J. Epstein, Applied Physics Letters 65 (1994) 2278-2280.

[7] R. B. Schultz, IEEE Transactions on Electromagnetic Compability EMC-10 (1968) 95-100.

[8] K. B. Cheng, S. Ramakrishna, K. C. Lee, Composites Part A: Applied Science and Manufacturing 31 (2000) 1039-1045.

[9] D. D. L. Chung, Carbon 39 (2001) 279-285.

[10] C. Y. Lee, H. G. Song, K. S. Jang, E. J. Oh, A. J. Epstein, J. Joo, Synthetic Metals 102 (1999) 1346-1349.

[11] Y. Duan, L. Shunhua, G. Hongtao, Science and Technology of Advanced Materials 6 (2005) 513-518.

[12] A. Kaynak, A. Polat, U. Yilmazer, Materials Research Bulletin 31 (1996) 1195-1206.

[13] Y. A. Shneyderman, Radio-Absorbing Materials, Foreign Technology Division, 1985.

[14] C. A. Grimes, Broadband EMC absorbing materials, in: E. Record (Ed.) 1993 Int'l.Symp., 1993, pp. 245-249.

[15] I. S. Seo, W. S. Chin, D. G. Lee, Composite Structures 66 (2004) 533-542.

[16] K. J. Vinoy, Kluwer Academic Publisher (1996).

[17] W. S. Chin, D. G. Lee, Composite Structures 77 (2007) 457-465.

[18] G. Hartsgrove, A. Kraszenski, A. Surowiec, Bioelectromagnetics 8 (1987) 29-36.

[19] P. Saville, A Review of Optimisation Techniques for Layered Radar Absorbing Materials, Technical Memorandum, Atlantic, 2004.

[20] A. Bhattacharyya, D. L. Sengupta, Radar Cross Section Analysis and Control, Artech House, 1991.

[21] Y. Naito, K. Suetake, IEEE Transactions on Microwave Theory and Techniques MT19 (1971) 65-&.

[22] P. Singh, V. K. Babbar, A. Razdan, S. L. Srivastava, R. K. Puri, Materials Science and Engineering B-Solid State Materials for Advanced Technology 67 (1999) 132-138.

[23] A. Bahadoor, Y. Wang, M. Afsar, Journal of Applied Physics 97 (2005) 10F105(101-103).

[24] T. Giannakopoulou, L. Kompotiatis, A. Kontogeorgakos, G. Kordas, Journal of Magnetism and Magnetic Materials 246 (2002) 360-365.

[25] Y. B. Feng, T. Qiu, C. Y. Shen, X. Y. Li, IEEE Transactions on Magnetics 42 (2006) 363-368.

[26] J. Li, J. Huang, Y. Qin, F. Ma, Materials Science and Engineering: B 138 (2007) 199-204.

[27] M. S. Pinho, M. L. Gregori, R. C. R. Nunes, B. G. Soares, European Polymer Journal 38 (2002) 2321-2327.

[28] J.-H. Oh, K.-S. Oh, C.-G. Kim, C.-S. Hong, Composites Part B 35 (2004) 49-56.

[29] N. Dishovsky, M. Grigorova, Materials Research Bulletin 35 (2000) 403-409.

[30] X. Luo, D. D. L. Chung, Composites Part B: Engineering 30 (1999) 227-231.

[31] S. Wen, D. D. L. Chung, Carbon 45 (2007) 505-513.

[32] T. Kim, D. Chung, Journal of Materials Engineering and Performance 15 (2006) 295-298.

[33] X. P. Shui, D. D. L. Chung, Journal of Materials Science 35 (2000) 1773-1785.

[34] R. A. Tellakula, V. K. Varadan, T. C. Shami, G. N. Mathur, Smart Materials & Structures 13 (2004) 1040-1044.

[35] N. Gagnon, Design and Study of a Free-Space Quasi-Optical Measurement System, in: School of Information Technology and Engineering University of Ottowa, 2002.

[36] D. R. Gagnon, IEEE Transactions on Microwave Theory and Techniques 39 (1991) 2237-2240.

[37] D. K. Ghodgaonkar, V. V. Varadan, V. K. Varadan, IEEE Transactions on Instrumentation and Measurement 38 (1989) 789-793.

[38] D. K. Ghodgaonkar, V. V. Varadan, V. K. Varadan, IEEE Transactions on Instrumentation and Measurement 39 (1990) 387-394.

[39] J. Baker, R. G. Geyer, J. H. Grosvenor, M. D. Janezic, C. A. Jones, IEEE Transactions on Dielectrics and Electrical Insulation 5 (1998) 571-577.

[40] G. R. Traut, IEEE Transactions on Components Packaging and Manufacturing Technology Part B-Advanced Packaging 18 (1995) 106-111.

[41] T. Ishikawa, Advances in inorganic fibers, in: Polymeric and Inorganic Fibers, vol 178, 2005, pp. 109-144.

[42] Composite Materials Handbook, Department of Defense Handbook, USA, 2002.

[43] S. Yajima, J. Hayashi, M. Omori, Chemistry Letters (1975) 931-934.

[44] P. J. Lamicq, G. A. Bernhart, M. M. Dauchier, J. G. Mace, American Ceramic Society Bulletin 65 (1986) 336-338.

[45] K. M. Prewo, J. J. Brennan, G. K. Layden, American Ceramic Society Bulletin 65 (1986) 305-&.

[46] S. Yajima, K. Okamura, T. Matsuzawa, Y. Hasegawa, T. Shishido, Nature 279 (1979) 706-707.

[47] S. M. Bleay, A. R. Chapman, G. Love, V. D. Scott, Journal of Materials Science 27 (1992) 5389-5396.

[48] C. Laffon, A. M. Flank, P. Lagarde, M. Laridjani, R. Hagege, P. Olry, J. Cotteret, J. Dixmier, J. L. Miquel, H. Hommel, A. P. Legrand, Journal of Materials Science 24 (1989) 1503-1512.

[49] T. Mah, N. L. Hecht, D. E. McCullum, J. R. Hoenigman, H. M. Kim, A. P. Katz, H. A. Lipsitt, Journal of Materials Science 19 (1984) 1191-1201.

[50] S. Yajima, American Ceramic Society Bulletin 62 (1983) 893-&.

[51] N. Hochet, M. H. Berger, A. R. Bunsell, Journal of Microscopy 185 (1997) 243-258.

[52] K. Kakimoto, T. Shimoo, K. Okamura, Materials Science and Engineering A-Structural Materials Properties Microstructure and Processing 217 (1996) 211-214.

[53] K. Kakimoto, T. Shimoo, K. Okamura, Journal of the Ceramic Society of Japan 105 (1997) 504-508.

[54] T. Shimoo, Y. Morisada, K. Okamura, Journal of American Ceramic Society 83 (2000) 3049-3056.

[55] T. Shimoo, Y. Morisada, K. Okamura, Journal of Materials Science 37 (2002) 4361-4368.

[56] M. Takeda, A. Urano, J.-i. Sakamoto, Y. Imai, Journal of American Ceramic Society 83 (2000) 1171-1176.

[57] K. Kumagawa, H. Yamaoka, M. Shibuya, T. Yamamura, Ceramic Engineering and Science Proceedings 18 (1997) 113-118.

[58] K. Okamura, T. Shimoo, K. Suzuya, K. Suzuki, Journal of the Ceramic Society of Japan 114 (2006) 445-454.

[59] Y. Kagawa, Y. Imahashi, H. Iba, T. Naganuma, K. Matsumura, Journal of Materials Science Letters 22 (2003) 159-161.

[60] Y. Kagawa, K. Matsumura, H. Iba, Y. Imahashi, Journal of Materials Science 42 (2007) 1116-1121.

[61] A. R. Bunsell, M. H. Berger, Journal of the European Ceramic Society 20 (2000) 2249-2260.

[62] Y. Saitow, K. Iwanaga, S. Itou, T. Fukumoto, T. Utsunomiya, 37th International SAMPE Symposium, 1992, pp. 808-819.

[63] V. Lavaste, M. H. Berger, A. R. Bunsell, J. Besson, Journal of Materials Science 30 (1995) 4215-4225.

[64] Committee on Advanced Fibers for High-Temperature Ceramic Composites, National Research Council Ceramic Fibers and Coatings: Advanced Materials for the Twenty-First Century, 1998.

[65] Ube Industries Co Ltd. (2001).

[66] L. Duffrene, J. Kieffer, Journal of. Physics and Chemistry of Solids 59 (1998) 1025-1037.

[67] T. Shimoo, Y. Morisada, K. Okamura, Journal of the American Ceramic Society 86 (2003) 838.

[68] H. Yamaoka, T. Ishikawa, K. Kumagawa, Journal of Materials Science 34 (1999) 1333-1339.